Broadband quantum noise reduction in AdV+ :

From frequency-dependent squeezing implementation to detection losses and scattered light mitigation

12th December 2022

Candidate : Eleonora Polini

Advisor : Edwige Tournefier
Co-advisors: Romain Bonnand, Romain Gouaty

Outline

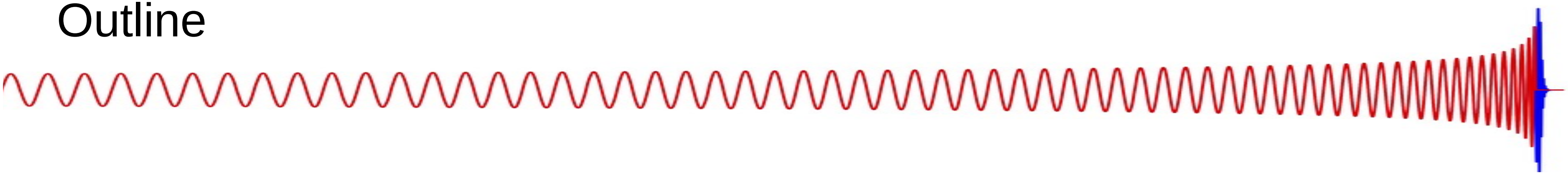

1. Gravitational waves: origin & detection

2. Quantum noise: origin & reduction strategy

3. The Virgo detector from the observing run O3 to O4

4. Frequency dependent squeezing system: installation and commissioning

5. Low loss Output Mode Cleaner: characterization, installation and commissioning

6. Scattered light noise: study and mitigation

7. Conclusions and next steps

Outline

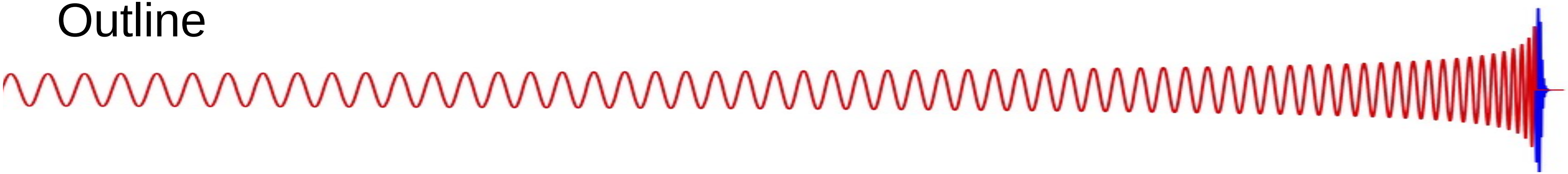

1. Gravitational waves: origin & detection

2. Quantum noise: origin & reduction strategy

3. The Virgo detector from the observing run O3 to O4

4. Frequency dependent squeezing system: installation and commissioning

5. Low loss Output Mode Cleaner: characterization, installation and commissioning

6. Scattered light noise: study and mitigation

7. Conclusions and next steps

Gravitational waves (GWs) are ‘ripples’ in the fabric of the space-time, propagating at the speed of light, caused by some of the most violent and energetic processes in the Universe.

$$g_{\mu\nu} = \eta_{\mu\nu} + h_{\mu\nu}$$

Smalll perturbation of the metric tensor

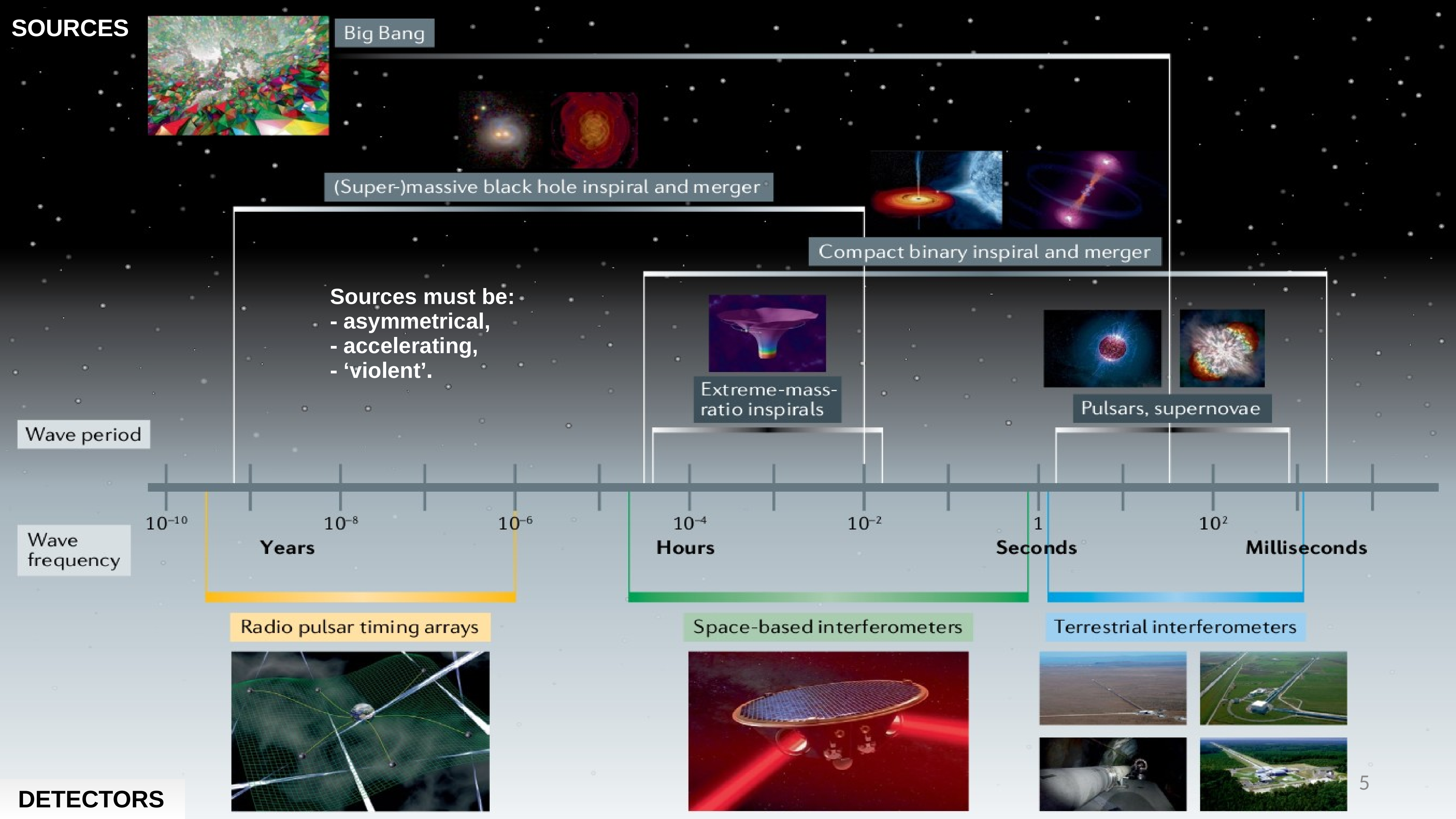
SOURCES
Big Bang
(Super-)massive black hole inspiral and merger
Compact binary inspiral and merger
Sources must be:
- asymmetrical,
- accelerating,
- 'violent'.
Extreme-mass-ratio inspirals
Pulsars, supernovae
Wave period
Wave frequency
10⁻¹⁰
10⁻⁸
10⁻⁶
10⁻⁴
10⁻²
1
10²
Years
Hours
Seconds
Milliseconds
Radio pulsar timing arrays
Space-based interferometers
Terrestrial interferometers
DETECTORS

Network of terrestrial GW detectors

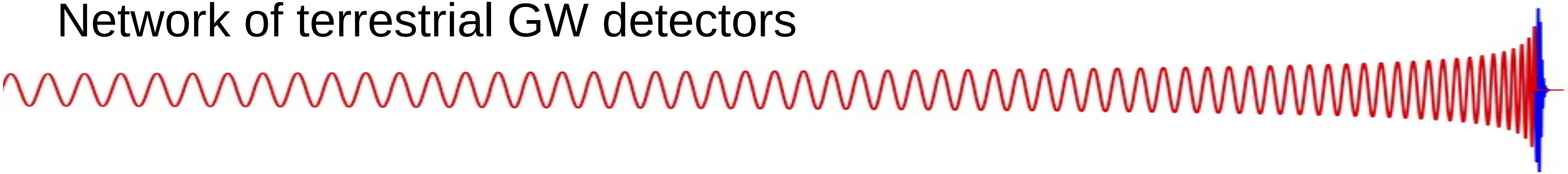

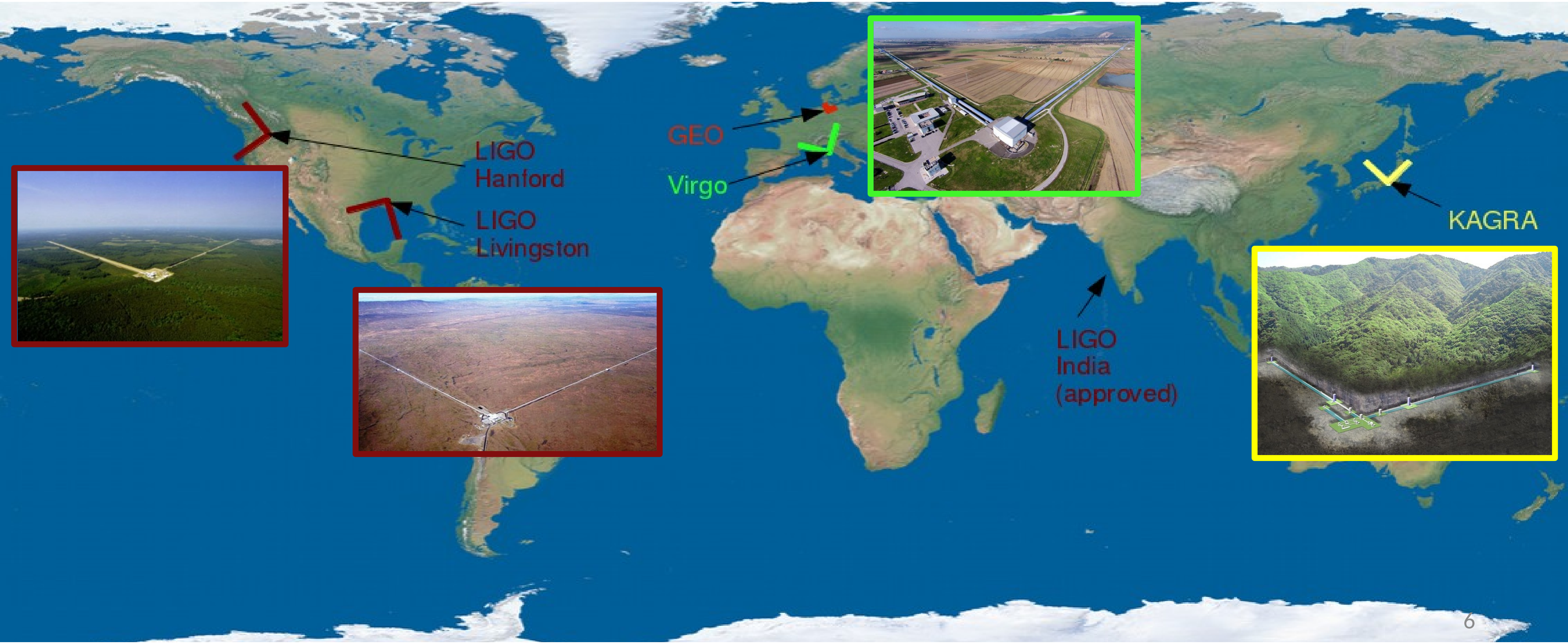

First direct detections of GWs

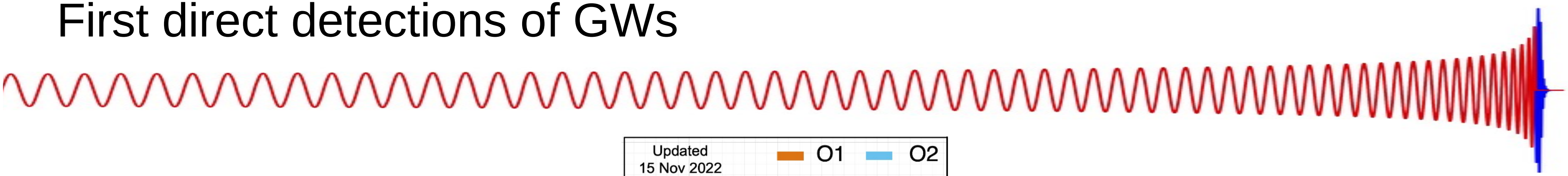

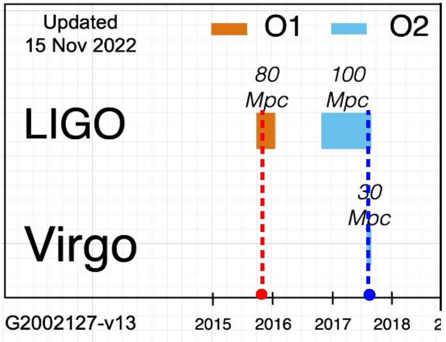

First GW direct observation by LIGO detectors of a binary black hole coalescence, 14th September 2015

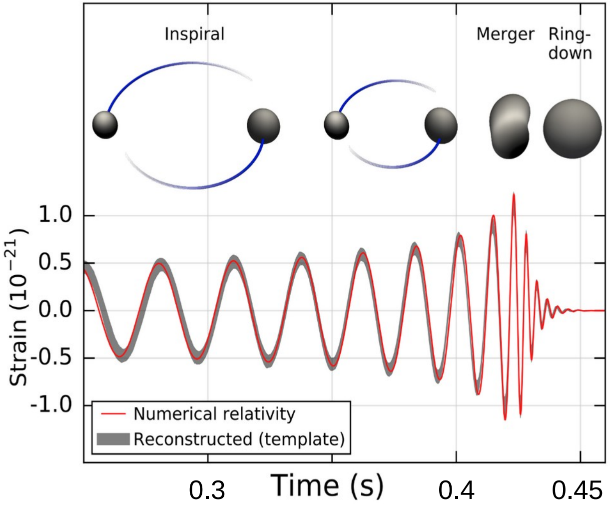

Binary neutron star coalescence detection by LIGO & Virgo detectors, 17th August 2017

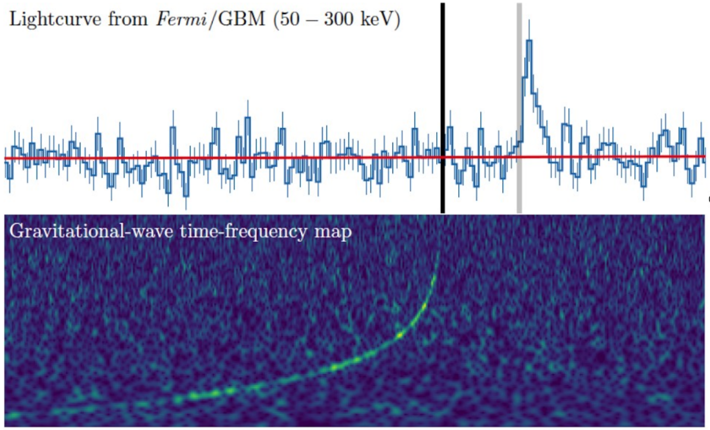

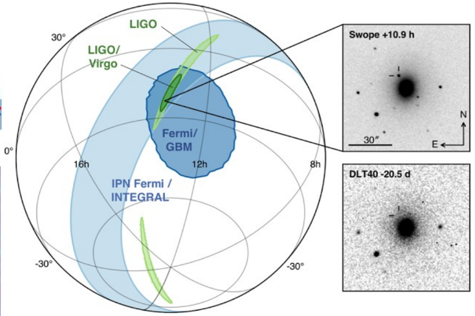

Observing runs and GW detections

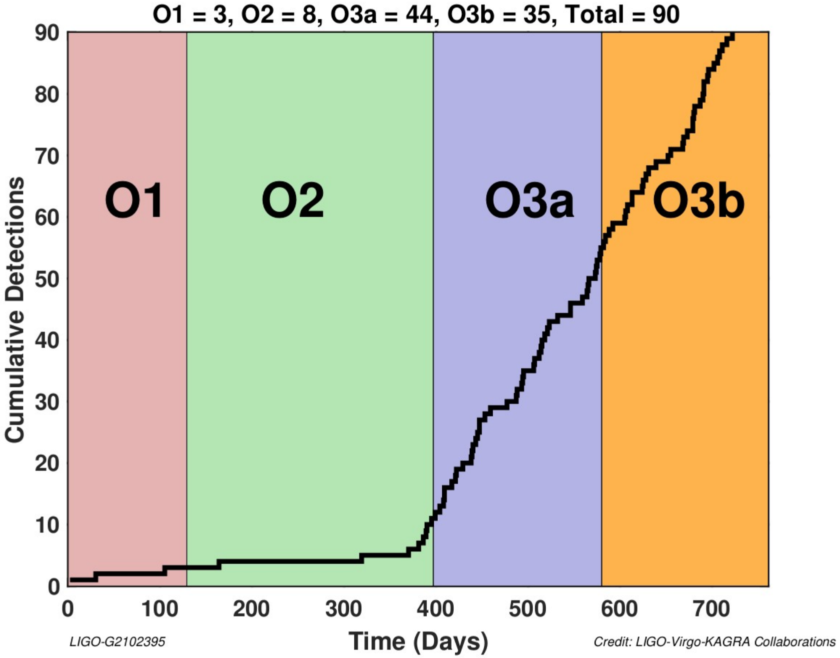

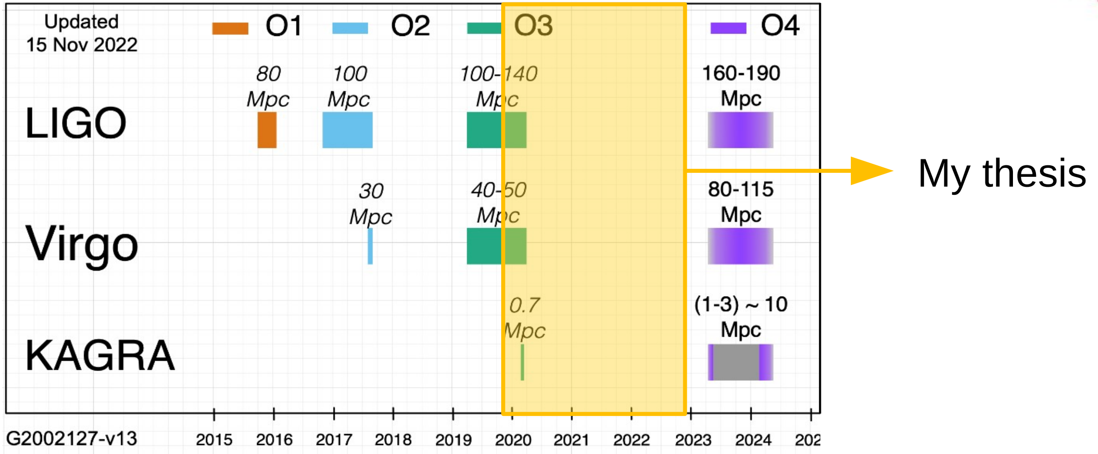

90 events detected up to now:
- 1 Binary Neutron Star (BNS) merger
- 2 Neutron Star – Black Hole (NSBH)
- All the others are Binary Black Hole (BBH)

Detection prospects for O4:
- Up to **three time** more events than in O3
- Improvement of the source localization
- Many other BNS events

Detection of gravitational waves

The most sensitive ground-based instrument is a **km-scale Michelson interferometer** whose mirrors are free-falling masses, i.e. suspended.

The gravitational wave induces a variation of the differential length of the arms, seen by a detector at the output port.

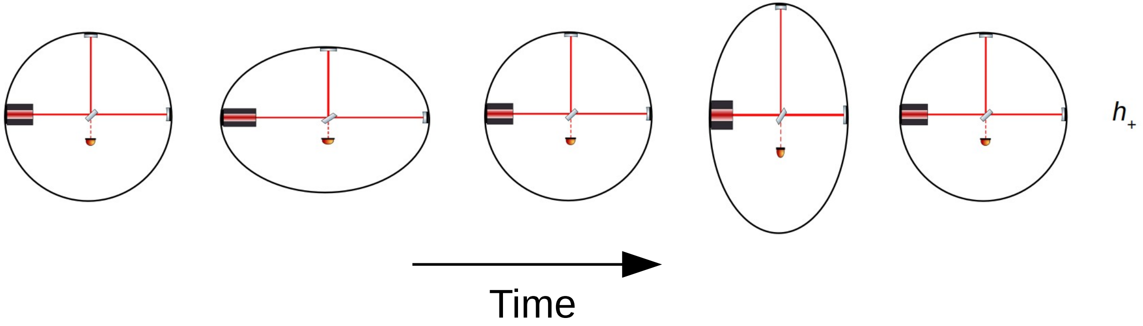

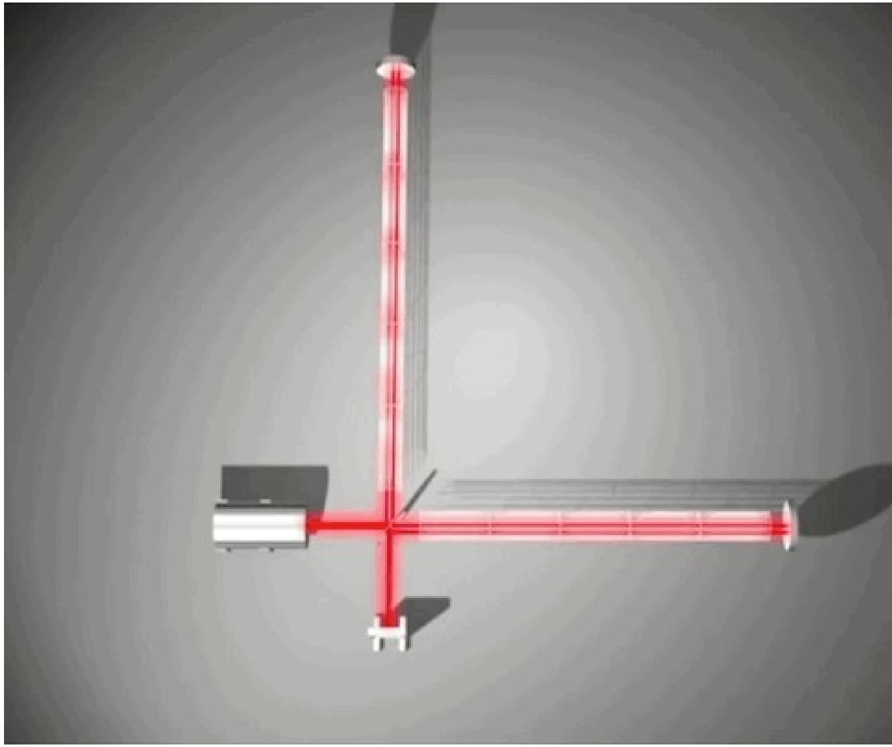

Detection of gravitational waves

The most sensitive ground-based instrument is a **km-scale Michelson interferometer** whose mirrors are free-falling masses, i.e. suspended.

The gravitational wave induces a variation of the differential length of the arms, seen by a detector at the output port.

The **GW amplitude or strain** is given by:

$$h = \frac{2\,\delta L_{\mathrm{GW}}}{L}$$

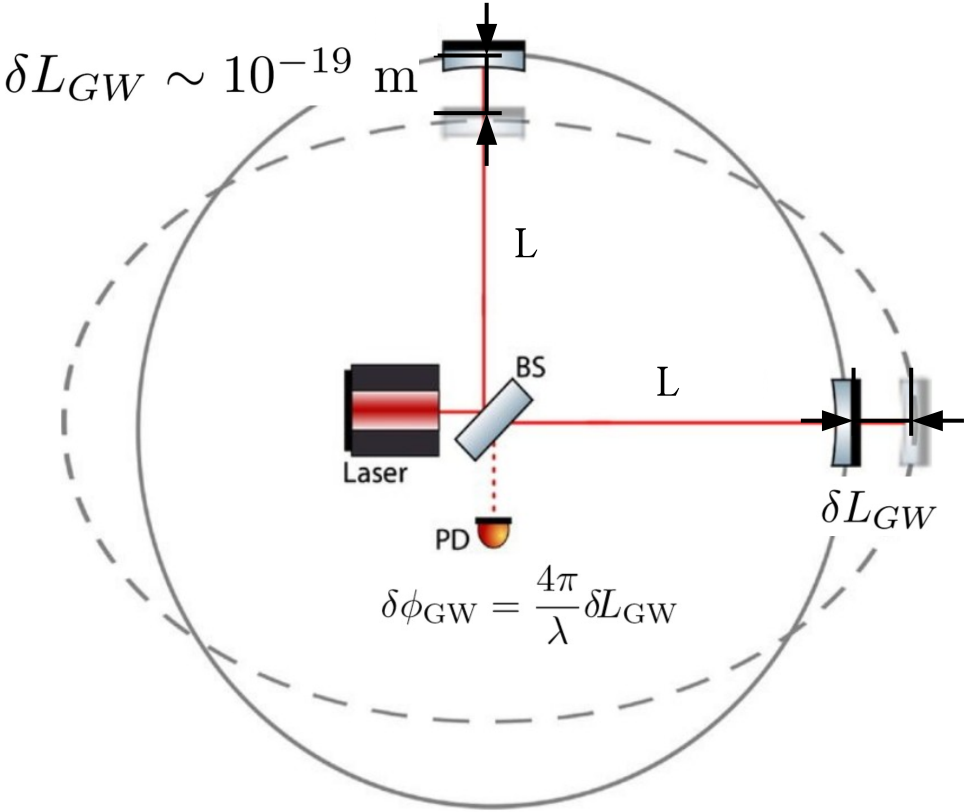

Detection of gravitational waves

Gravitational waves signals are ‘hidden’ by several noises

h(t) = signal(t) + noise(t)

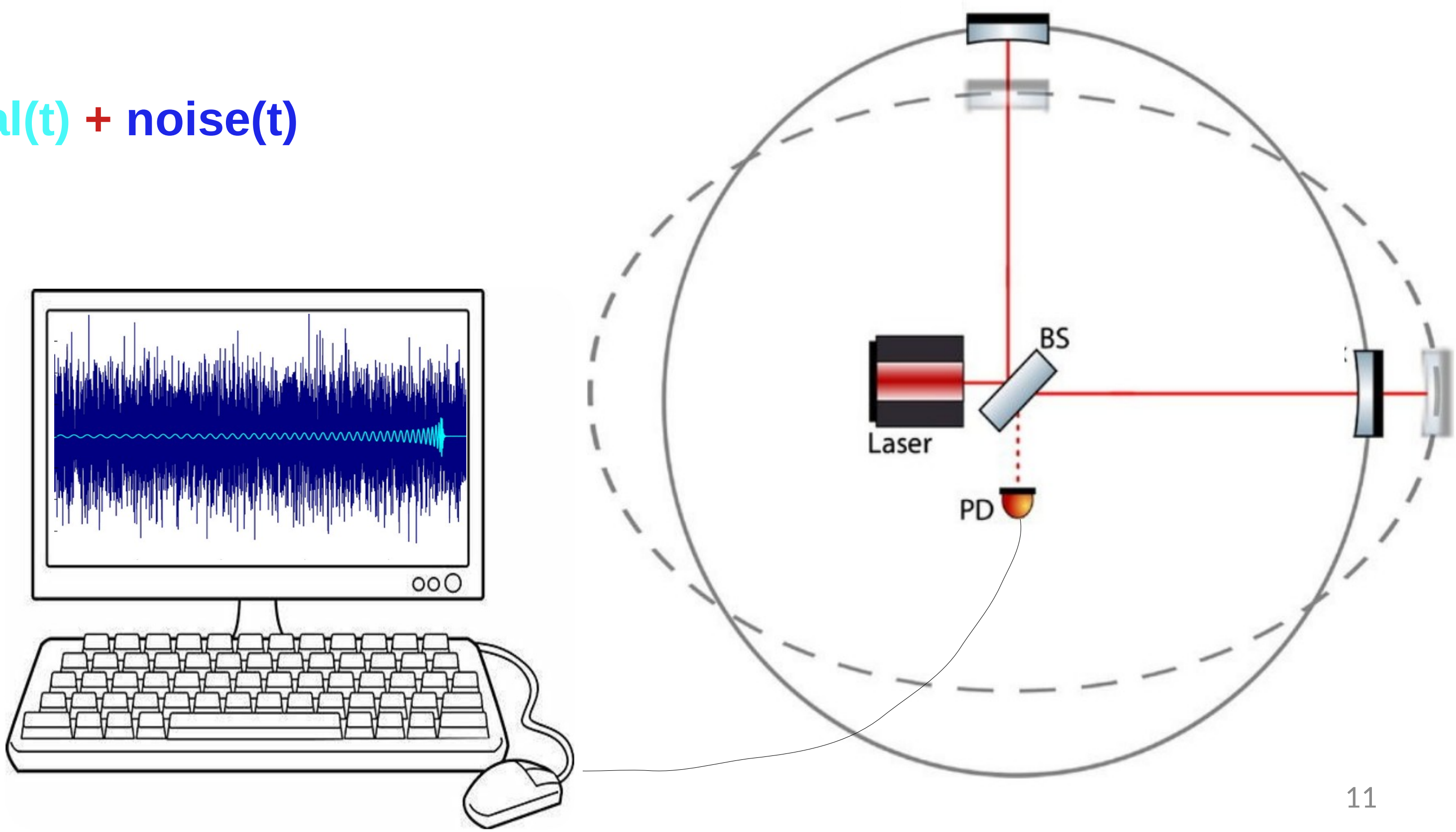

Real interferometer

- **Suspended mirrors** to filter seismic noise

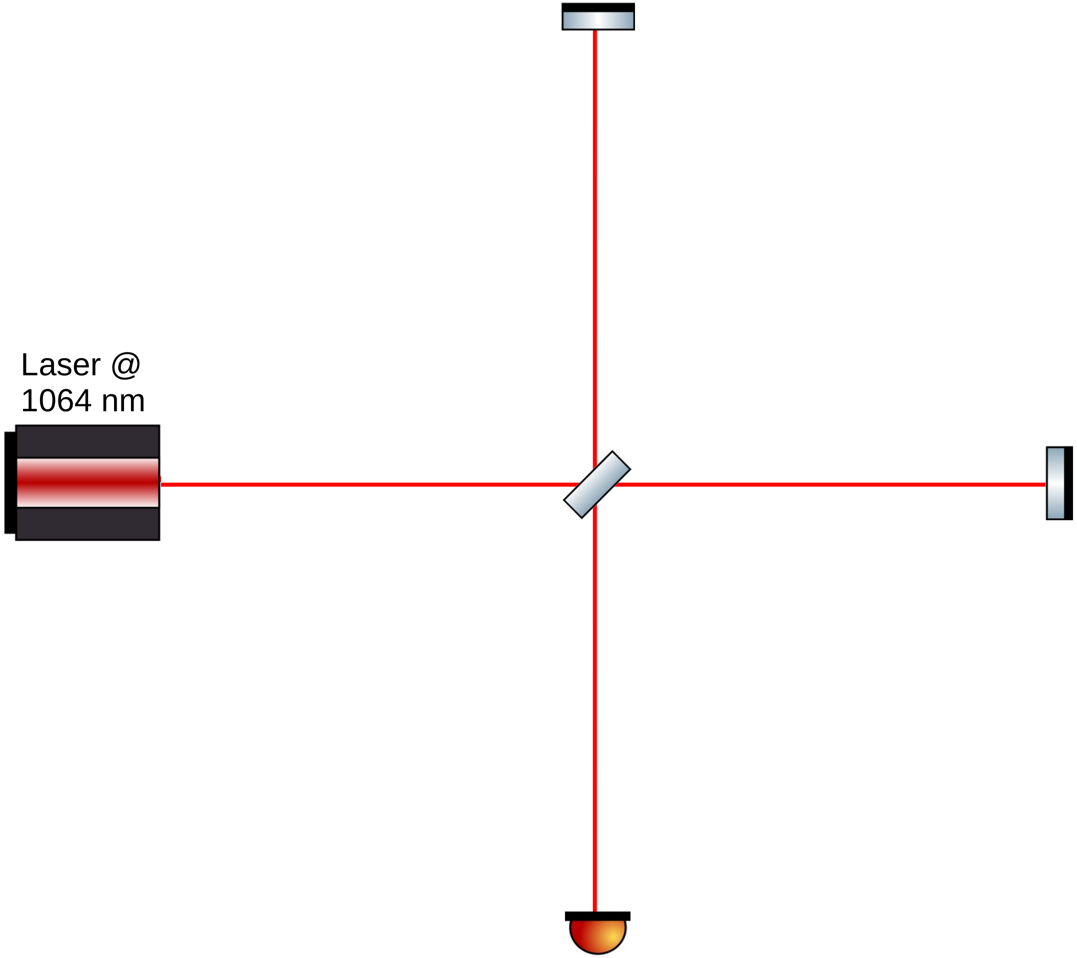

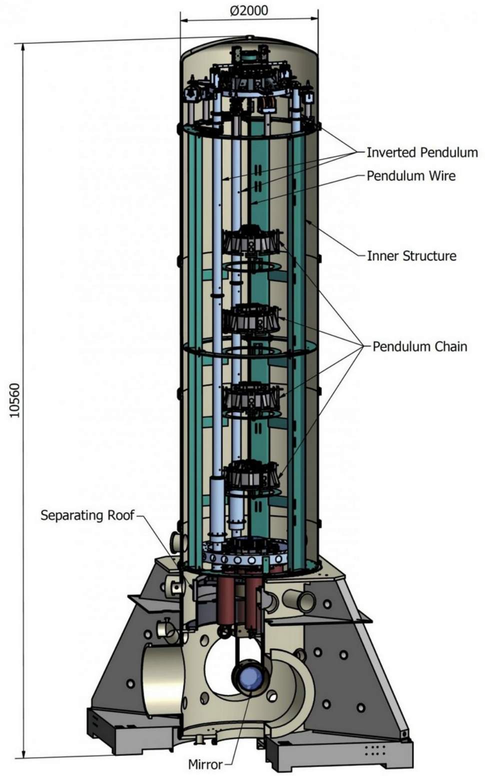

Real interferometer

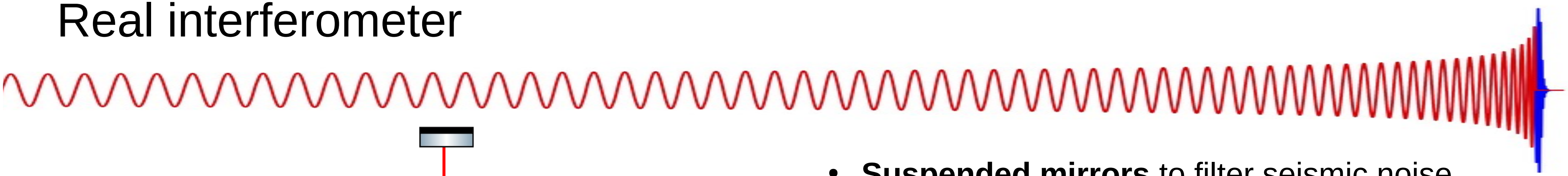

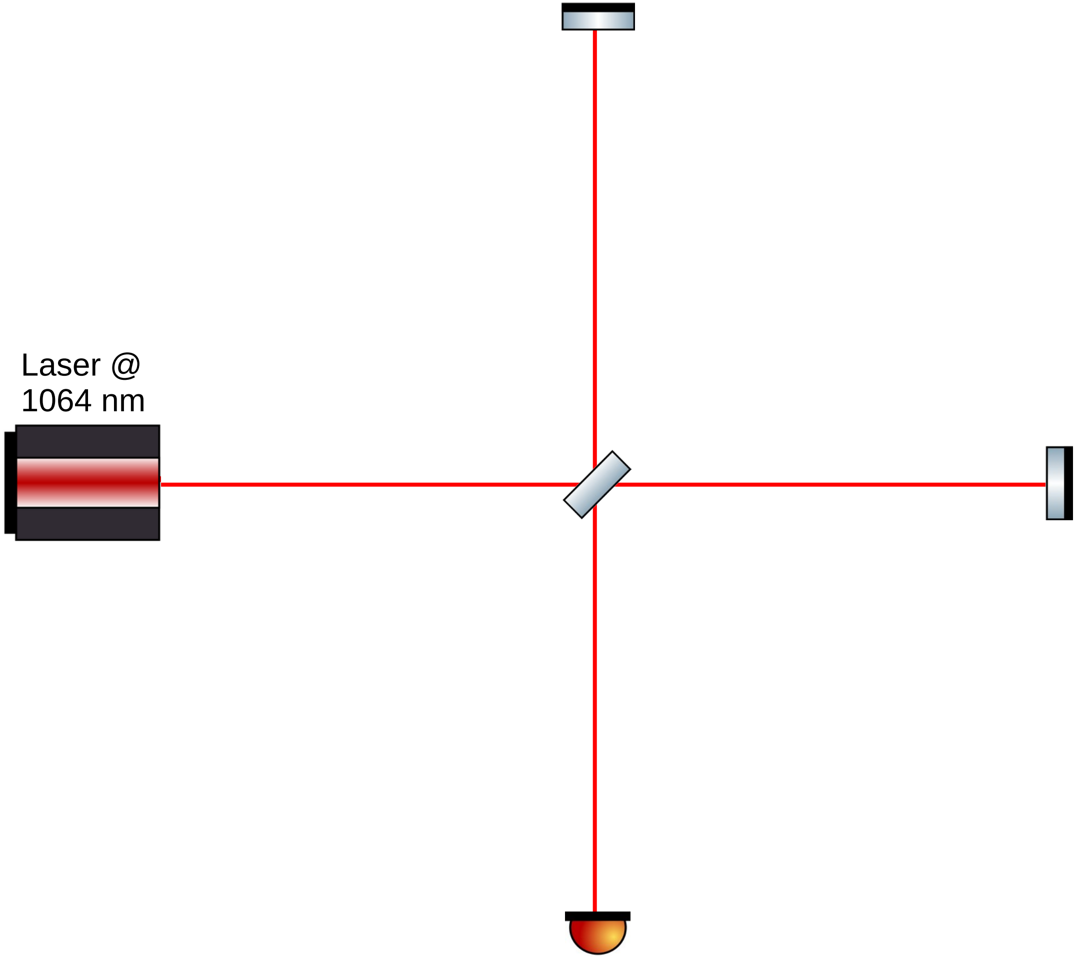

- **Suspended mirrors** to filter seismic noise
- **Whole system in vacuum (10^{-8} mbar)** to avoid the gases refractive index variation

Real interferometer

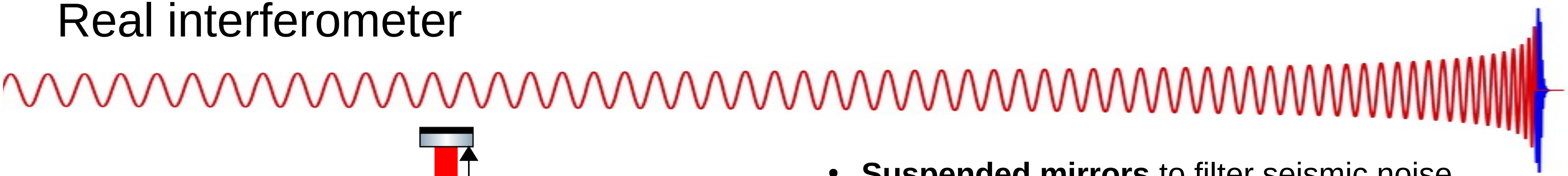

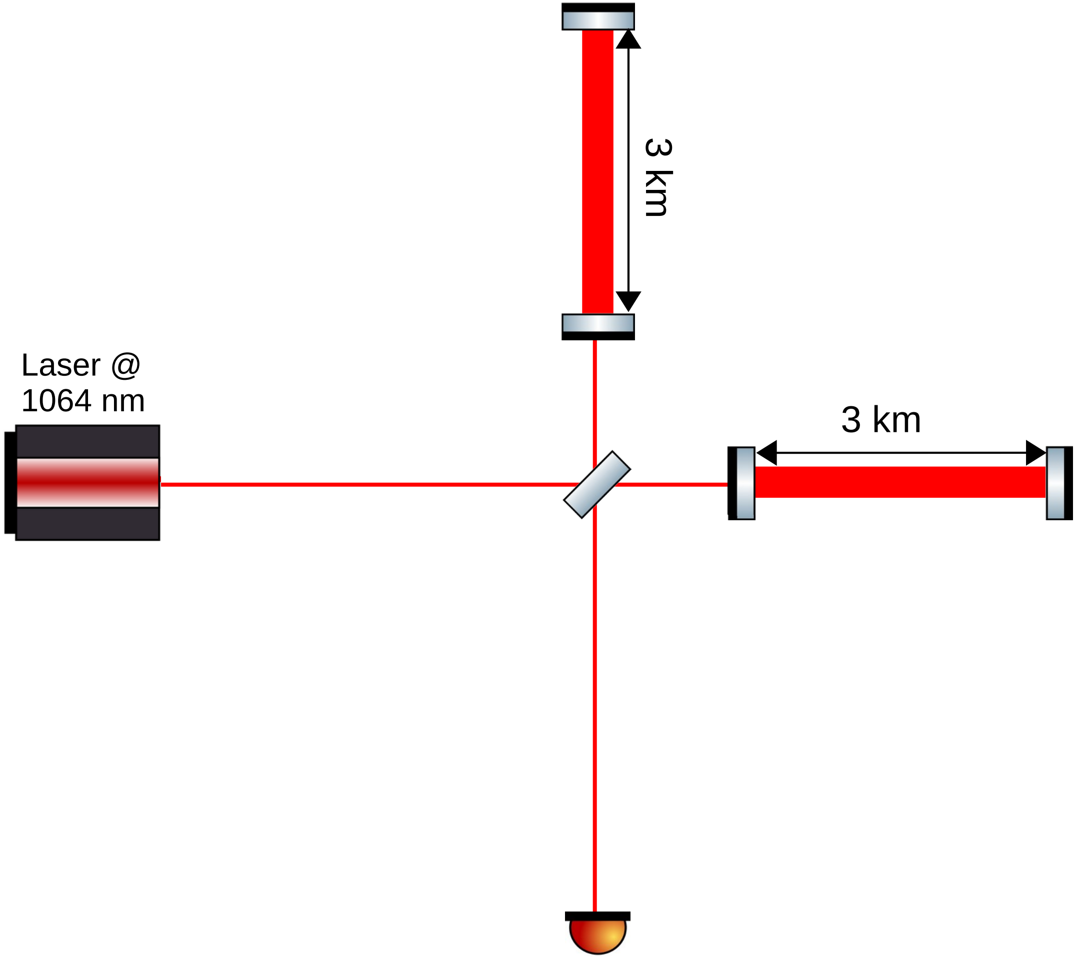

- **Suspended mirrors** to filter seismic noise
- **Whole system in vacuum (10^{-8} mbar)** to avoid the gases refractive index variation
- **Fabry-Perot cavities** to increase the effective length of the arms

Real interferometer

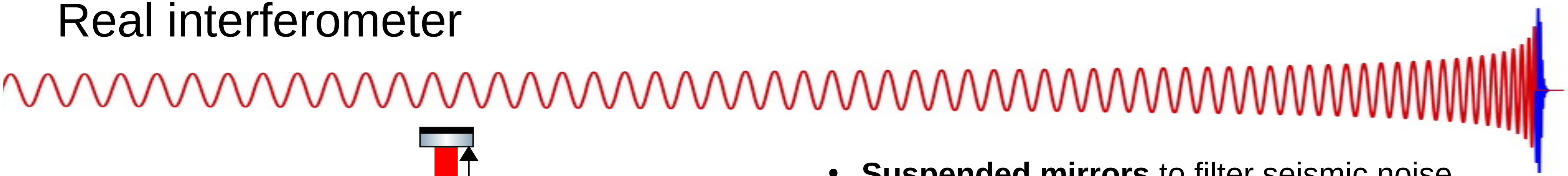

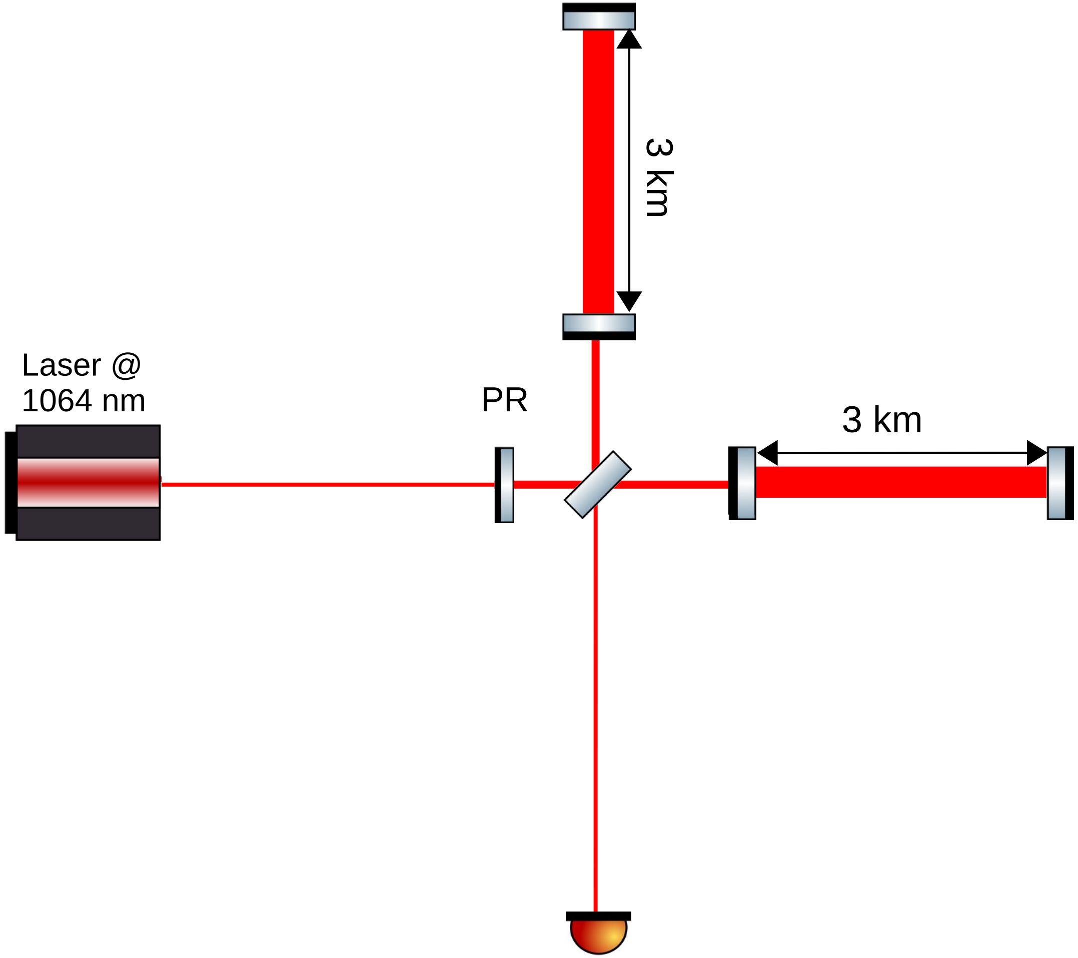

- **Suspended mirrors** to filter seismic noise
- **Whole system in vacuum (10^{-8} mbar)** to avoid the gases refractive index variation
- **Fabry-Perot cavities** to increase the effective length of the arms
- **Power Recycling mirror** to increase the power circulating in the interferometer

Real interferometer

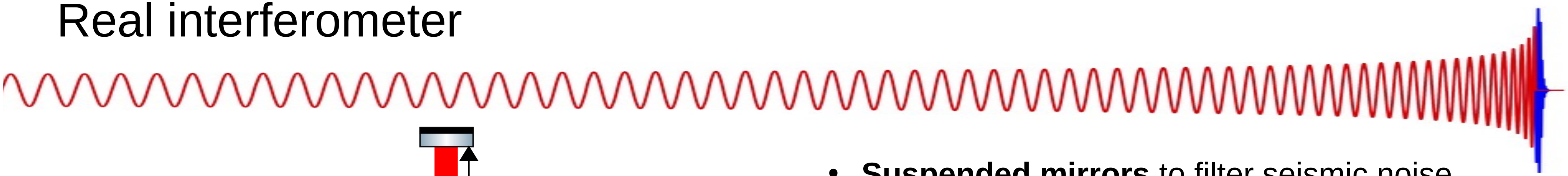

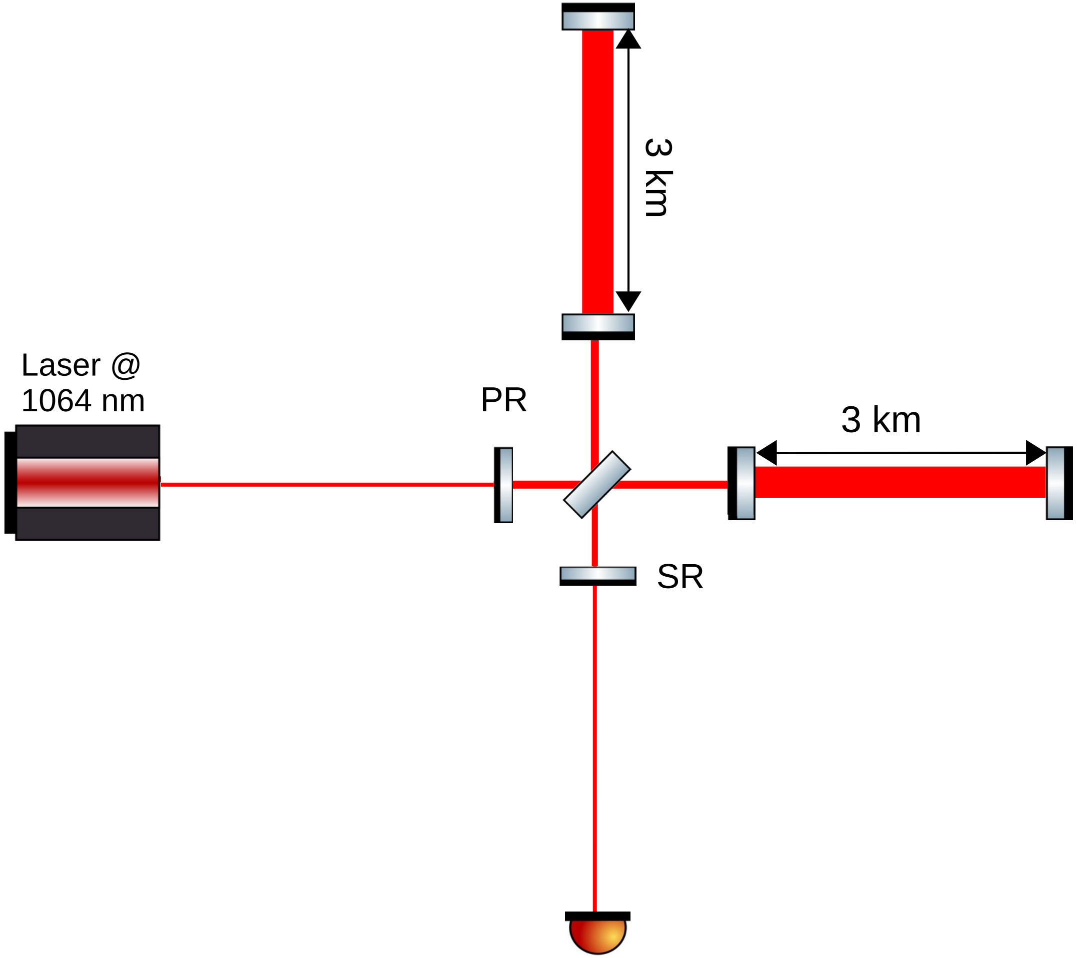

- **Suspended mirrors** to filter seismic noise
- **Whole system in vacuum (10^{-8} mbar)** to avoid the gases refractive index variation
- **Fabry-Perot cavities** to increase the effective length of the arms
- **Power Recycling mirror** to increase the power circulating in the interferometer
- **Signal Recycling mirror** to amplify the gravitational wave signal

Real interferometer

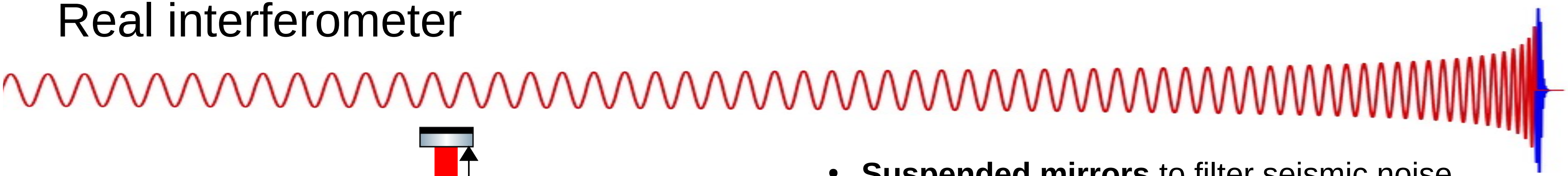

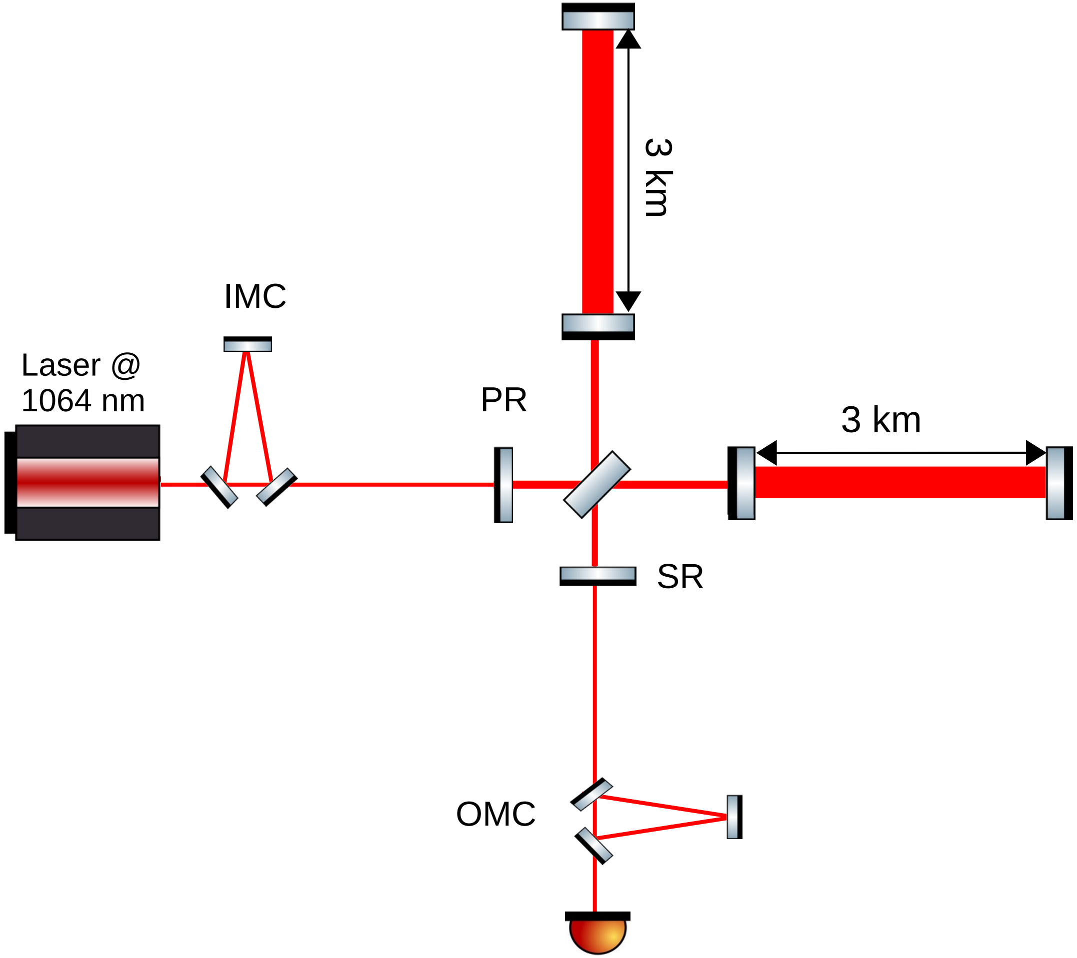

- **Suspended mirrors** to filter seismic noise
- **Whole system in vacuum (10^{-8} mbar)** to avoid the gases refractive index variation
- **Fabry-Perot cavities** to increase the effective length of the arms
- **Power Recycling mirror** to increase the power circulating in the interferometer
- **Signal Recycling mirror** to amplify the gravitational wave signal
- **Input and Output Mode Cleaner cavities** to filter the laser beam

Real interferometer

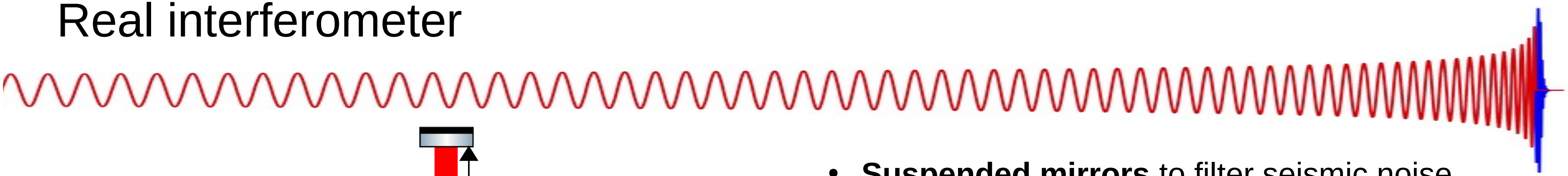

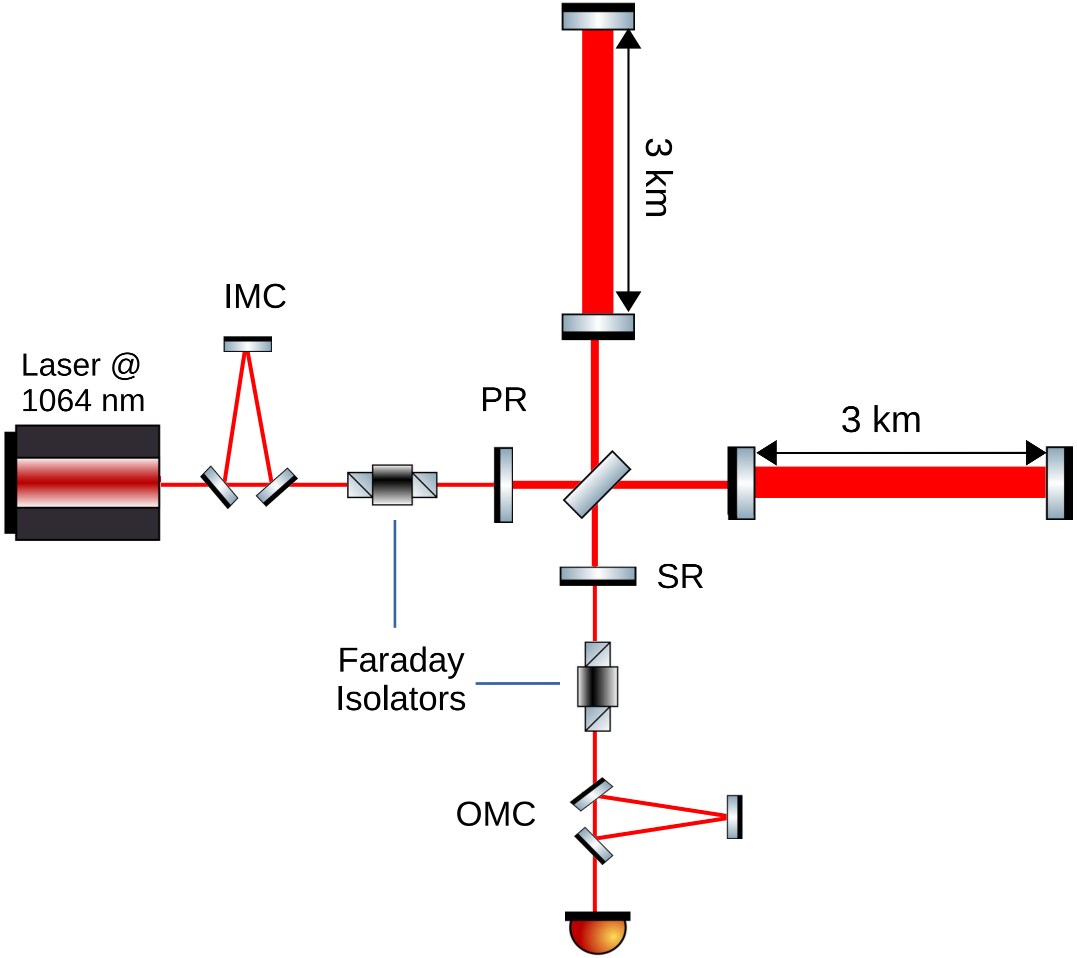

- **Suspended mirrors** to filter seismic noise
- **Whole system in vacuum (10^{-8} mbar)** to avoid the gases refractive index variation
- **Fabry-Perot cavities** to increase the effective length of the arms
- **Power Recycling mirror** to increase the power circulating in the interferometer
- **Signal Recycling mirror** to amplify the gravitational wave signal
- **Input and Output Mode Cleaner cavities** to filter the laser beam
- **Faraday Isolators** to attenuate back-reflected and back-scattered light

Noise sources

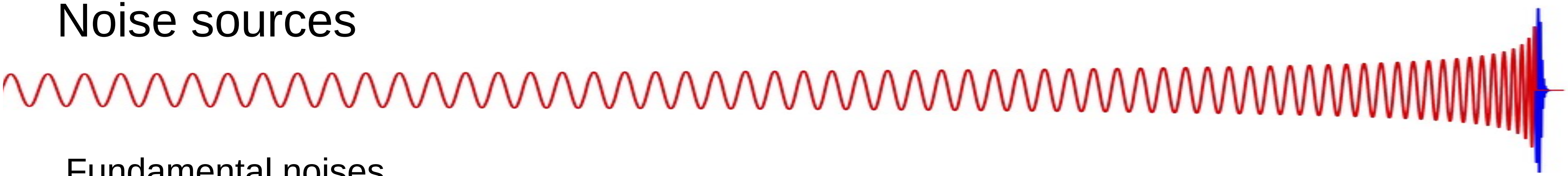

Fundamental noises

- Thermal noise
- Seismic noise
- Newtonian noise
- Quantum noise

Technical noises

- Scattered light noise
- Electronic noise
- Control noise
- …

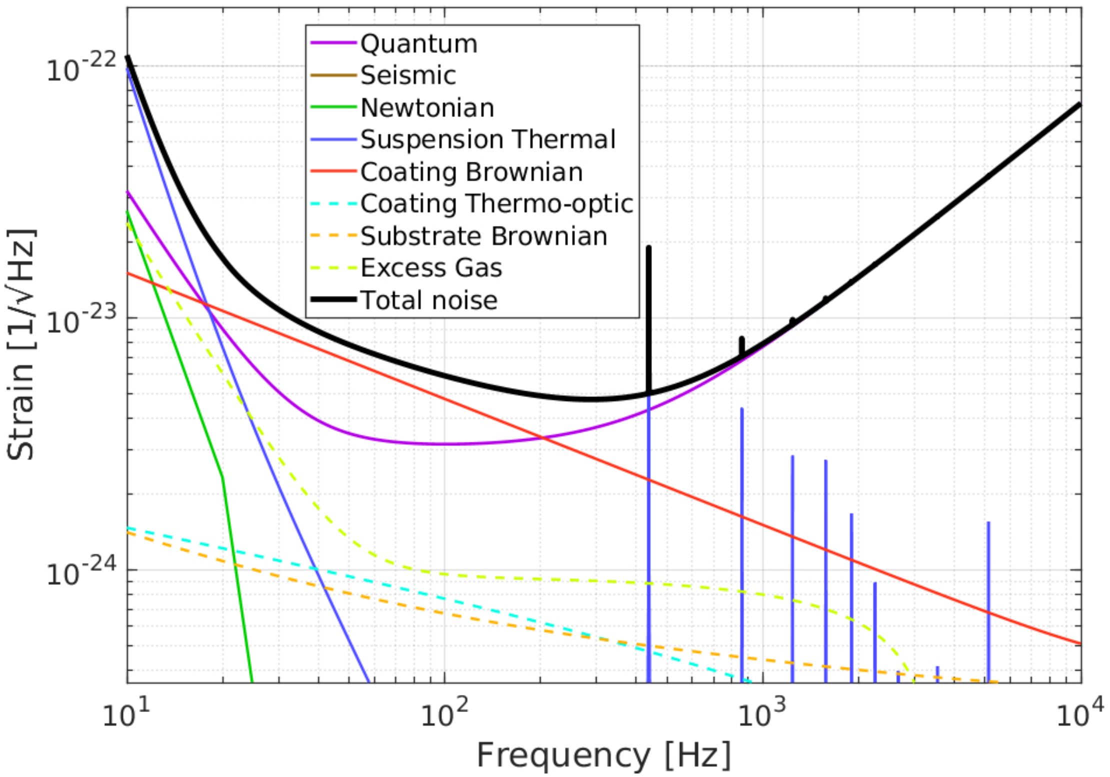

Noise sources

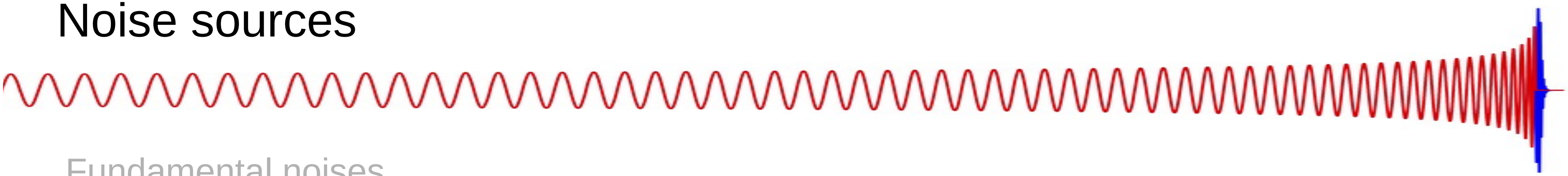

Fundamental noises

- Thermal noise
- Seismic noise
- Newtonian noise
- Quantum noise

Technical noises

- Scattered light noise
- Electronic noise
- Control noise
- …

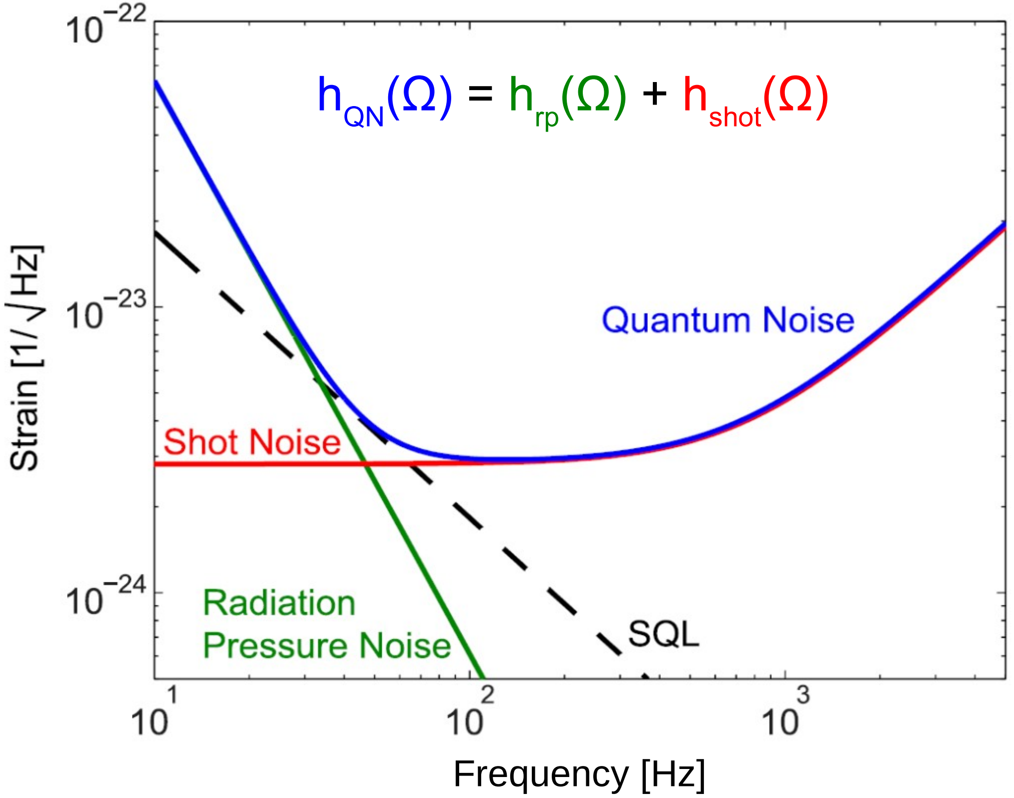

Outline

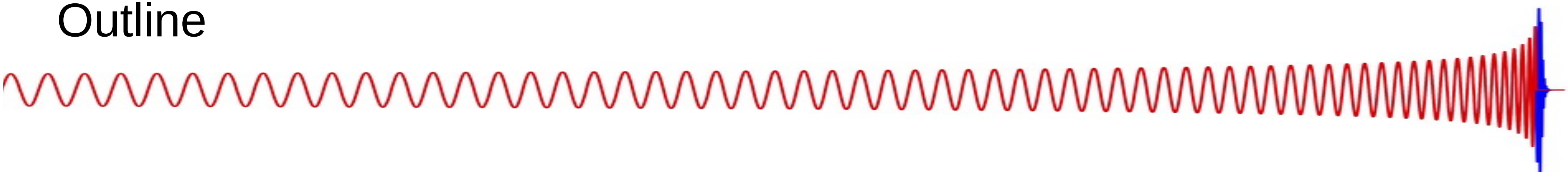

1. Gravitational waves: origin & detection
2. Quantum noise: origin & reduction strategy
3. The Virgo detector from the observing run O3 to O4
4. Frequency dependent squeezing system: installation and commissioning
5. Low loss Output Mode Cleaner: characterization, installation and commissioning
6. Scattered light noise: study and mitigation
7. Conclusions and next steps

Quantum nature of light

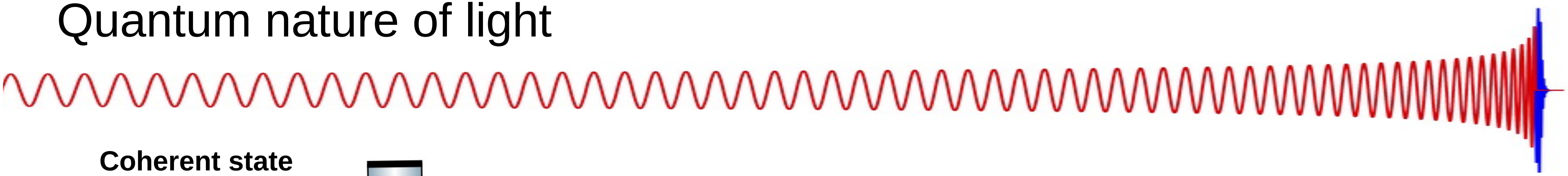

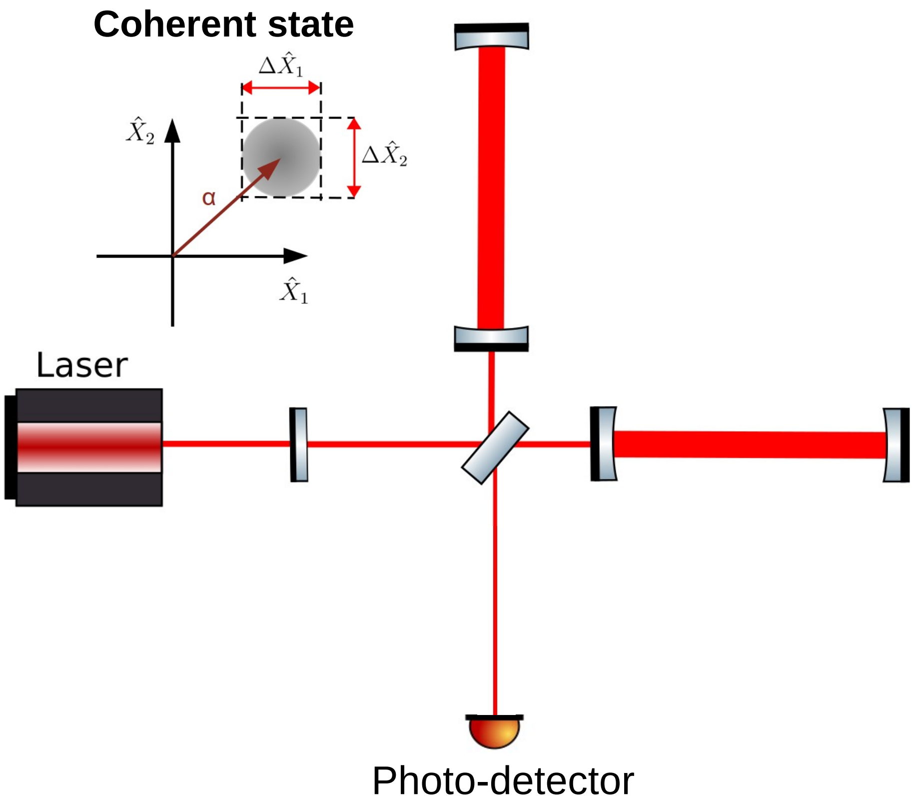

The laser field in the quantum formalism is

$$\hat{E}(t) = 2E_0\left[\left(\hat{X}_1 + \Delta\hat{X}_1\right)\cos(\omega t) + \left(\hat{X}_2 + \Delta\hat{X}_2\right)\sin(\omega t)\right]$$

Amplitude operator — Amplitude fluctuations — Phase operator — Phase fluctuations

Coherent states are **minimum uncertainty states**, i.e. their fluctuations according to Heisenberg Uncertainty Principle are:

$$\left(\Delta\hat{X}_1\right)^2\left(\Delta\hat{X}_2\right)^2 = \frac{1}{16}$$

Origin of quantum noise

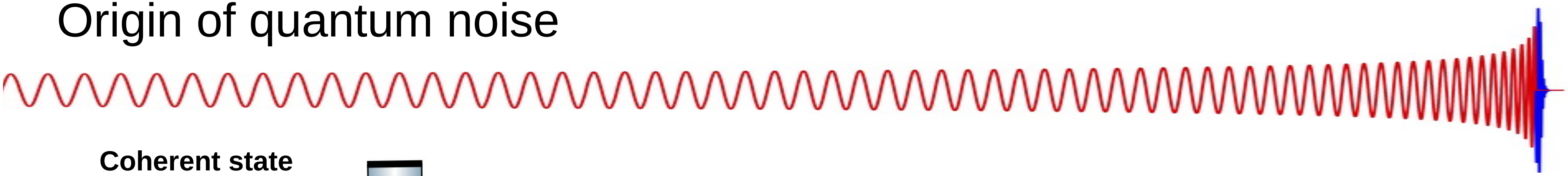

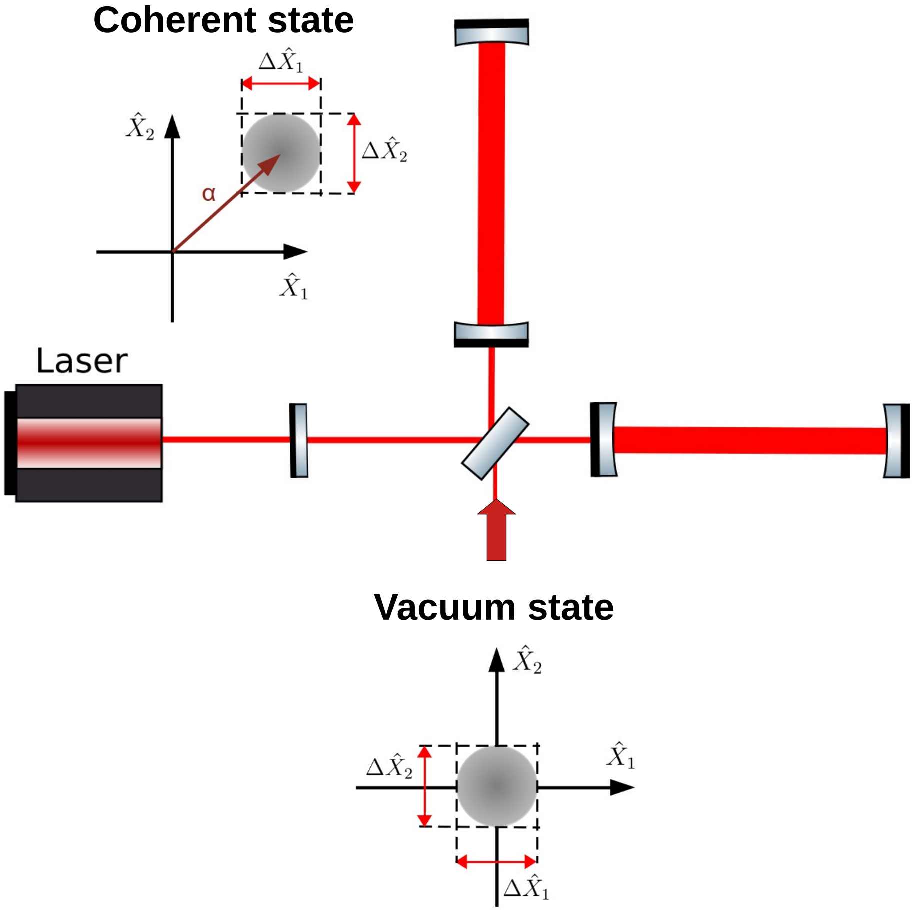

Quantum noise arises from **vacuum fluctuations** entering the output port of the detector.

Amplitude fluctuations (ΔX_1) accounts as **radiation pressure noise**.

Phase fluctuations (ΔX_2) accounts as **shot noise**.

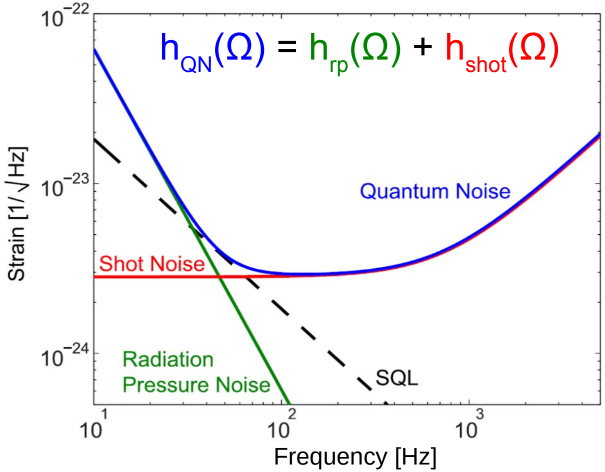

Quantum noise reduction

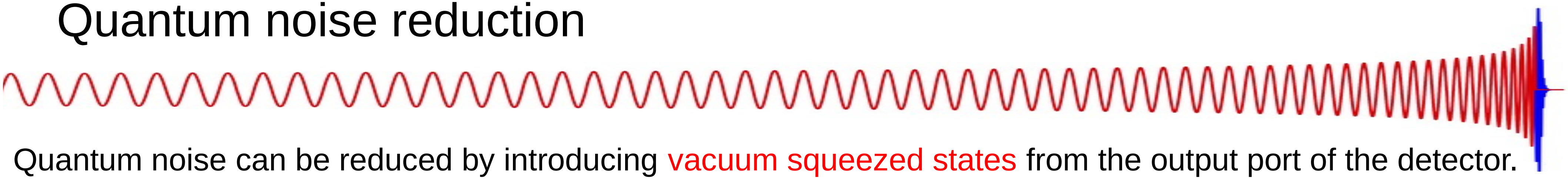

Quantum noise can be reduced by introducing vacuum squeezed states from the output port of the detector.

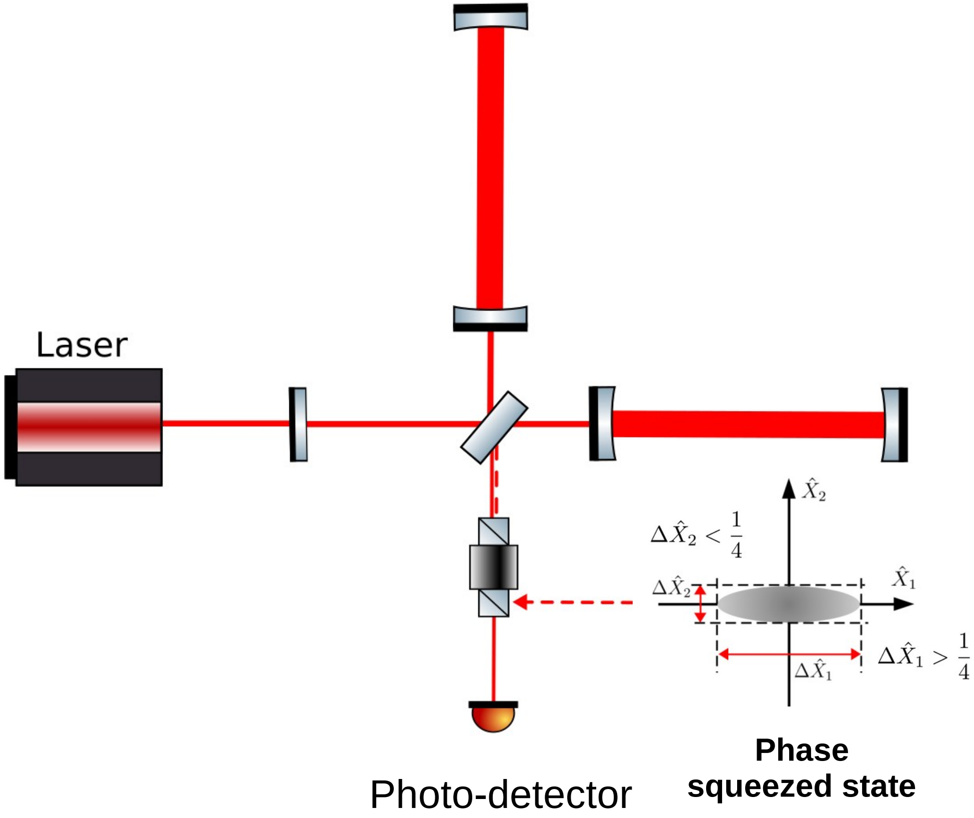

Squeezed states are minimum uncertainty states whose fluctuations are reduced in one direction and increased in the other with respect to the vacuum states.

Vacuum squeezed states at the generic angle ϑ:

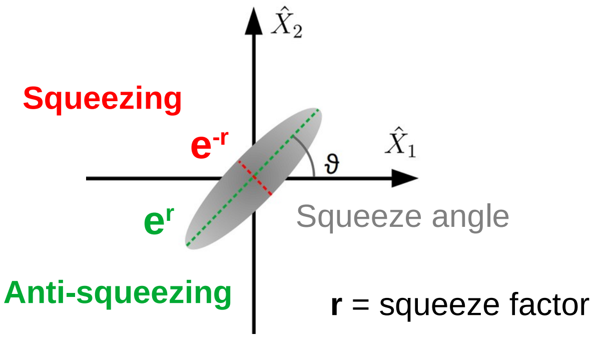

Quantum noise reduction

Vacuum squeezed states have been injected in the GW detectors during the observing run O3.

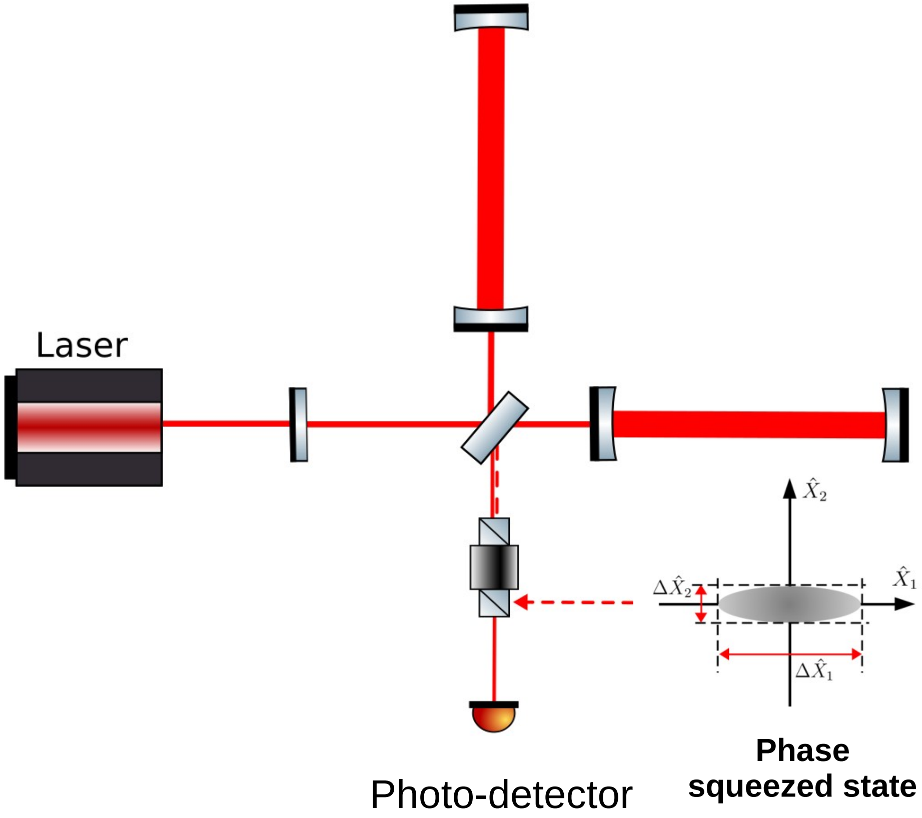

Frequency independent squeezing (FIS):

- Reduced the quantum noise at high frequency
- Increased the quantum noise at low frequency

$$h_{FIS}(\Omega) = h_{rp}(\Omega) \cdot e^{r} + h_{shot}(\Omega) \cdot e^{-r}$$

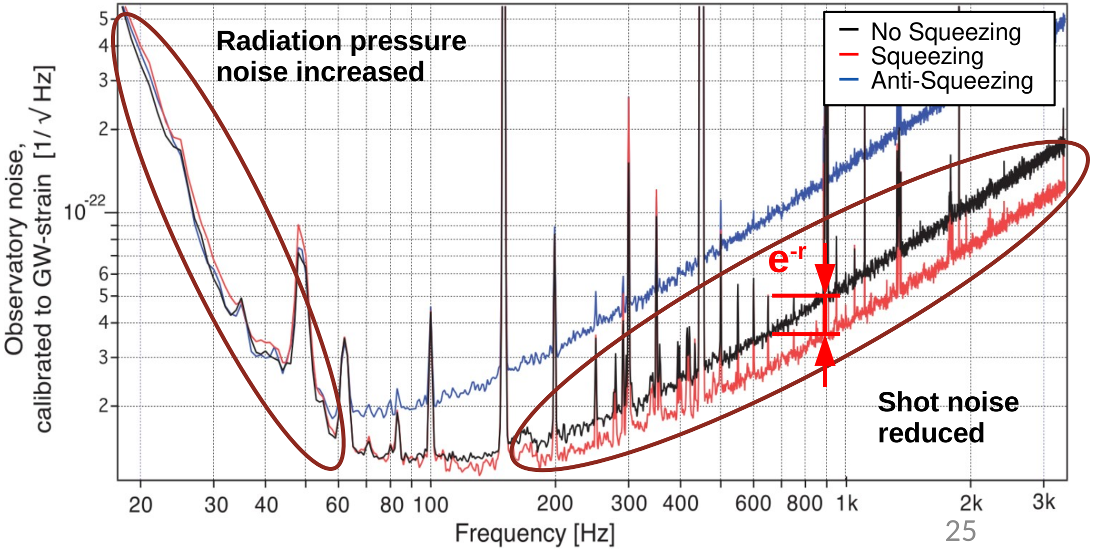

Quantum noise broadband reduction

Frequency dependent squeezing (FDS) allows a broadband quantum noise reduction.

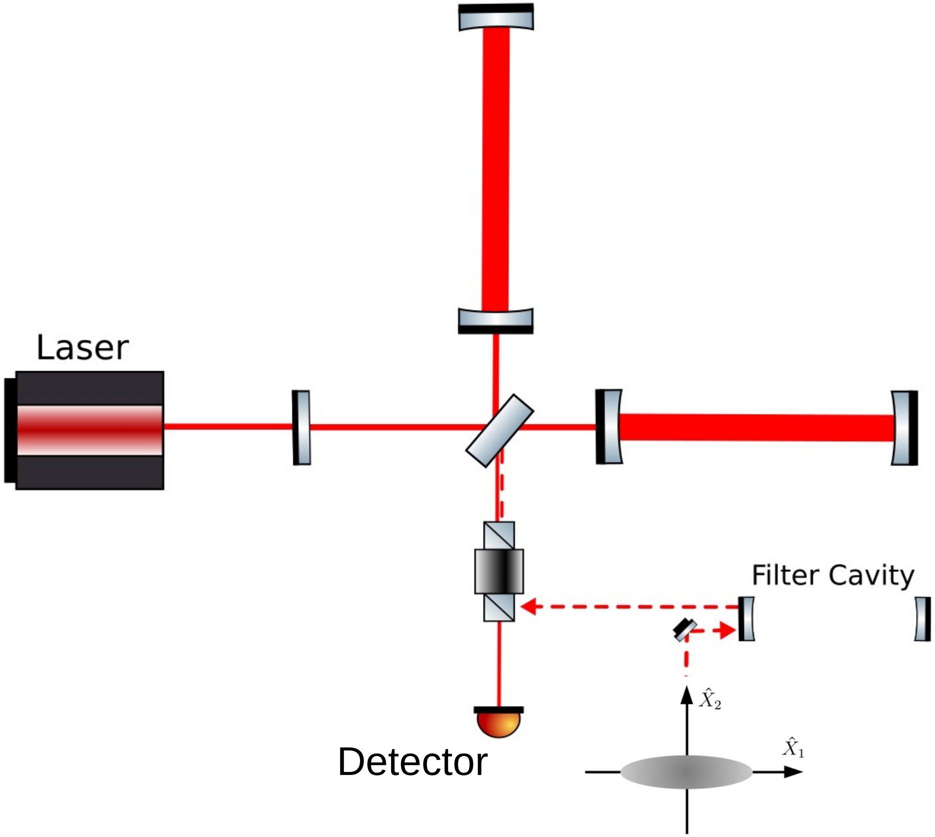

$$h_{FDS}(\Omega) = [h_{shot}(\Omega) + h_{rp}(\Omega)] \cdot e^{-r}$$

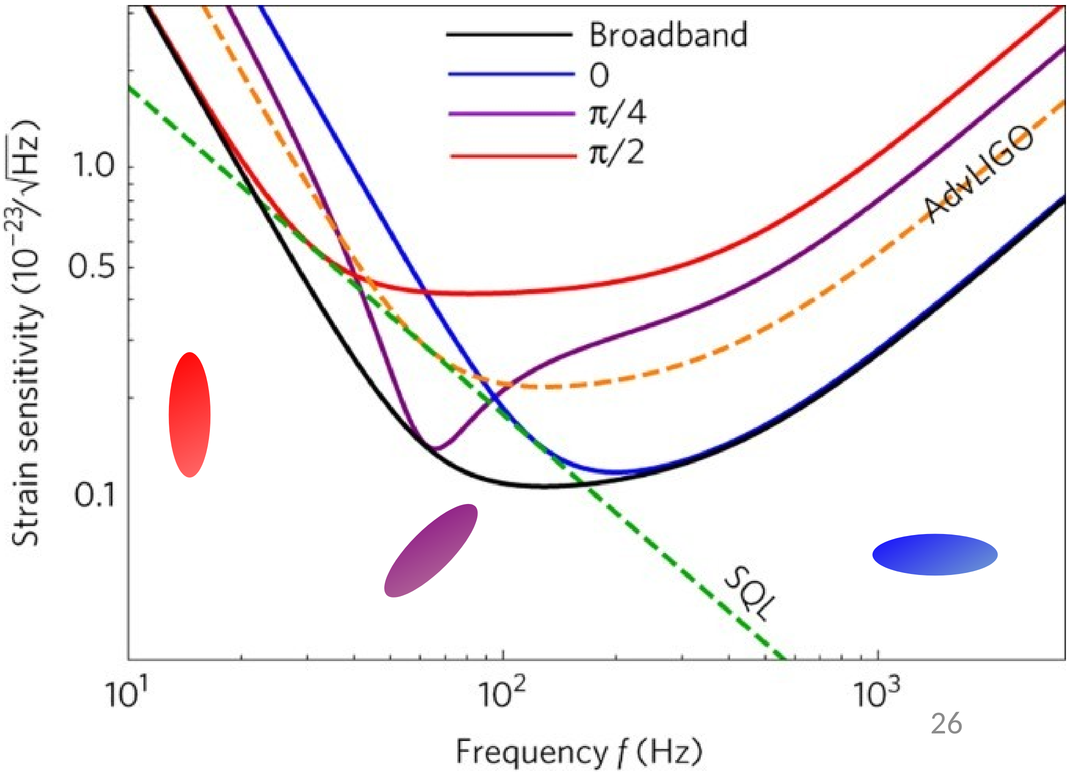

Quantum noise broadband reduction

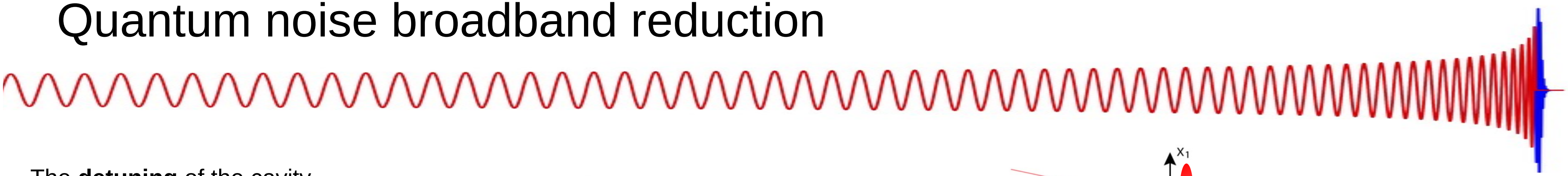

The **detuning** of the cavity $\Delta\omega_{fc}$ needs to be equal to the frequency Ω where

$$\mathbf{h_{shot}(\Omega) = h_{rp}(\Omega)}$$

↓

Frequency Dependent Squeezing @ $\Omega = \Delta\omega_{fc}$

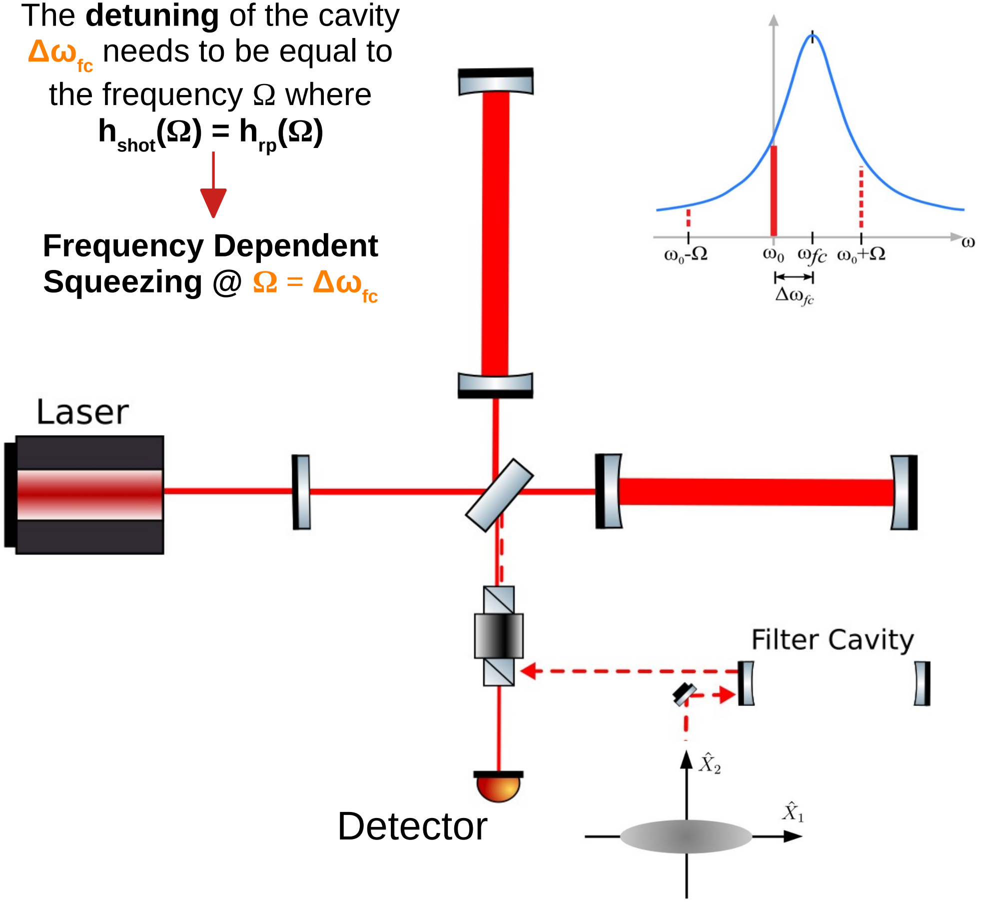

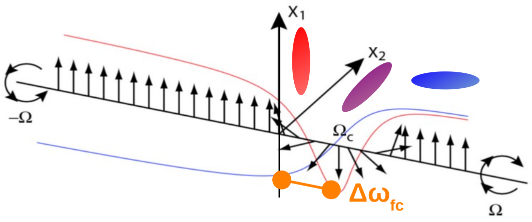

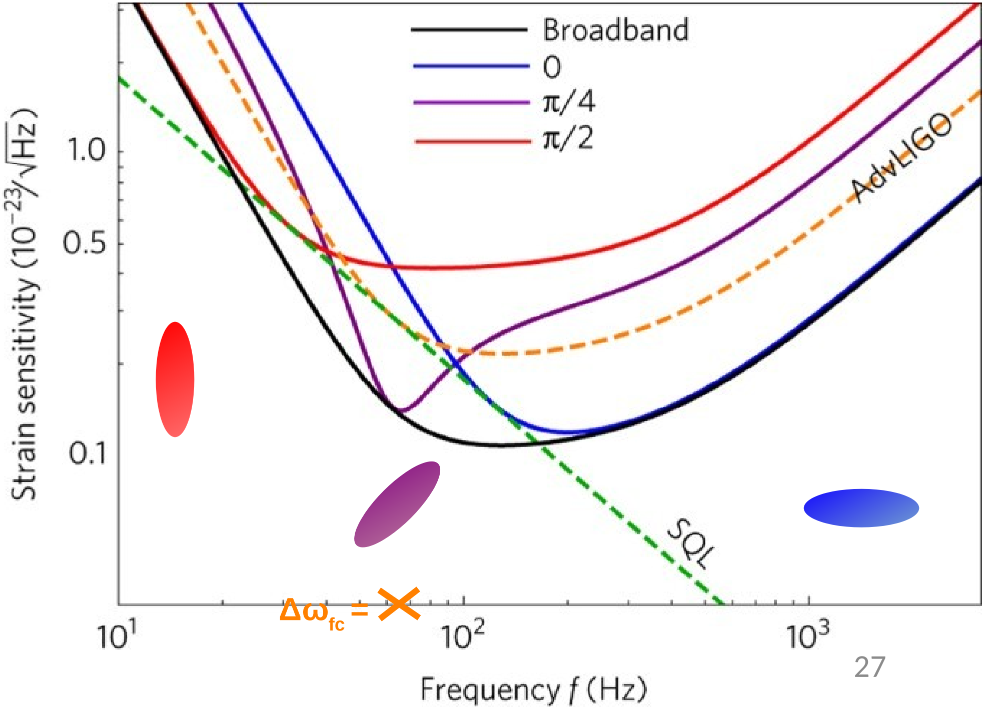

Squeezing degradation mechanisms

- **Optical losses** can be modeled as a recombination of the squeezing with a vacuum state inside a beam splitter, resulting in a reduction of the squeezing level.

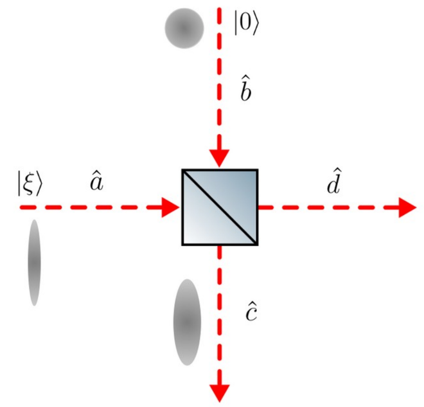

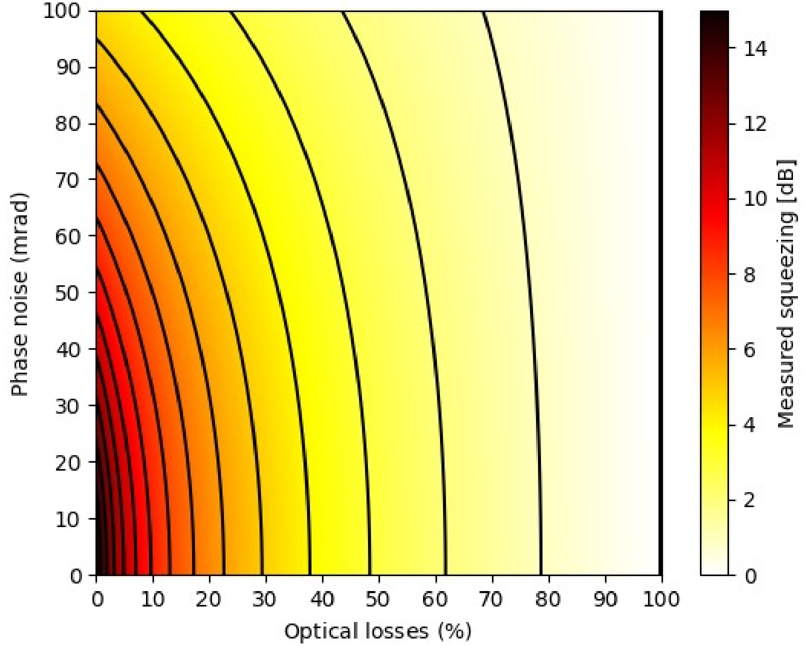

- **Phase noise** mixes the fluctuations in the two quadrature degrading the measured squeezing level.

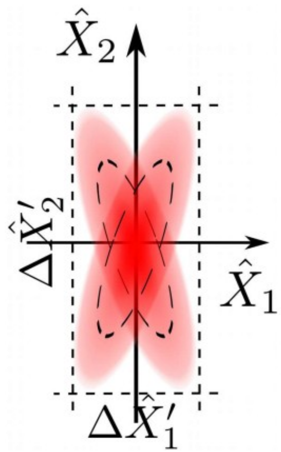

Squeezing degradation mechanisms

- **Optical losses** can be modeled as a recombination of the squeezing with a vacuum state inside a beam splitter, resulting in a reduction of the squeezing level.

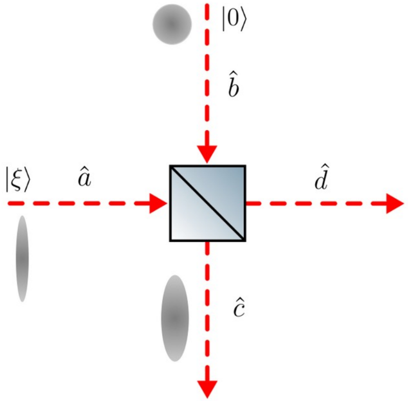

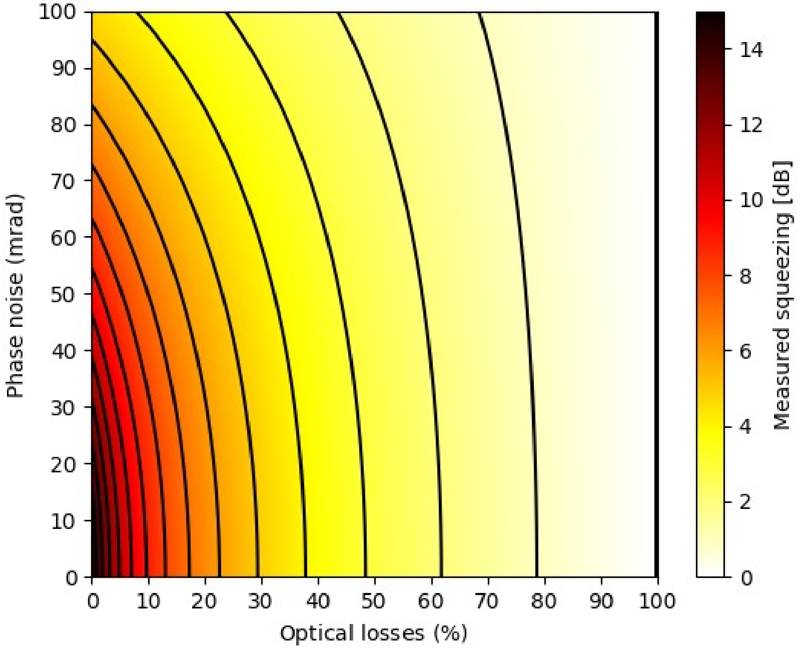

- **Phase noise** mixes the fluctuations in the two quadrature degrading the measured squeezing level.

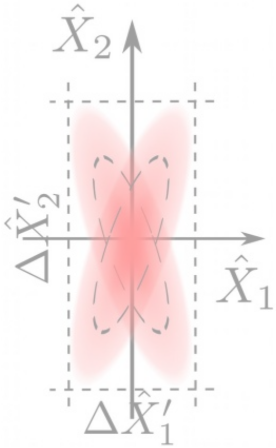

Outline

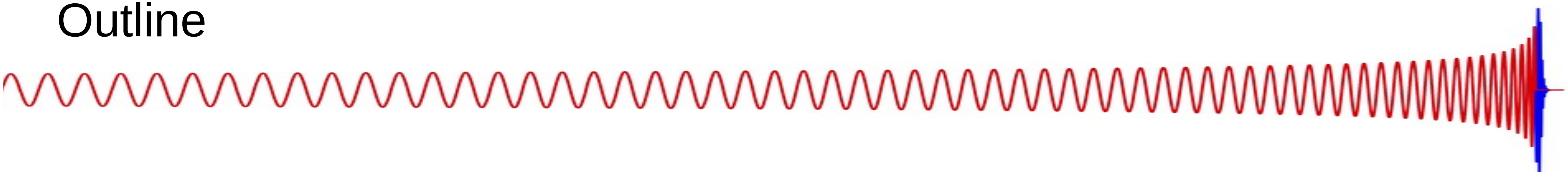

1. Gravitational waves: origin & detection
2. Quantum noise: origin & reduction strategy
3. The Virgo detector from the observing run O3 to O4
4. Frequency dependent squeezing system: installation and commissioning
5. Low loss Output Mode Cleaner: characterization, installation and commissioning
6. Scattered light noise: study and mitigation
7. Conclusions and next steps

Virgo upgrades between O3 and O4

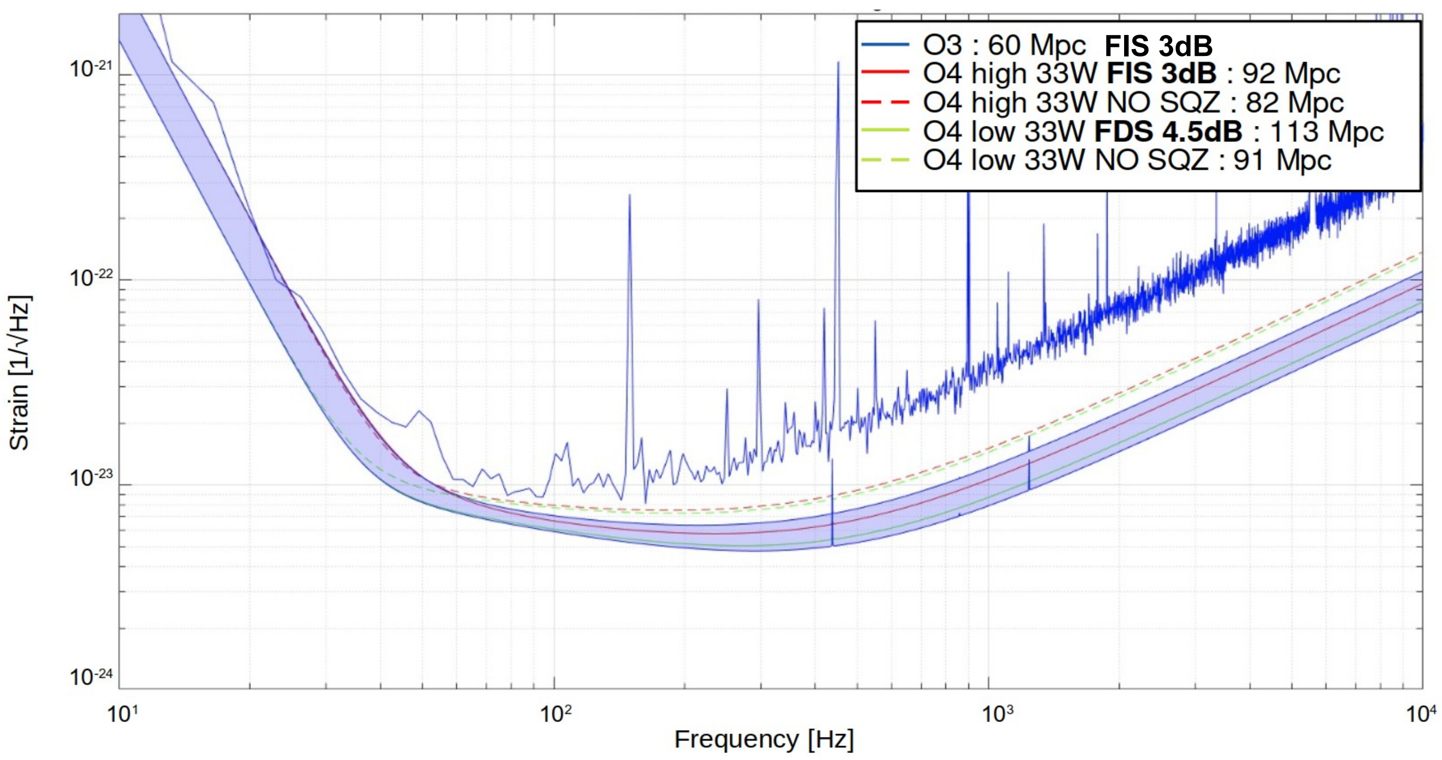

Main upgrades:

- Increase of laser power from 25W to 33W
- Signal Recycling
- Frequency Dependent Squeezing @ Ω = 25Hz

Other improvements:

- Low loss high finesse Output Mode Cleaner
- Scattered light mitigation

My main contributions

- Scattered light noise study and mitigation

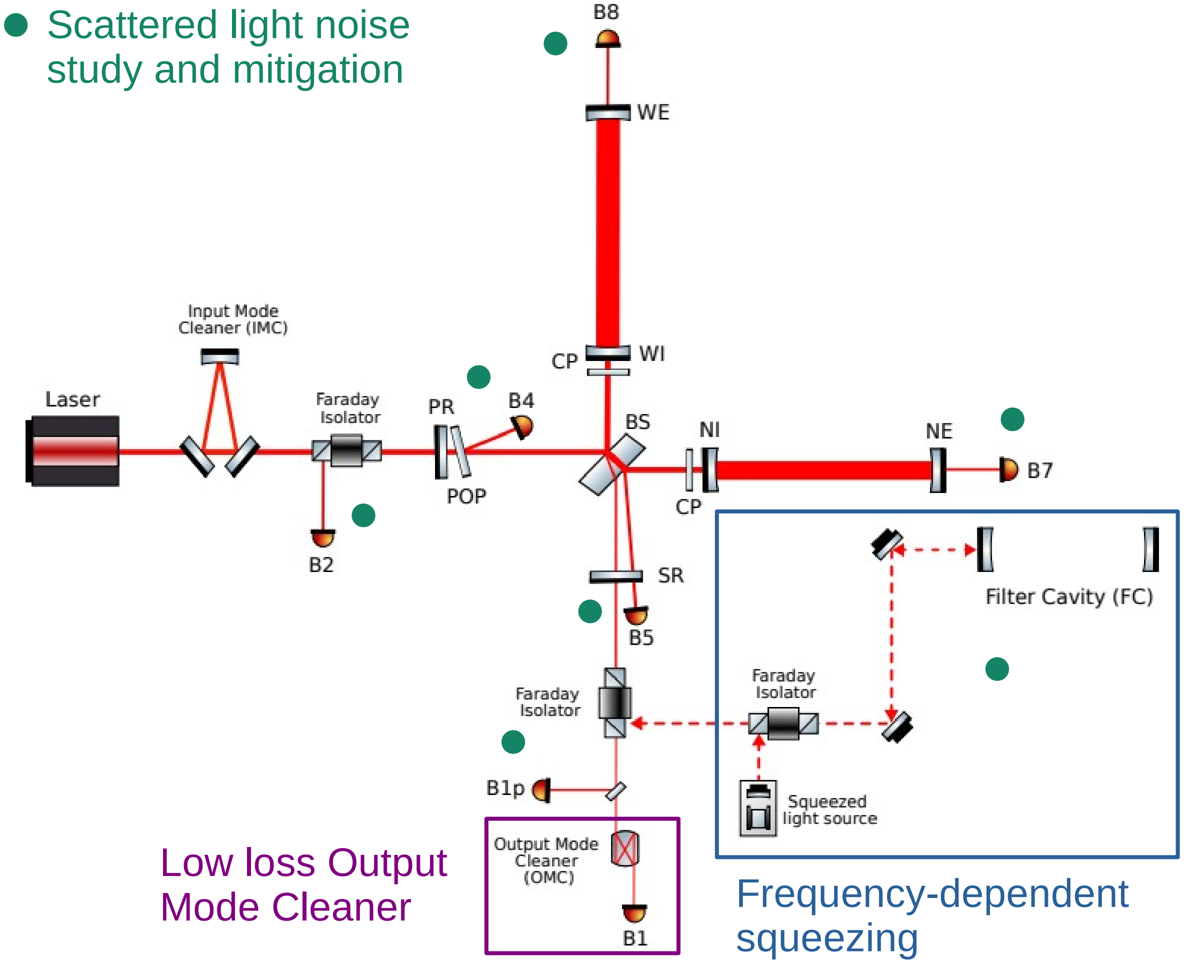

Low loss Output Mode Cleaner

Frequency-dependent squeezing

Frequency dependent squeezing implementation:

- Higher reduction of shot noise
- Reduction of radiation pressure noise

Optical losses reduction:

- New low loss output mode cleaner

Scattered light noise reduction:

- Study and mitigation of scattered light on optical benches
- Measurement of scattered light with an optical set-up at LAPP

Outline

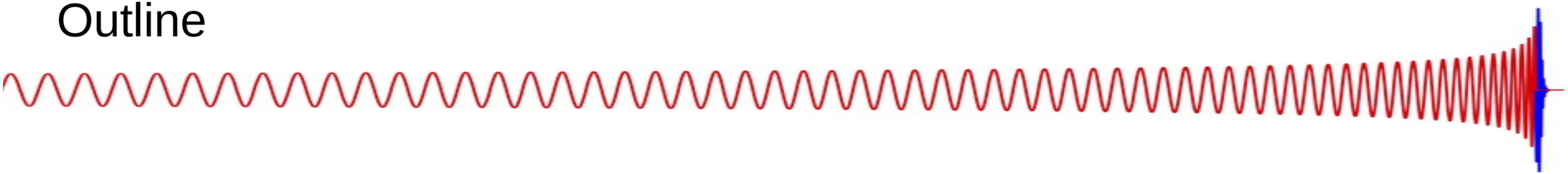

1. Gravitational waves: origin & detection
2. Quantum noise: origin & reduction strategy
3. The Virgo detector from the observing run O3 to O4
4. Frequency dependent squeezing system: installation and commissioning
5. Low loss Output Mode Cleaner: characterization, installation and commissioning
6. Scattered light noise: study and mitigation
7. Conclusions and next steps

FDS system implemented in AdV+

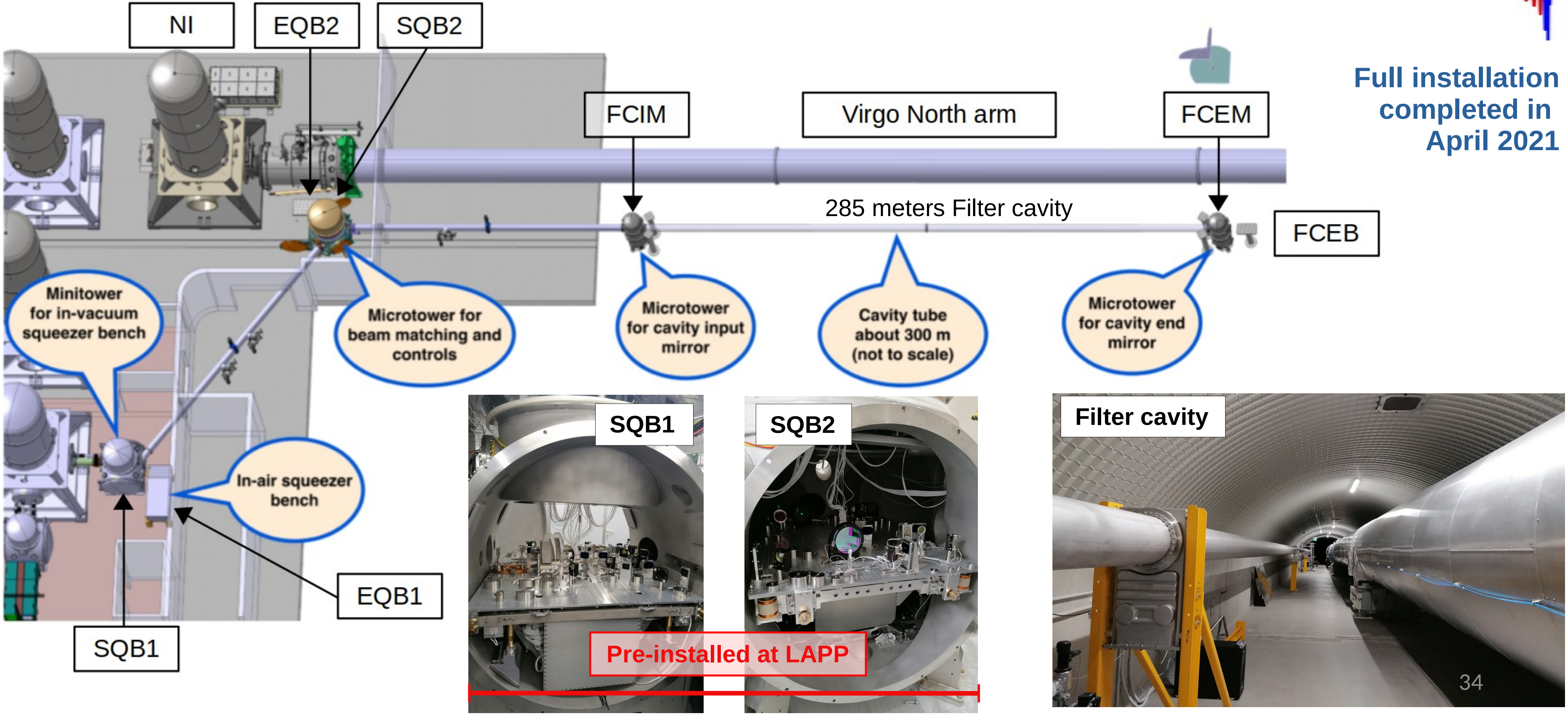

Full installation completed in April 2021

FDS system overview

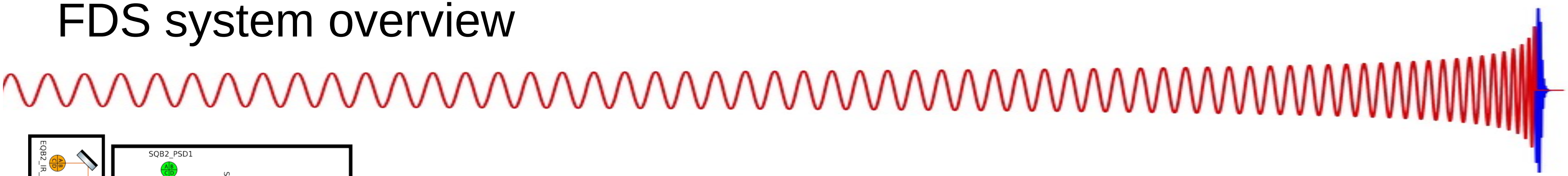

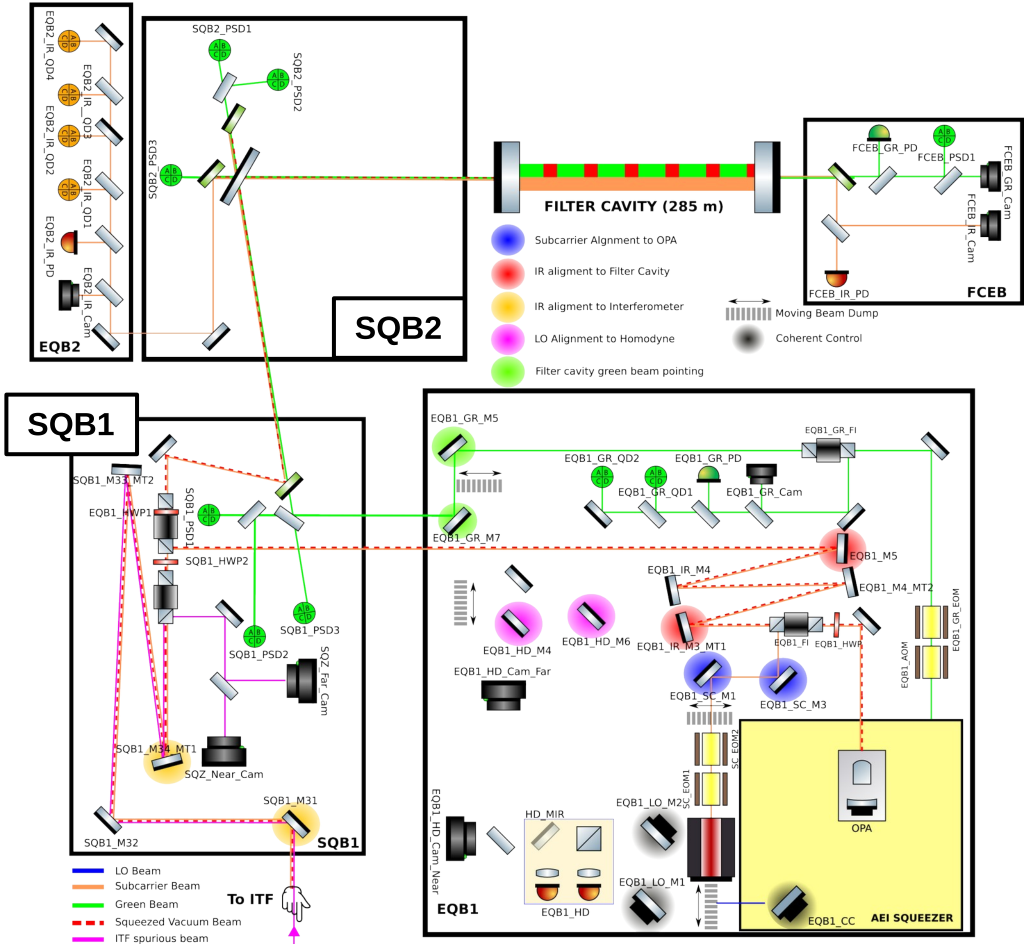

Squeezed Vacuum Beam

Sub-carrier beam: to align the IR beam and to control the filter cavity

Local Oscillator (LO) beam: to perform squeezing measurement

Green beam: control and automatic alignment of the filter cavity, control of suspended benches

ITF spurious beam: to overlap the squeezed beam with the ITF beam:

- alignment (beam tilt and shift)
- mode matching (beam parameters)

FDS system timeline

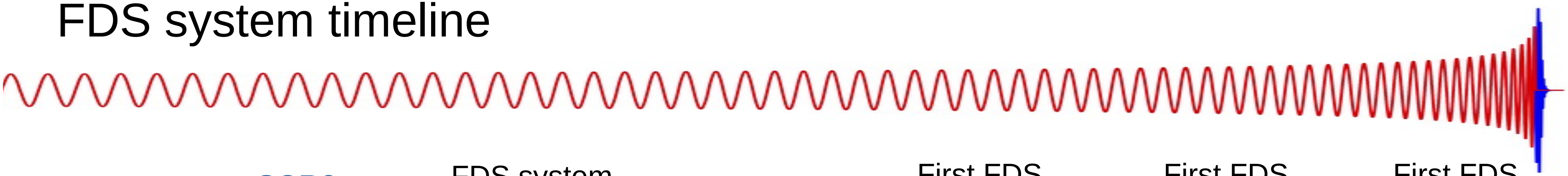

- **SQB1** at LAPP and on site — Jan 2021
- **SQB2** at LAPP and on site — April 2021
- FDS system aligned and FC locked on green — June 2021
- FC locked on IR — Oct 2021
- First FDS demonstration detuning ~300Hz — Nov 2021
- First FDS measurement beating the shot noise — Feb 2022
- First FDS measurement at 25 Hz — June 2022

FDS system timeline

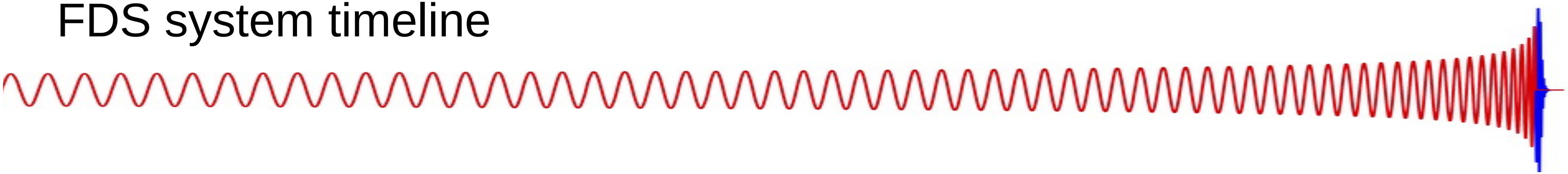

- **Jan 2021** — **SQB1** at LAPP and on site
- **April 2021** — **SQB2** at LAPP and on site
- **June 2021** — FDS system aligned and FC locked on green
- **Oct 2021** — FC locked on IR
- **Nov 2021** — First FDS demonstration detuning ~300Hz
- **Feb 2022** — First FDS measurement beating the shot noise
- **June 2022** — First FDS measurement at 25 Hz

Pre-installation of suspended benches at LAPP

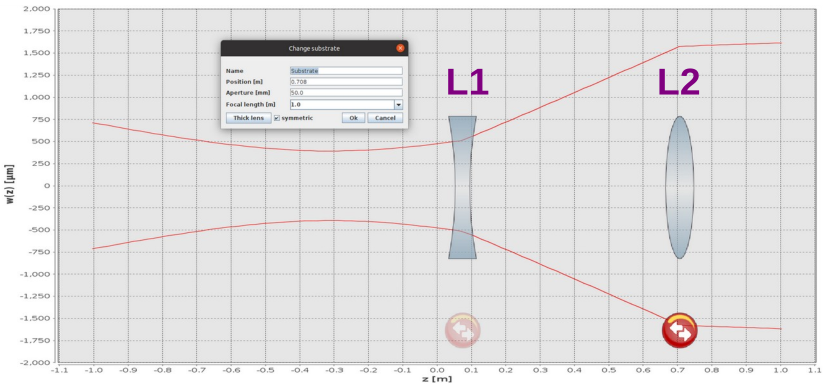

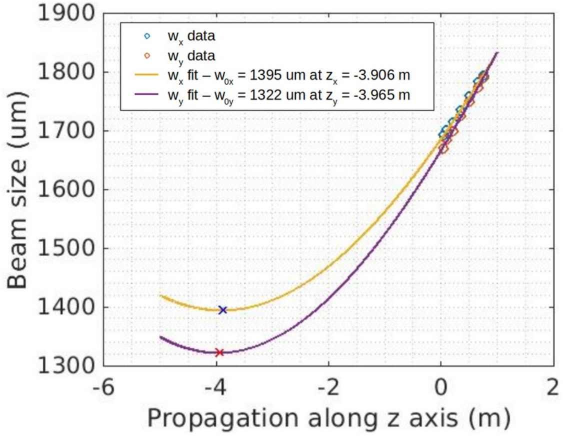

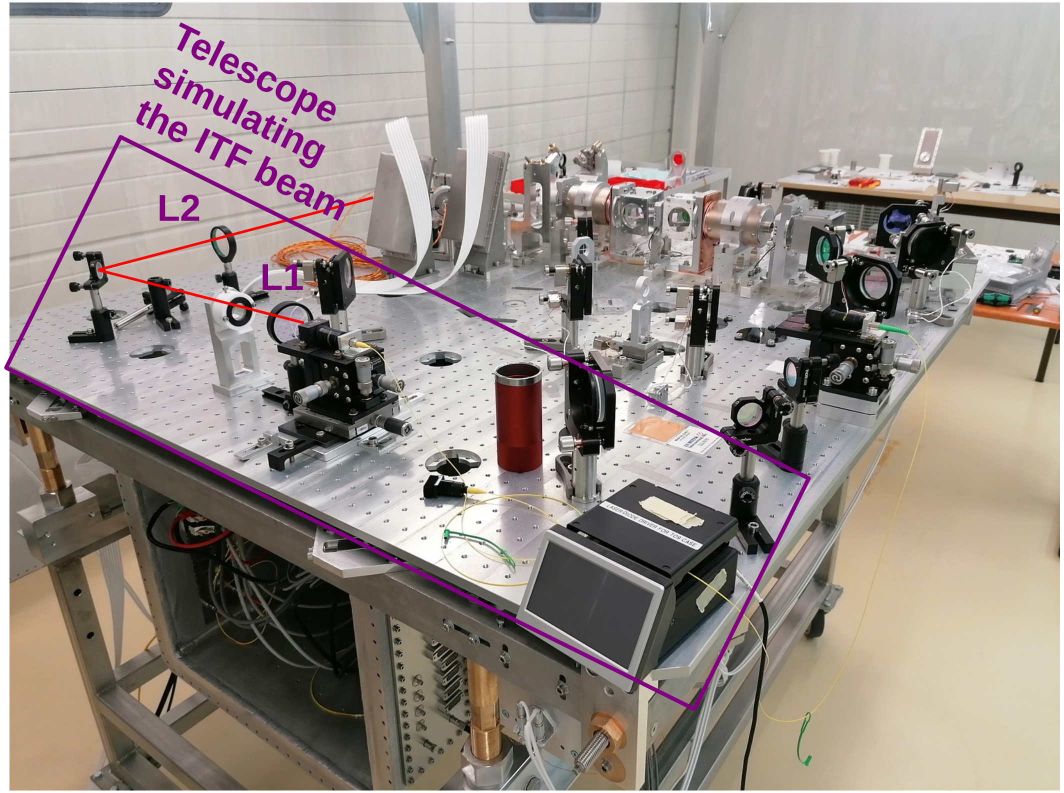

Commissioning of suspended benches on site

Suspension

Vacuum chamber

Bench

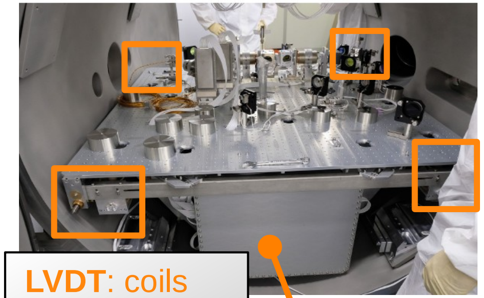

LVDT: coils for angular bench control

Electronics

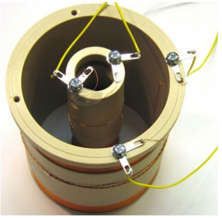

Angular dofs: controlled with LVDTs on the bench and the frame

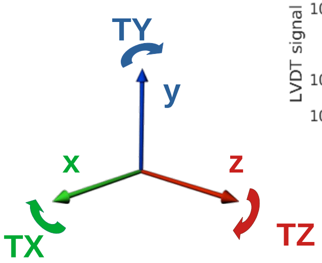

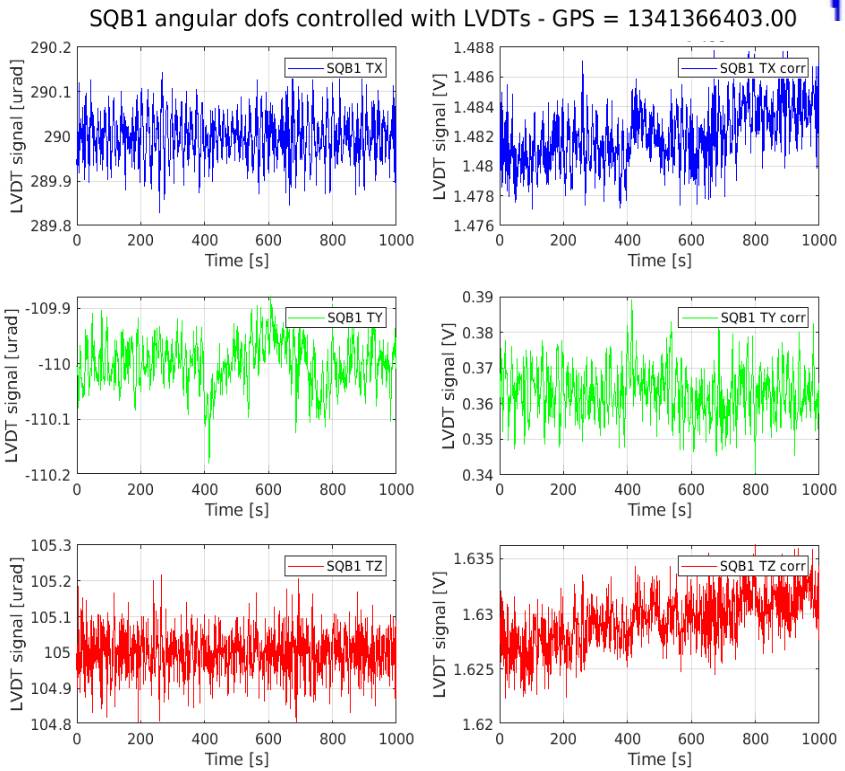

Residual angular noise < 2 urad rms
Residual longitudinal noise < 10 um rms

FDS system timeline

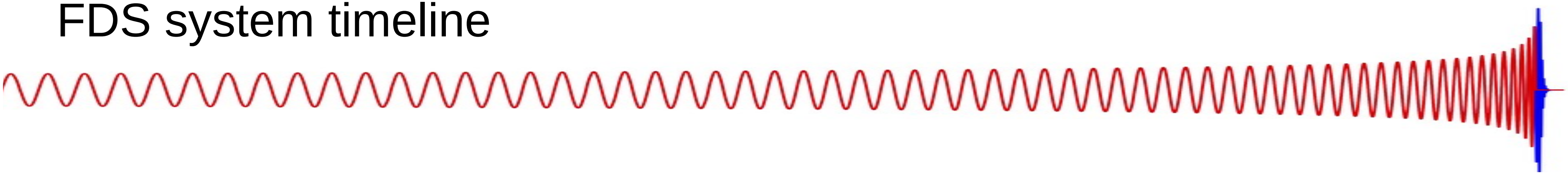

- **Jan 2021** — **SQB1** at LAPP and on site
- **April 2021** — **SQB2** at LAPP and on site
- **June 2021** — FDS system aligned and FC locked on green
- **Oct 2021** — FC locked on IR
- **Nov 2021** — First FDS demonstration detuning ~300Hz
- **Feb 2022** — First FDS measurement beating the shot noise
- **June 2022** — First FDS measurement at 25 Hz

Position Sensor Devices to control the suspended benches

Alternative strategy to control the suspended benches: to sense the bench angular degrees of freedom with respect to the beam rather than to the LVDTs referred to ground

- ✓ Test, installation and alignment

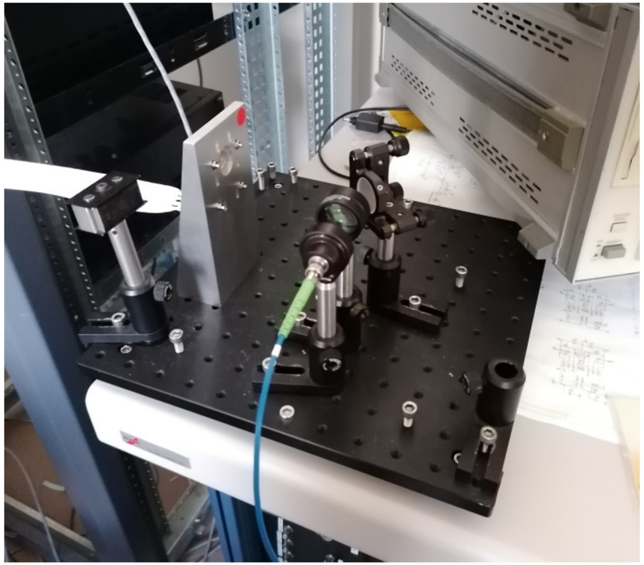

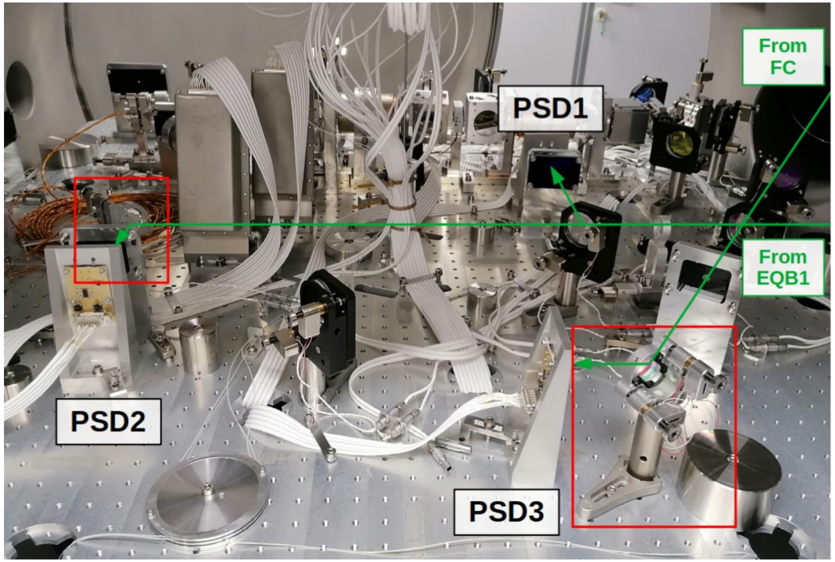

Position Sensor Devices to control the suspended benches

✓ Angular dofs reconstructed from the PSDs signal

1. Bench displacements (in TX, TY, TZ) → coefficient matrix M_c
2. Sensing matrix ($M_s = M_c^{-1}$) → $\overrightarrow{dof} = M_s \cdot \overrightarrow{PSD}$

Sensing with:

LVDTs

PSDs: sensing matrix M_A

PSDs: sensing matrices M_B and M_C

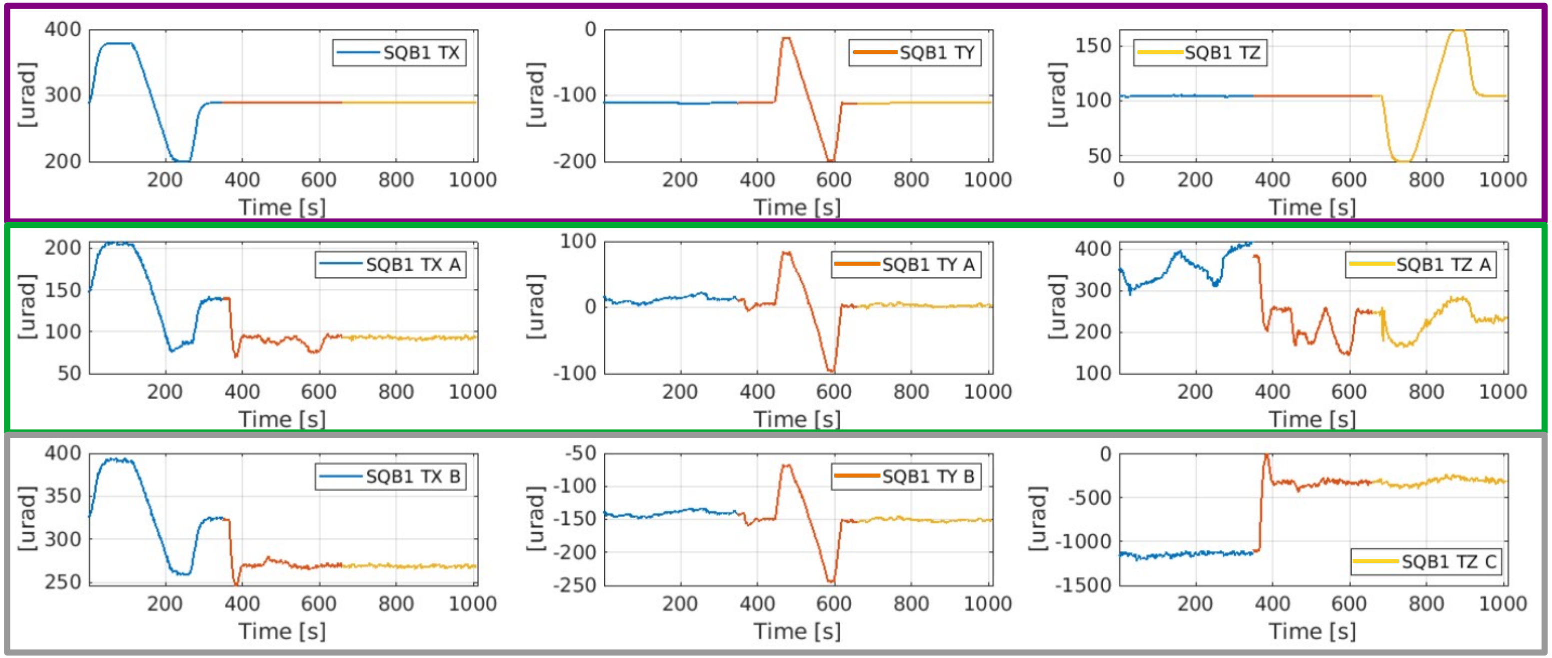

Position Sensor Devices to control the suspended benches

✓ Suspended benches angular sensing with LVDT + PSD and correction on LVDTs

SQB1 TX sensing (LVDT +PSD) and correction (LVDT)

PSD vertical and horizontal signals

Seismometer near SQB1 signals

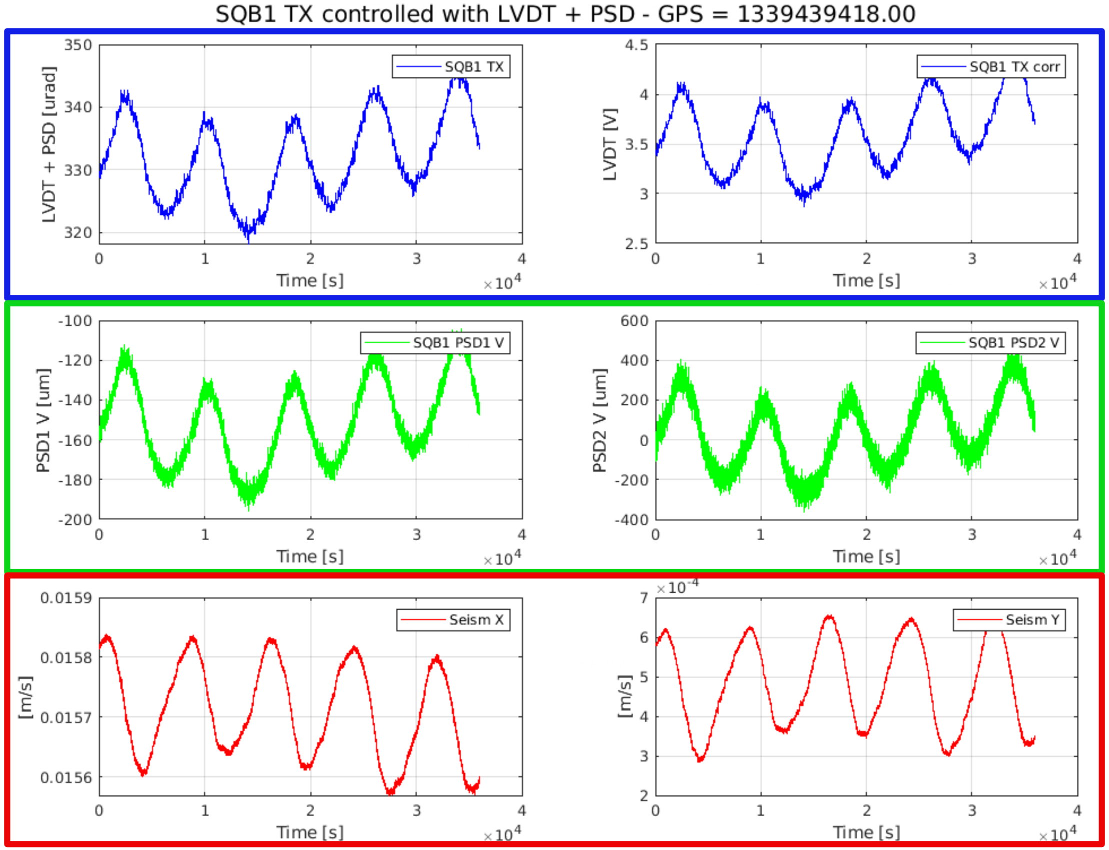

FDS system timeline

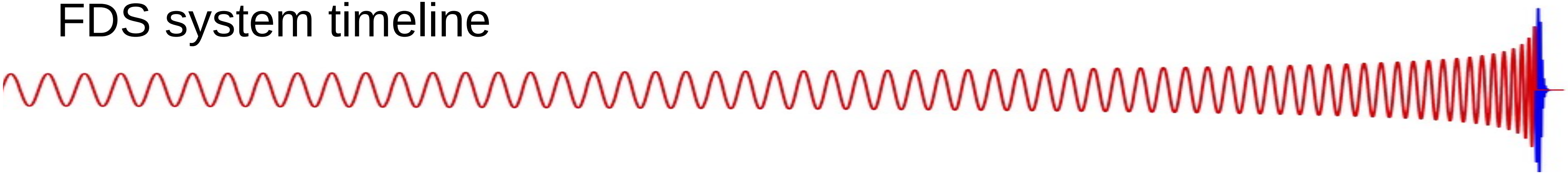

SQB1 at LAPP and on site	SQB2 at LAPP and on site	FDS system aligned and FC locked on green	FC locked on IR	First FDS demonstration detuning ~300Hz	First FDS measurement beating the shot noise	First FDS measurement at 25 Hz
Jan 2021	April 2021	June 2021	Oct 2021	Nov 2021	Feb 2022	June 2022

Homodyne detection principle

The **homodyne detection** cancels the photodiodes common classical noises through the interference of two beams: the Local Oscillator (LO) beam and the detected beam.

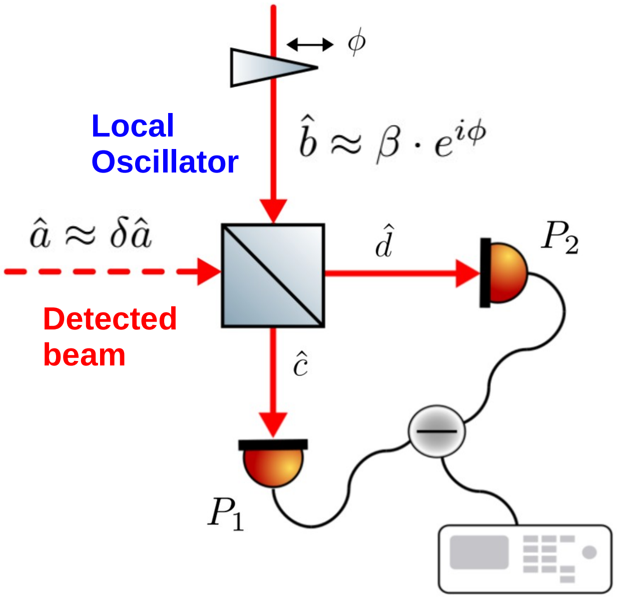

The output beams are:

$$\hat{c} = \frac{1}{\sqrt{2}}(\hat{a} + \hat{b}) \qquad \hat{d} = \frac{1}{\sqrt{2}}(\hat{a} - \hat{b})$$

The detected quantity is:

$$P_1 - P_2 = \hat{c}^\dagger \hat{c} - \hat{d}^\dagger \hat{d} = 2 \cdot \Re(\hat{a} \cdot \hat{b}) \propto \beta \cdot \delta\hat{a}$$

FDS homodyne detection

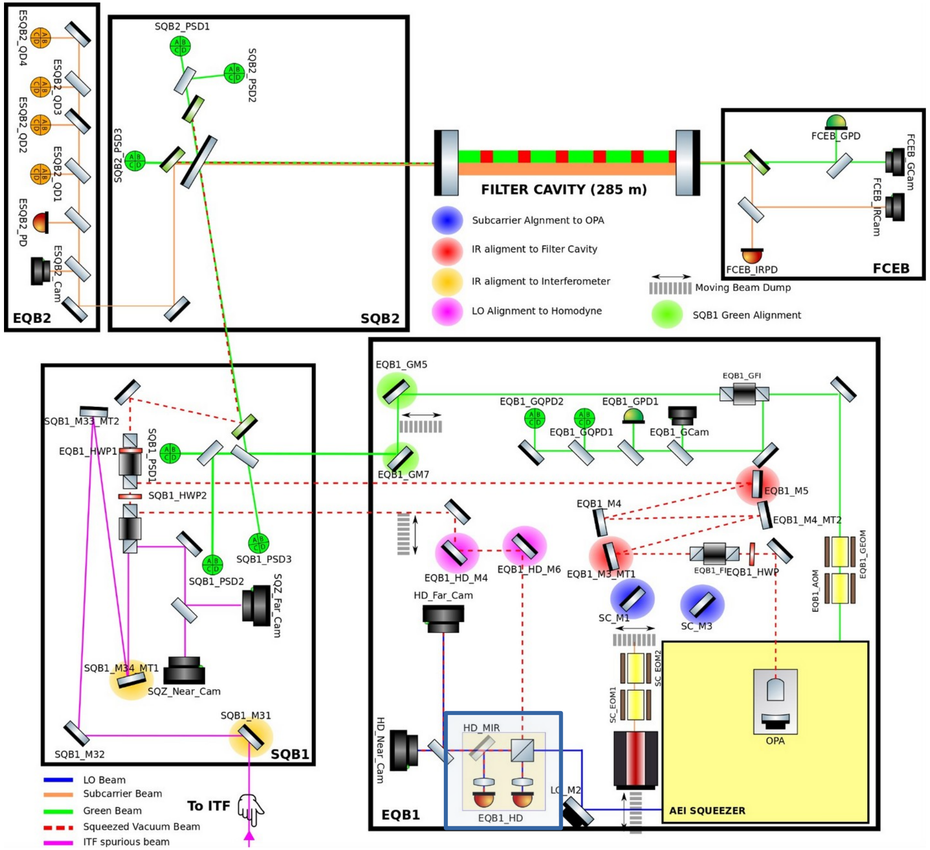

The **homodyne detection** allows to measure the squeezing quadrature ϕ amplified proportionally to the LO amplitude β:

$$P_1 - P_2 \propto \beta \cdot \delta \hat{X}^a_\phi$$

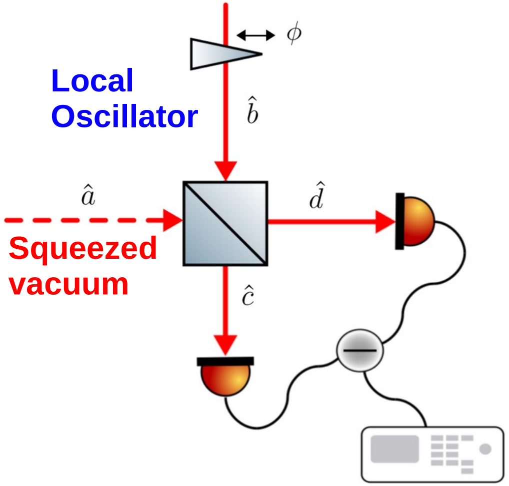

First FDS demonstration @ 360 Hz

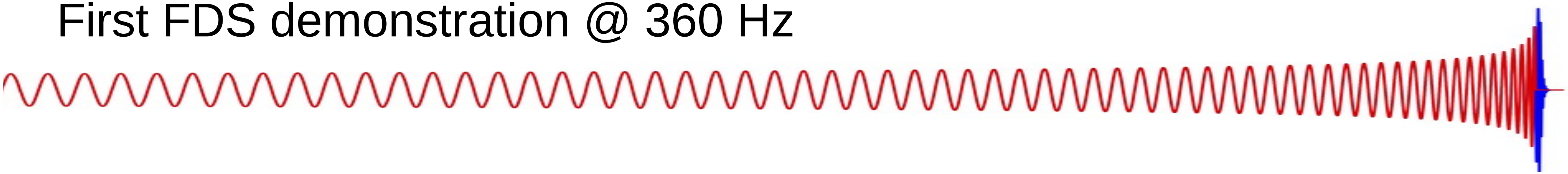

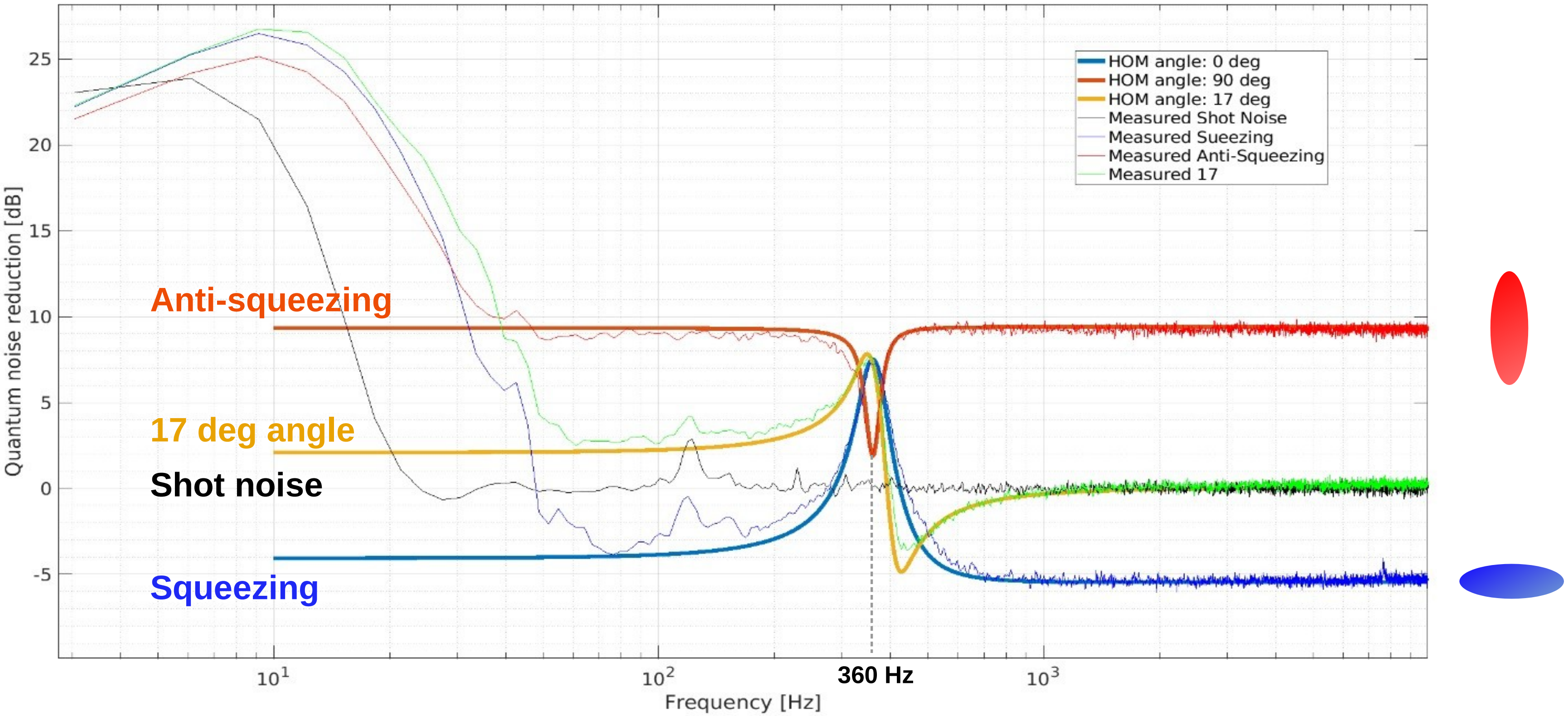

First FDS demonstration

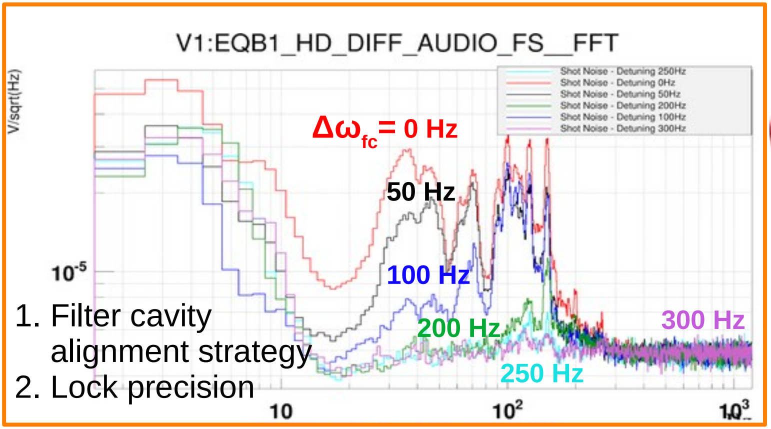

1. Filter cavity alignment strategy
2. Lock precision

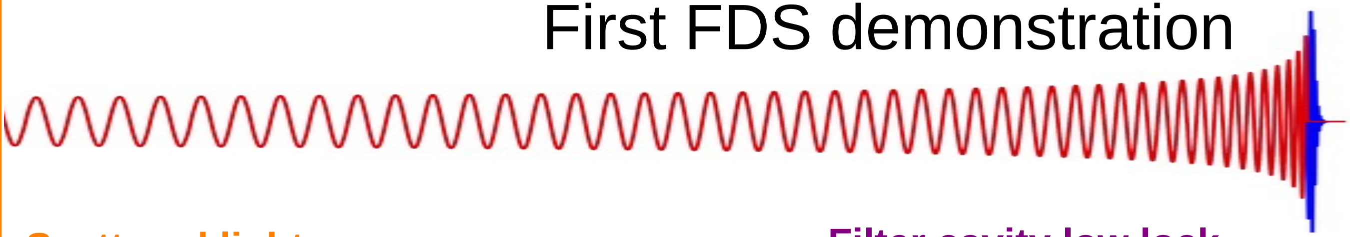

Scattered light:
LO back-scattered from homodyne photodiodes

Filter cavity low lock precision

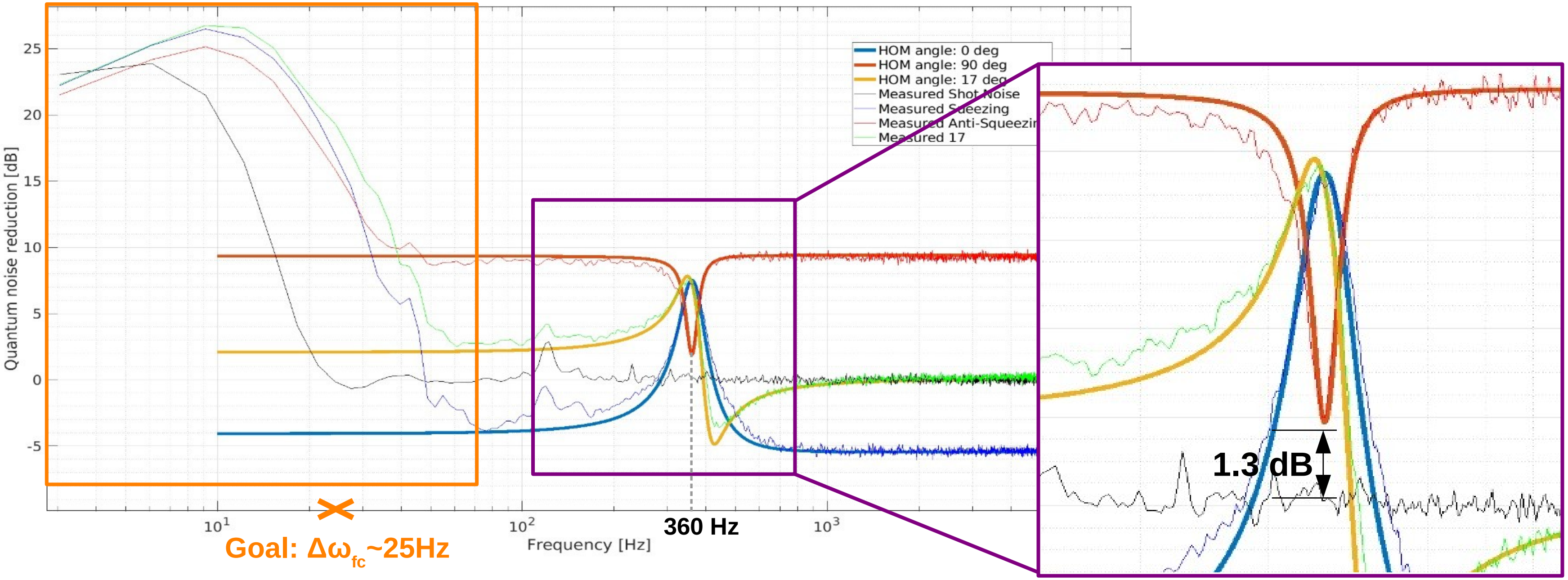

Scattered light noise origin

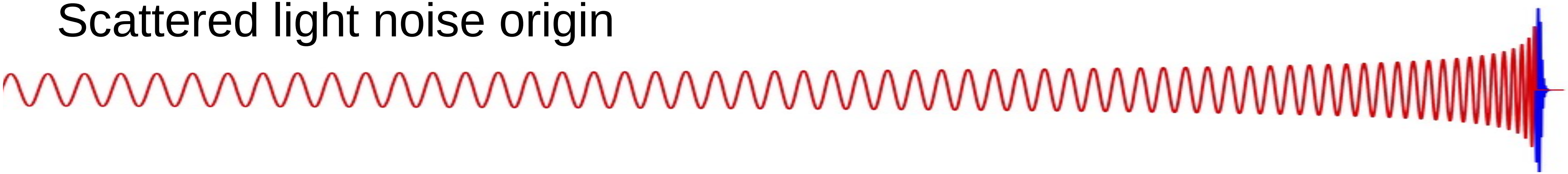

Scattered light is generated by the **LO beam** diffused by the homodyne photodiodes.

It propagates along the optical system and it is modulated by the difference in path length **δα(t)** + **δφ(t)** between the **LO beam** and the **scattered light field**.

This results in a noise at low frequency on the differential channel of the homodyne detector.

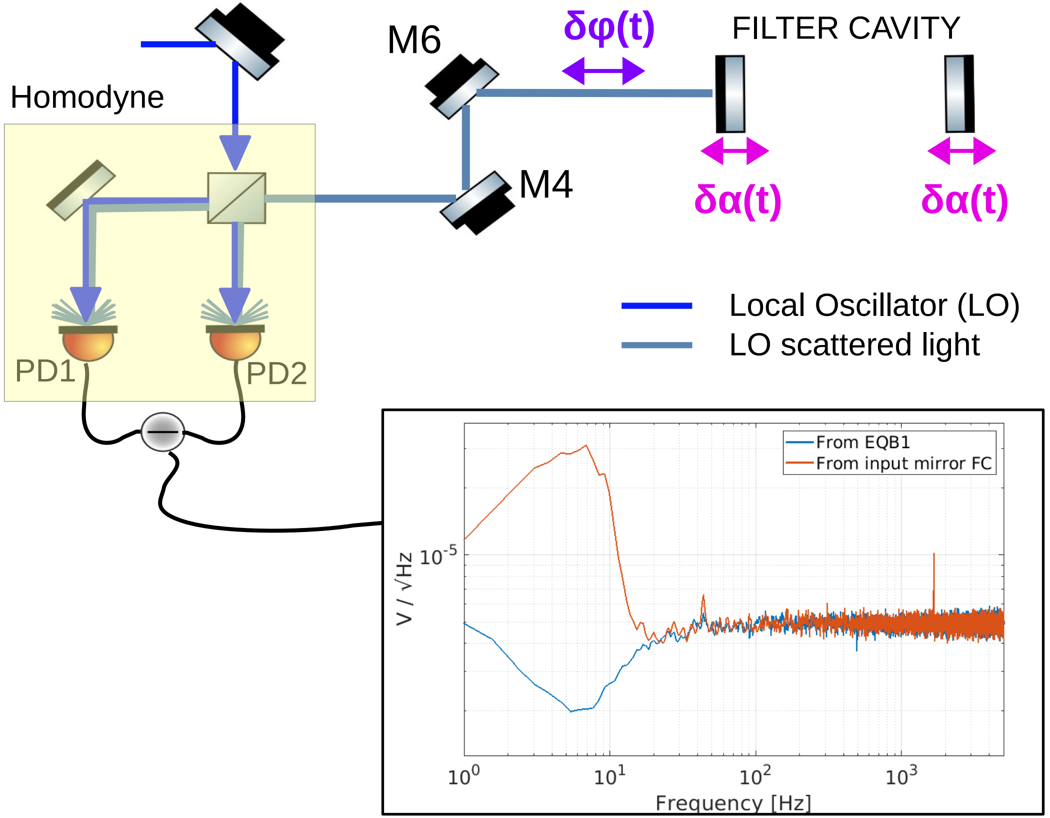

Scattered Light Loop implementation

I implemented a **feedback control loop (SLL)** to compensate for the path length difference **δα(t)** + **δφ(t).**

- A modulation at 500Hz is sent to the actuator on M4.
- The differential homodyne signal is demodulated at the same frequency to obtain the error signal.
- It is filtered and sent to the actuator on M4 to correct the scattered light noise.

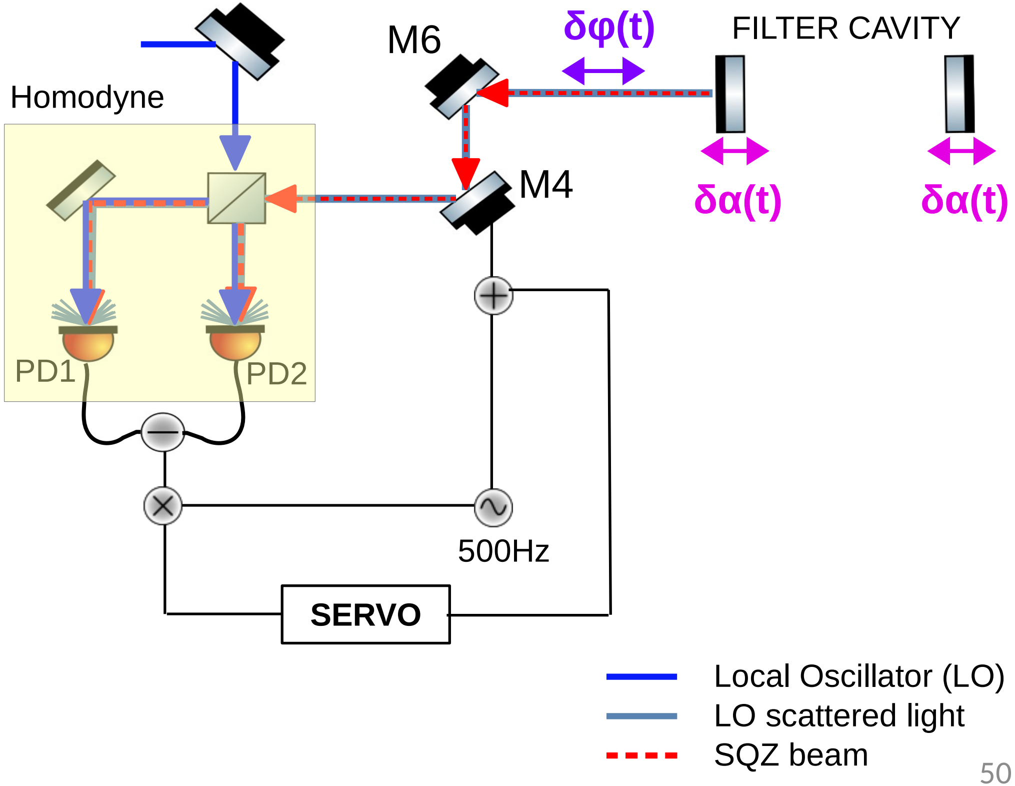

Scattered Light Loop performance

Results:
- Reduction of 25 dB for shot noise measurements;
- SLL can be used during squeezing measurements.

Next steps:
- Replacement of the actuator with one with higher dynamic range.

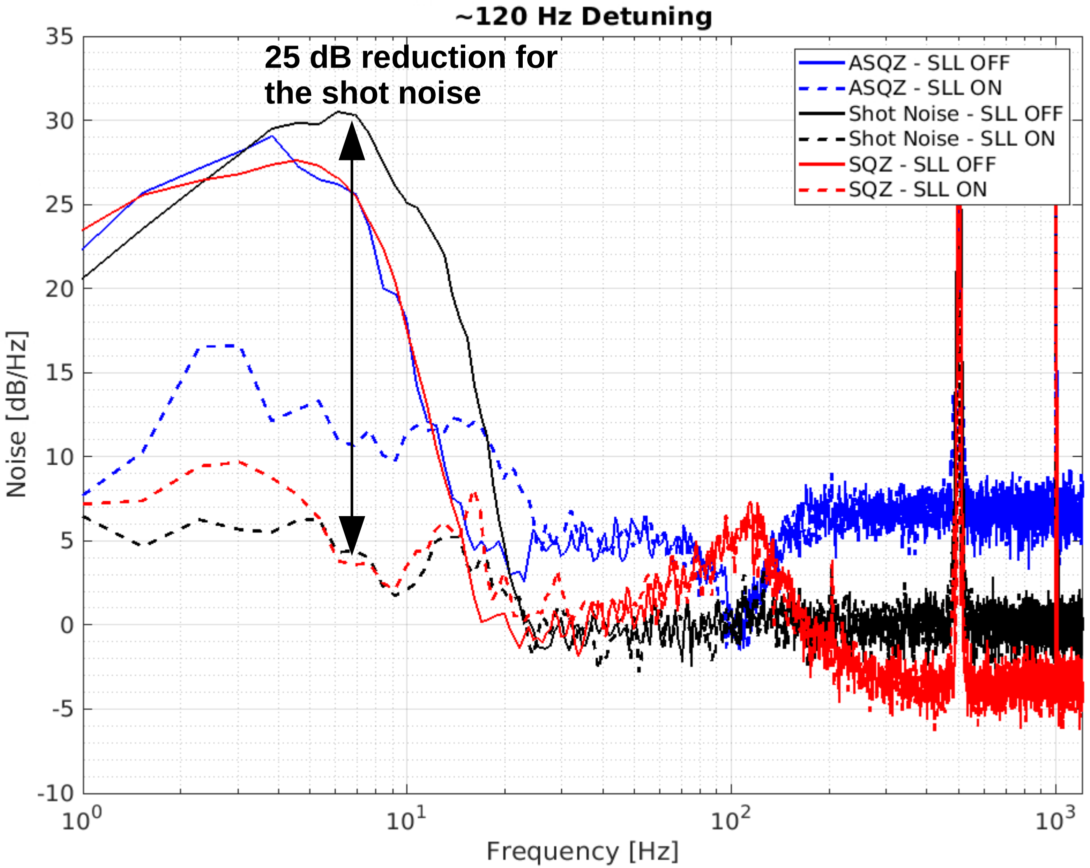

Filter cavity lock precision improvement

Before:
- Filter cavity locked acting ONLY on the cavity end mirror
- ~ 8 Hz of lock precision

After:
- Filter cavity locked acting BOTH on the cavity end mirror and the squeezer laser frequency
- ~ 1 Hz of lock precision

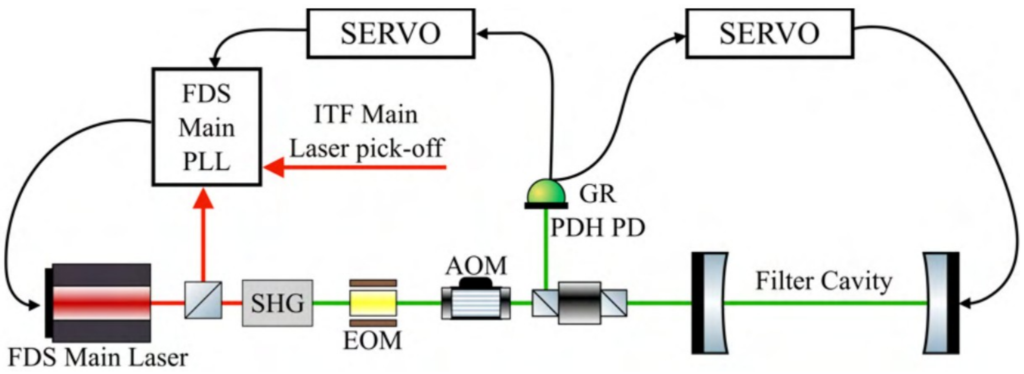

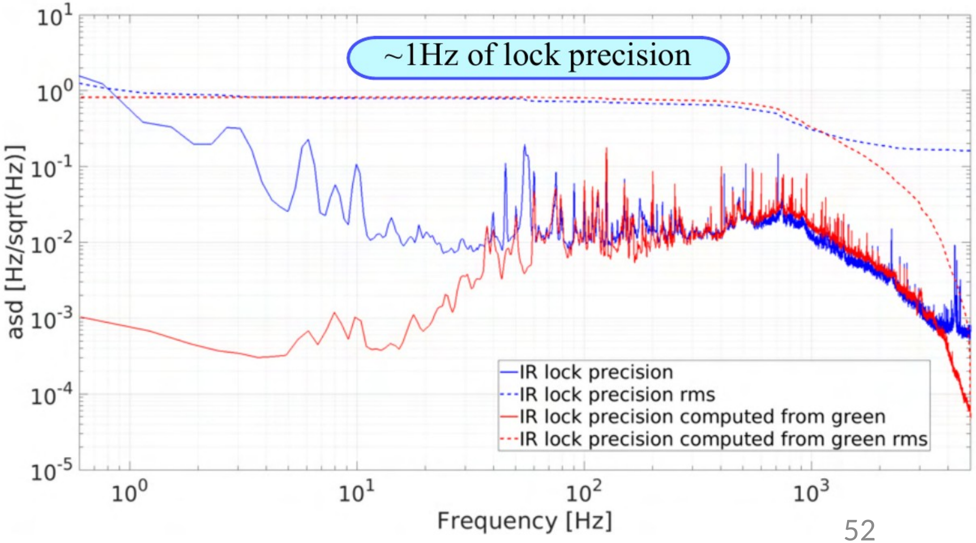

FDS system timeline

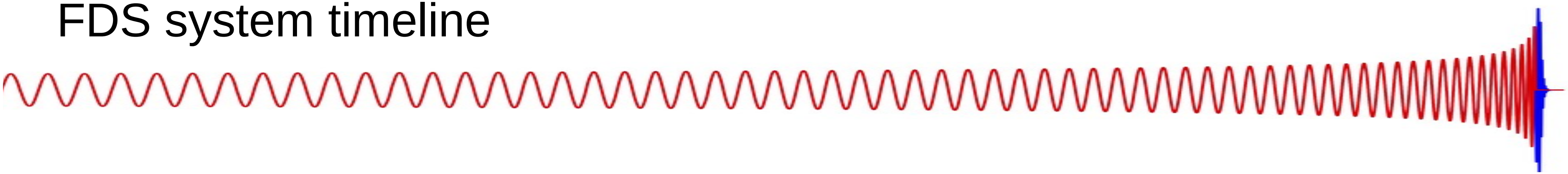

- **SQB1** at LAPP and on site — Jan 2021
- **SQB2** at LAPP and on site — April 2021
- FDS system aligned and FC locked on green — June 2021
- FC locked on IR — Oct 2021
- First FDS demonstration detuning ~300Hz — Nov 2021
- First FDS measurement beating the shot noise — Feb 2022
- First FDS measurement at 25 Hz — June 2022

Milestone!

FDS measurement at 25 Hz

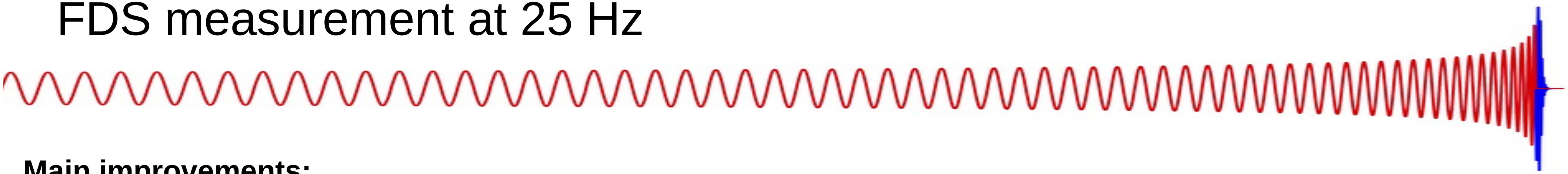

Main improvements:

- Lock precision
- Different filter cavity alignment strategy
- Low seismic activity during summer (stray light bump at < 10 Hz)

Results:

- Detuning: 25 Hz
- Optical losses: 14%
- Phase Noise: 25 mrad

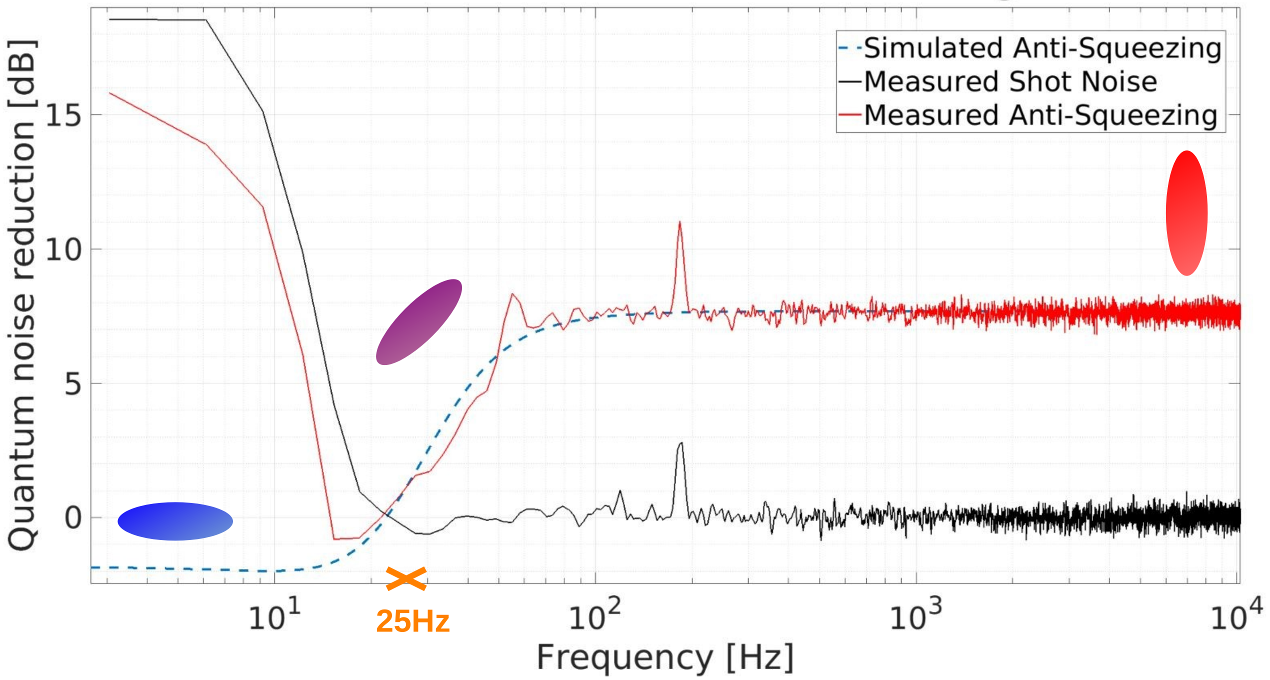

Outline

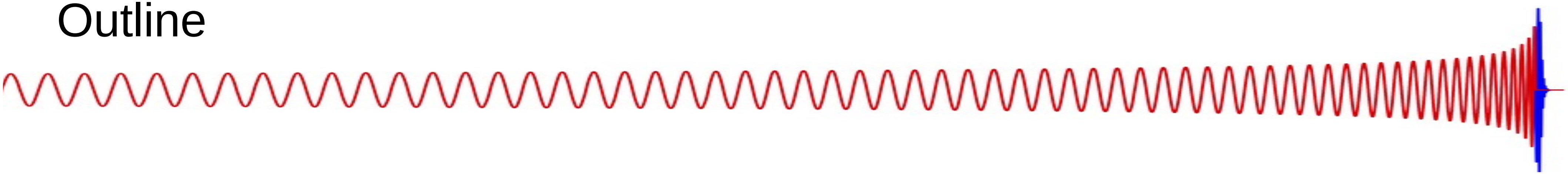

1. Gravitational waves: origin & detection
2. Quantum noise: origin & reduction strategy
3. The Virgo detector from the observing run O3 to O4
4. Frequency dependent squeezing system: installation and commissioning
5. Low loss Output Mode Cleaner: characterization, installation and commissioning
6. Scattered light noise: study and mitigation
7. Conclusions and next steps

FDS injection in ITF preparation

Beam from/to ITF characterized :

- Beam from ITF measured on SQB1
- Beam from FC measured on SQB1
- Beam from FC to EQB1 measured

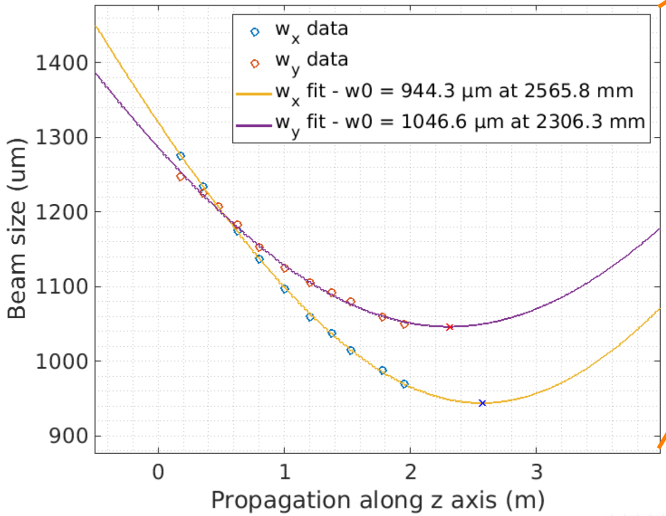

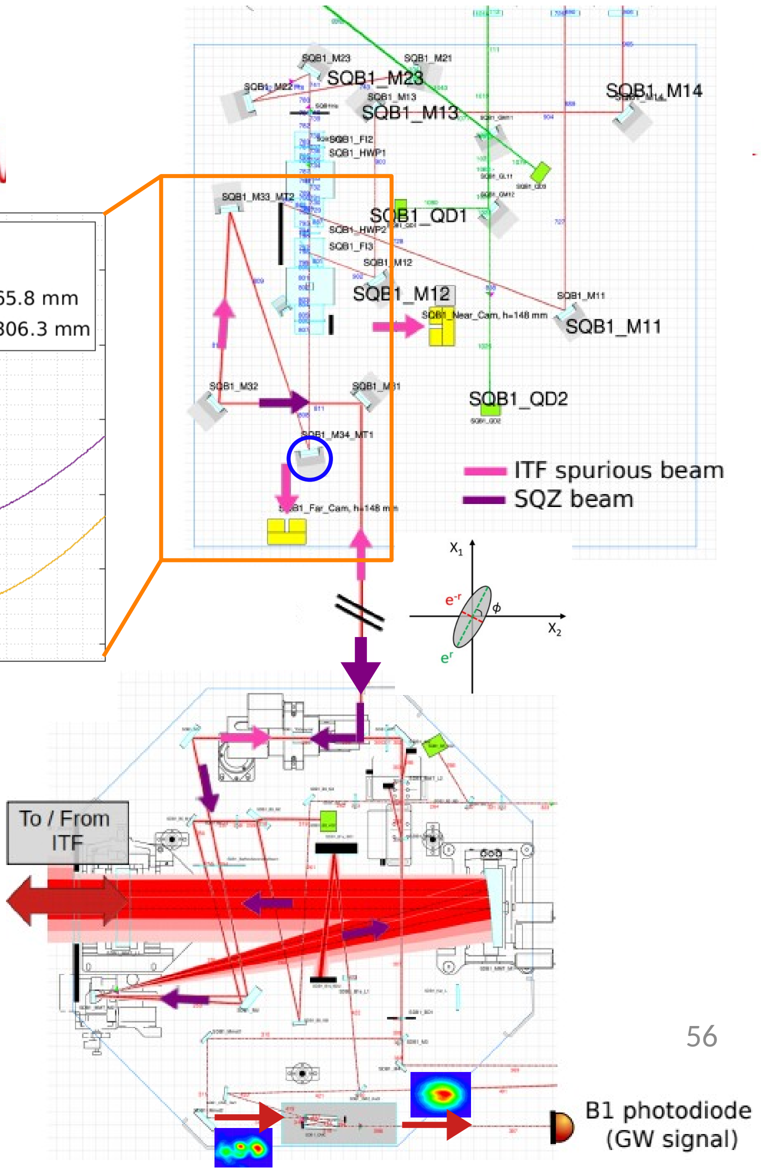

In May 2022:
Squeezed beam - ITF beam estimated mode matching ~ 84% :(

Replacement of one mirror of the telescope on SQB1

In October 2022:
Squeezed beam - ITF beam estimated mode matching ~ 99% :)

Output Mode Cleaner replacement

Motivation: need to replace two output mode cleaners cavity with a single one to reduce detection losses to maintain the squeezing performance

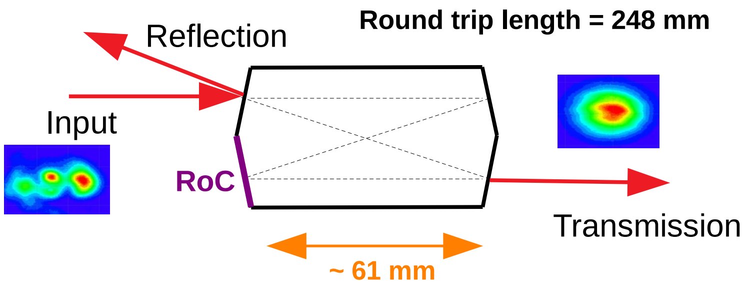

Properties	O3 OMC cavities	O4 OMC cavity
Finesse (F)	123	1000
Micro-roughness (σ_{RMS})	0.3 nm RMS	$\leq$ 0.1 nm RMS
Radius of Curvature (ρ)	1700 mm	1700 mm
Material	Suprasil 3001 (fused silica)	Suprasil 3001 (fused silica)

Loss sources	Measured during O3	Target for O4
ITF-OMC1 matching	8%	3%
OMC1-OMC2 matching	2.5%	0
OMC internal losses	2%	1.5%
Total losses	12.5%	4.5%

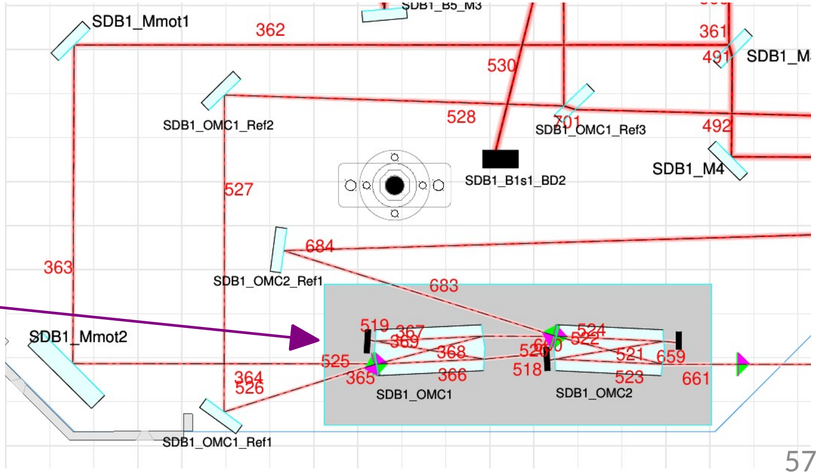

OMC characterization at LAPP

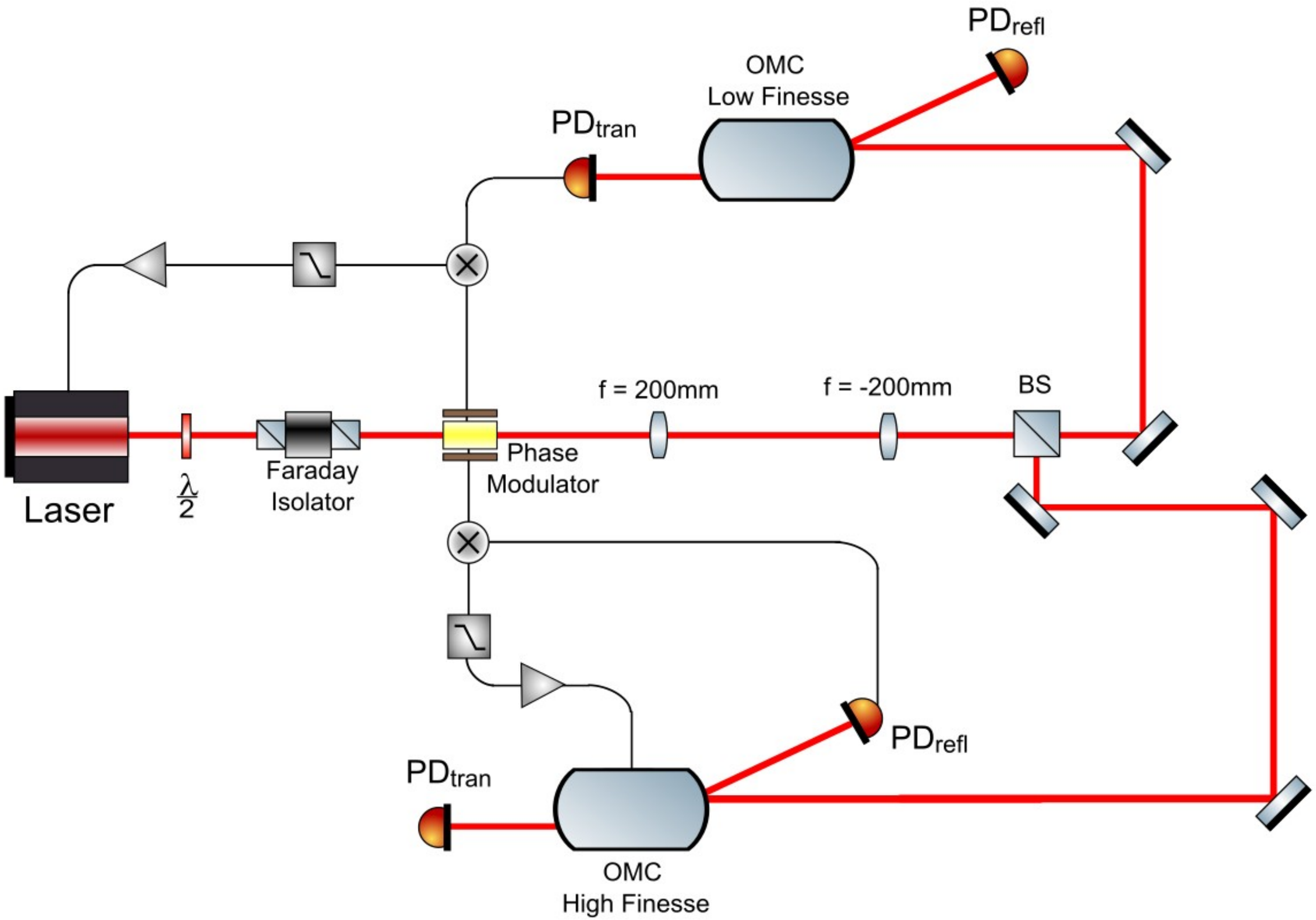

- **Alignment** of the OMC
- **Lock** of the OMC with Peltier and PZT
- **Laser frequency stabilization** with a low finesse OMC spare
- Measurement of
  - Finesse
  - Radius of curvature
  - Internal losses

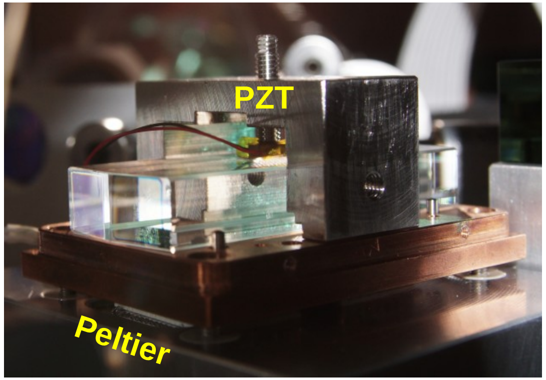

OMC internal losses measurement at LAPP

Losses have been measured from power measurement with a calibrated integrating sphere:

$$L = 1 - \frac{P_R}{P_{in}} - \frac{P_T}{P_{in}}$$

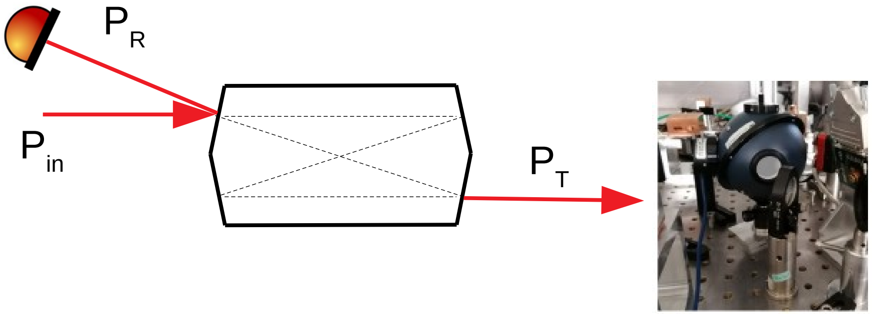

P_T measured locking the OMC with the PD in reflection and averaging several measurements (same for P_R).

We got $\mathbf{L_{meas} = (2.0 \pm 0.1)\ \%}$.

Losses source	**Value per round-trip**
Suprasil absorption	(7.5 ± 5) ppm
Coating absorption	(4 ± 4) ppm
Surface scattering	(14 ± 2) ppm
Rayleigh scattering	(17.0 ± 0.5) ppm
HR residual transmission	(2.5 ± 0.4) ppm
Total	(45 ± 12) ppm

The estimation of internal losses needs to be multiplied by the number of round-trips inside the cavity:

$$\mathbf{L_{exp} = N \times L_{round\ trip} = (1.5 \pm 0.4)\ \%.}$$

The two values are in agreement.

Installations on SDB1

1. Low loss **Output mode Cleaner**

2. Motorized **waveplates** for a fine polarization tuning

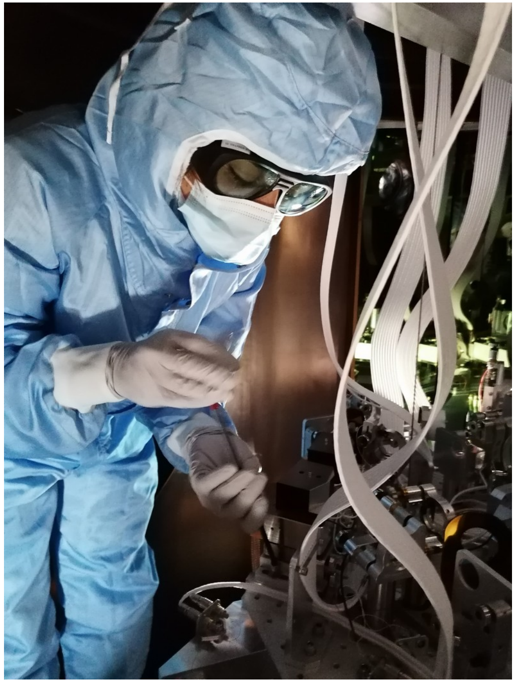

2.

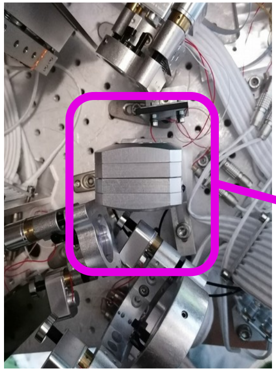

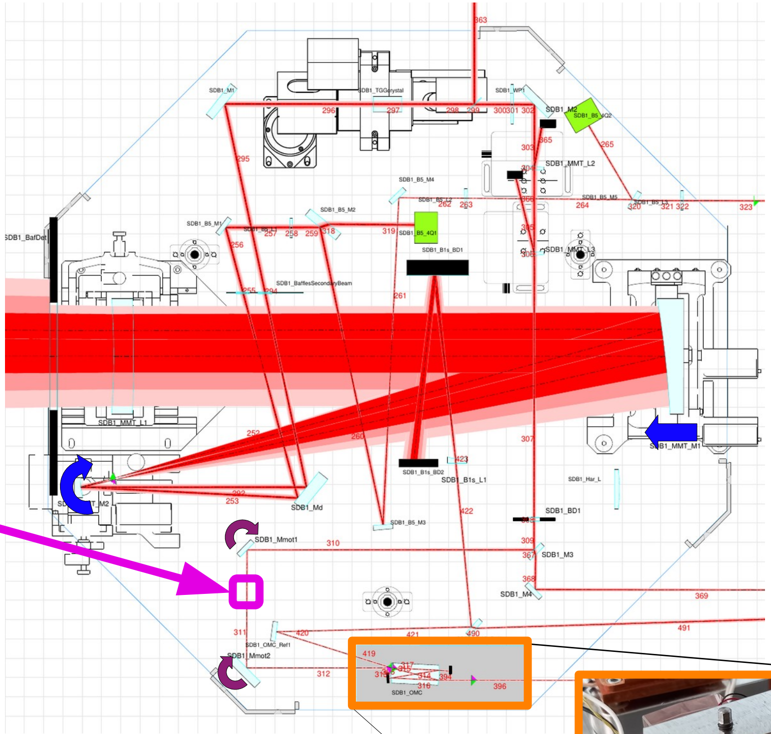

1.

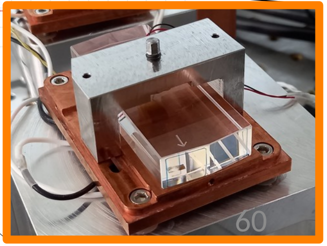

- Alignment
- Mode matching
- Polarization tuning

OMC loss budget

Alignment, **mode matching** and **polarization tuning** performed with direct beam from Virgo laser.

Alignment ~ 99.5%

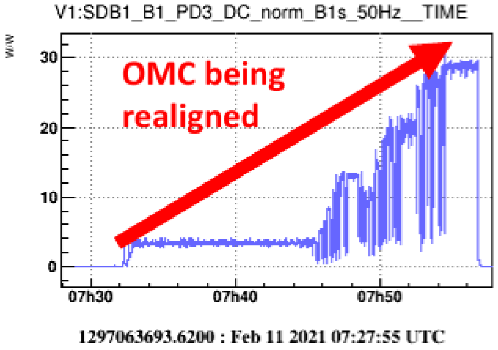

Mode matching ~ 99.3%

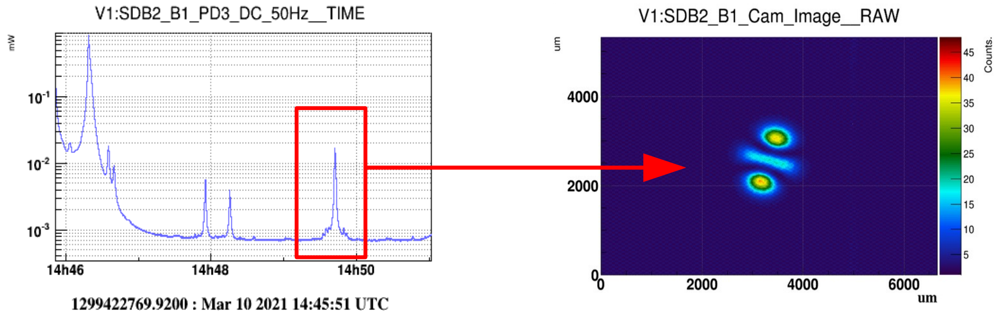

Polarization tuning ~ 99.9%

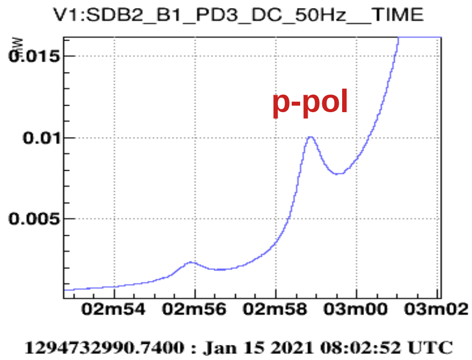

Losses	Measured during O3	Target for O4	Measured for O4
ITF-OMC	8%	3%	1.2%*
OMC 1-2	2.5%	0%	0%
Internal	2%	1.5%	2%
Total	**12.5%**	**4.5%**	**3.2%**

* Misalignment: 0.5% +
Mode Mismatch: 0.64% +
Polarization mistune: 0.08%
= **1.2%**

Squeezing loss budget: O3 vs O4

Optical losses	FIS measured during O3	FDS expected for O4
Injection losses	12.4%	9.4%
Detection losses	18.9%	9.7%
ITF losses	~ 4%	~ 5%
Total losses	35.3%	24.1%
Shot noise reduction	(3.2 ± 0.1) dB	(6.5 ± 0.5) dB

Outline

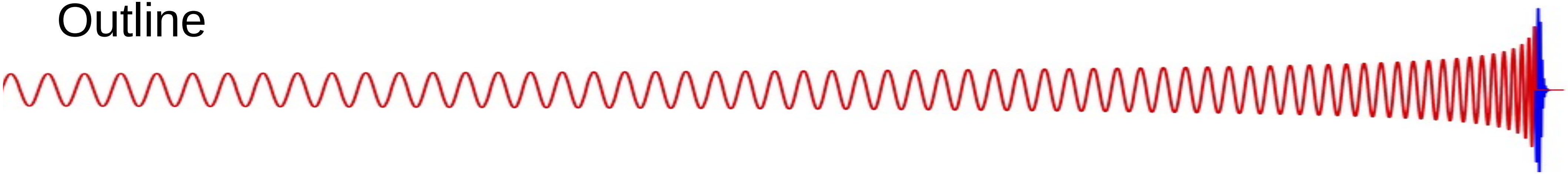

1. Gravitational waves: origin & detection
2. Quantum noise: origin & reduction strategy
3. The Virgo detector from the observing run O3 to O4
4. Frequency dependent squeezing system: installation and commissioning
5. Low loss Output Mode Cleaner: characterization, installation and commissioning
6. Scattered light noise: study and mitigation
7. Conclusions and next steps

Stray light noise from suspended benches in O3

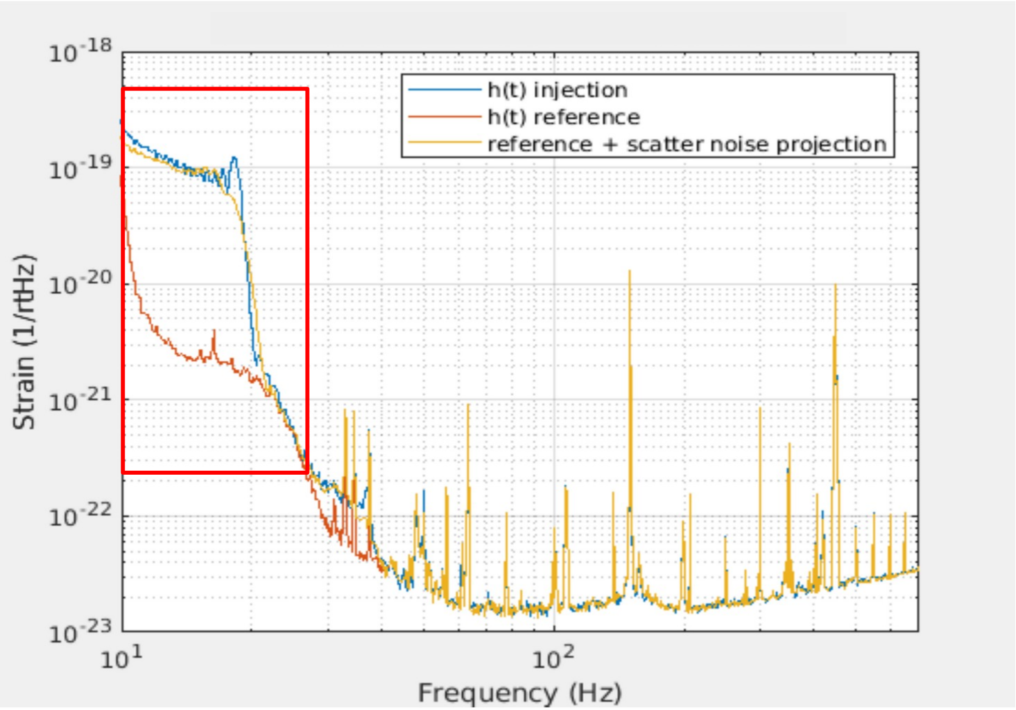

Stray light noise from **SDB1** measurement during O3.

Stray light noise has been measured during O3 by introducing a displacement $z_r(t)$ to the suspended benches.

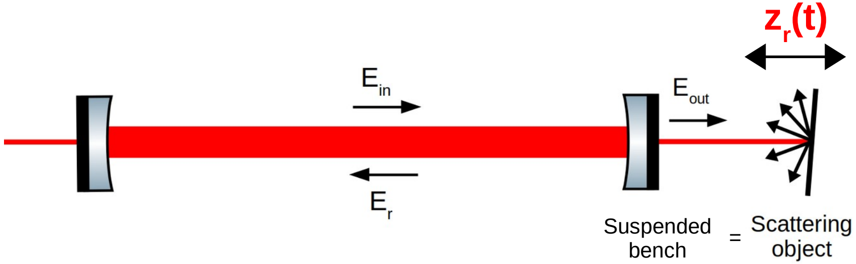

Stray light noise can hide the reduction of radiation pressure noise brought by frequency-dependent squeezing!

Would it be the case during O4??

Stray light projection ingredients for O4

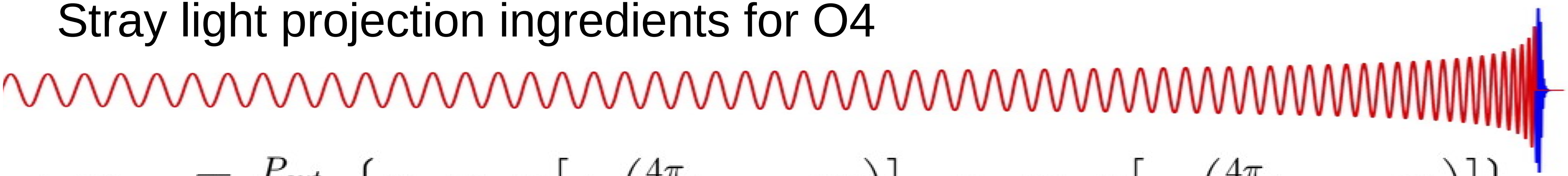

$$h_r(f) = \sqrt{f_r} \cdot \frac{P_{out}}{P_{in}} \cdot \left\{ K_{n_\phi}(f) \cdot \mathcal{F}\left[\sin\left(\frac{4\pi}{\lambda}(z_0 + \underline{z_r(t)})\right)\right] + K_{\frac{\delta P}{P}}(f) \cdot \mathcal{F}\left[\cos\left(\frac{4\pi}{\lambda}(z_0 + \underline{z_r(t)})\right)\right] \right\}$$

Fourier transform of the phase / amplitude components of the bench displacement wrt to ITF reference, with $z_r(t)$ considered during high seismic activity periods during the commissioning for O4

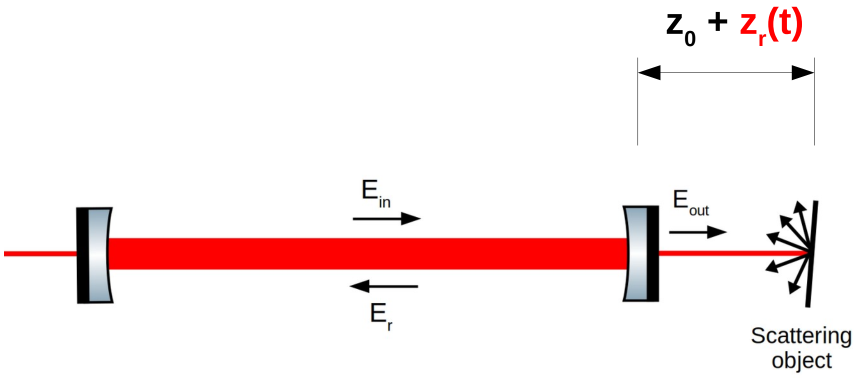

Stray light projection ingredients for O4

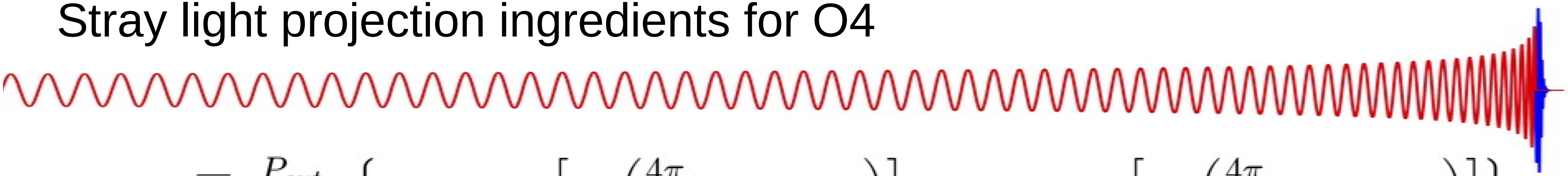

$$h_r(f) = \sqrt{f_r} \cdot \frac{P_{out}}{P_{in}} \cdot \left\{ \underline{K_{n_\phi}(f)} \cdot \mathcal{F}\left[\sin\left(\frac{4\pi}{\lambda}(z_0 + z_r(t))\right)\right] + \underline{K_{\frac{\delta P}{P}}(f)} \cdot \mathcal{F}\left[\cos\left(\frac{4\pi}{\lambda}(z_0 + z_r(t))\right)\right]\right\}$$

Phase Transfer Function **Amplitude Transfer Function**

The TF describes the opto-mechanical response of the detector and depends on the optical configuration of the ITF in O4

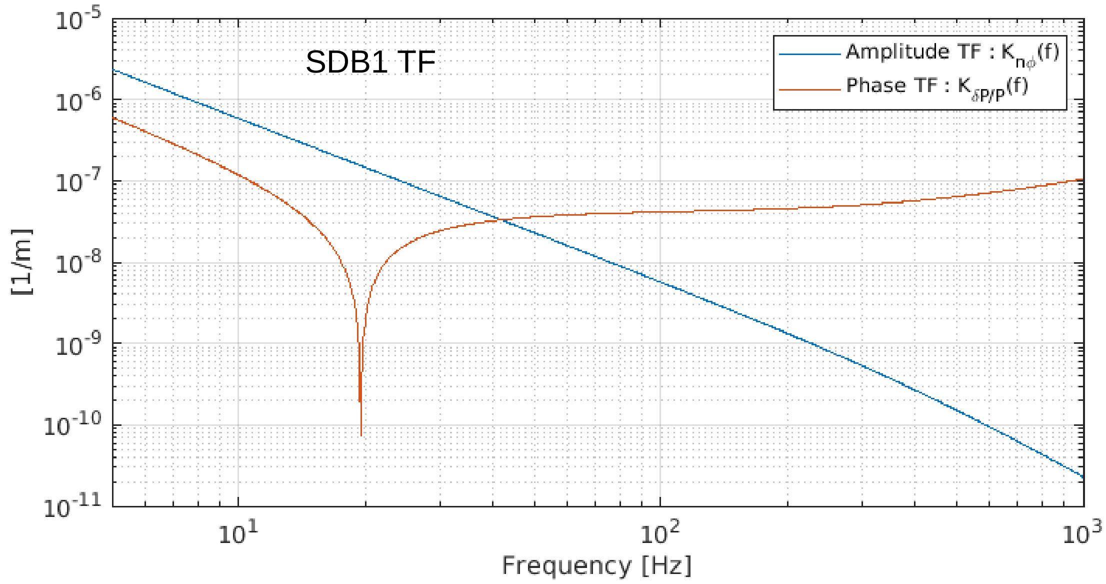

Stray light projection ingredients for O4

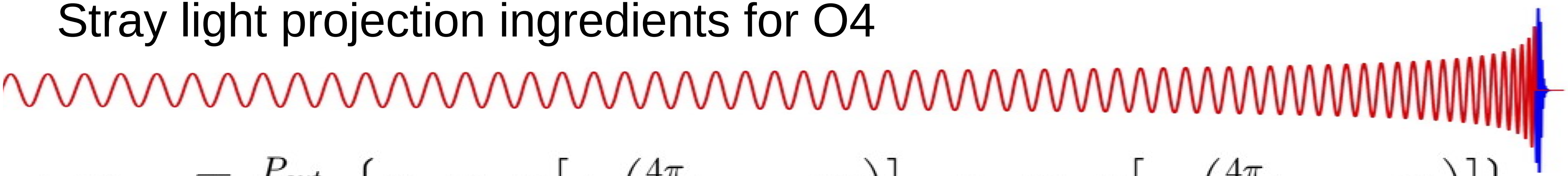

$$h_r(f) = \sqrt{f_r} \cdot \frac{P_{out}}{P_{in}} \cdot \left\{ K_{n_\phi}(f) \cdot \mathcal{F}\left[\sin\left(\frac{4\pi}{\lambda}(z_0 + z_r(t))\right)\right] + K_{\frac{\delta P}{P}}(f) \cdot \mathcal{F}\left[\cos\left(\frac{4\pi}{\lambda}(z_0 + z_r(t))\right)\right]\right\}$$

Fraction of stray light re-coupled with the main mode of the interferometer: $f_r = f_{sc} + f_{Rayleigh} + f_{sp} + f_{extra}$

Secondary beams mitigation for O4

Ghost beams are unwanted secondary beams due to not perfect coating of optical components.

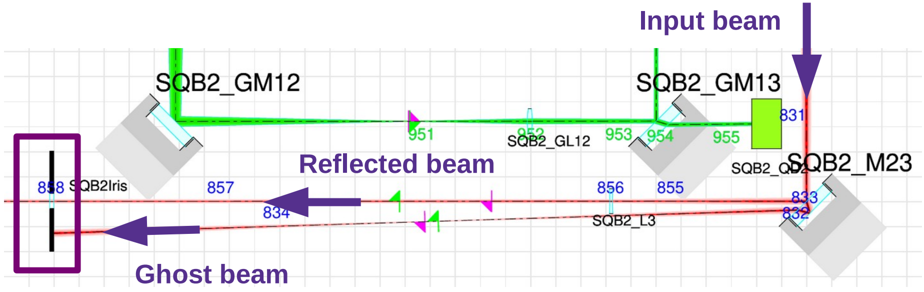

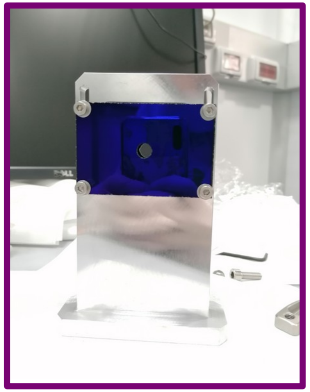

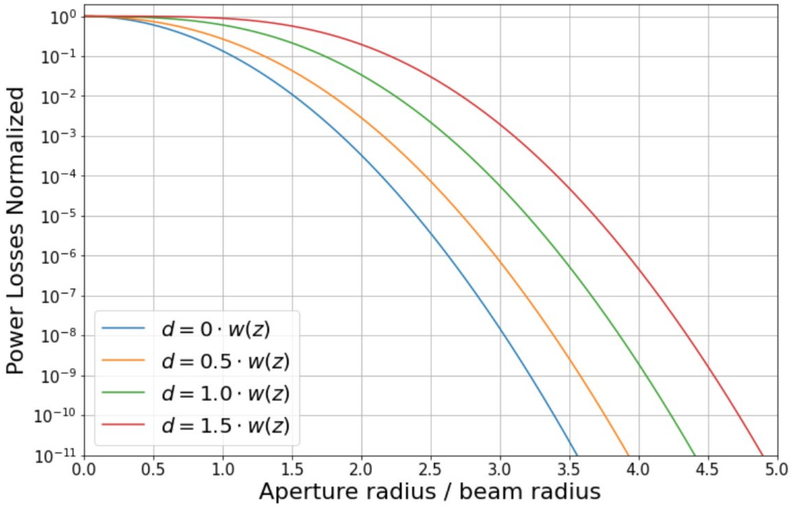

Systematic ghost beams **tracing** and **dumping** for all the benches and pipes of AdV+.

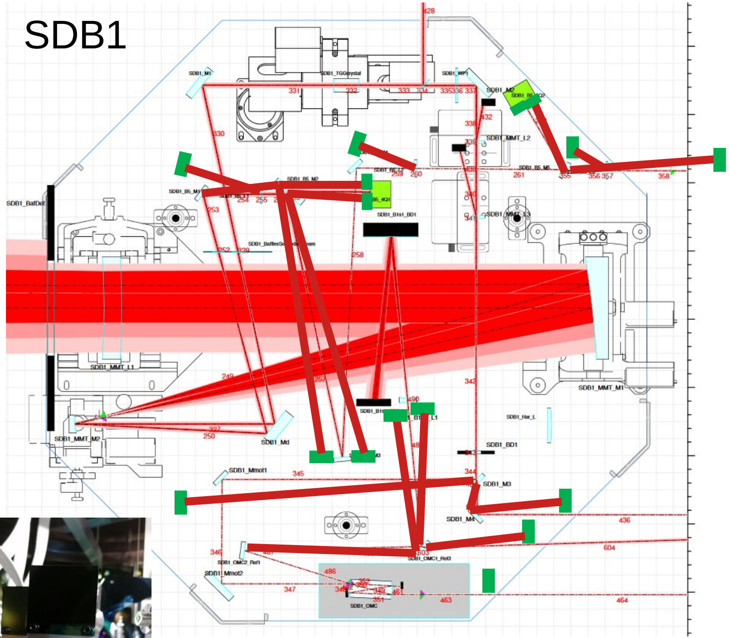

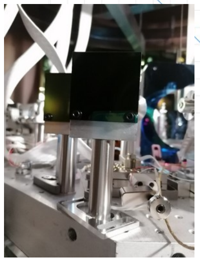

: beam dump

Secondary beams mitigation for O4

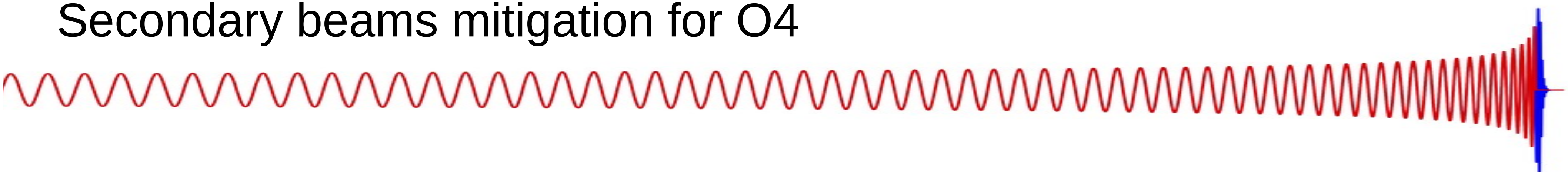

Mitigation strategies adopted for AdV+:

1. Wedge optimization
2. Diaphragms installation
3. Baffle installation
4. Absorbing disks behind mirrors
5. Diaphragms on quadrants
6. Small beam dumps
7. Dumpers on photodiodes
8. Lens tilting
9. Absorbing screws

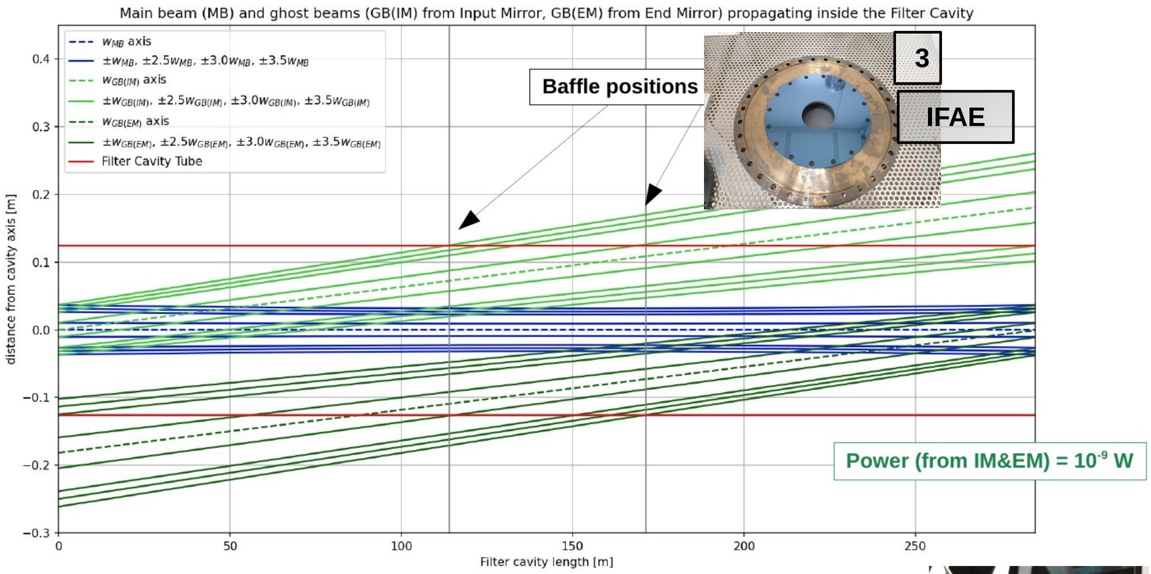

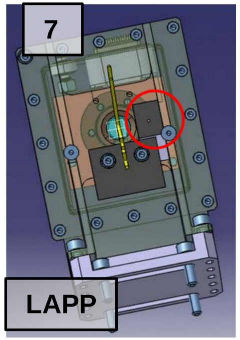

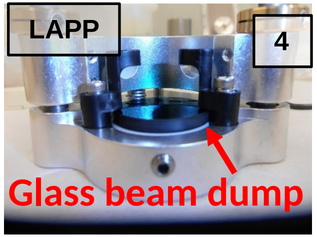

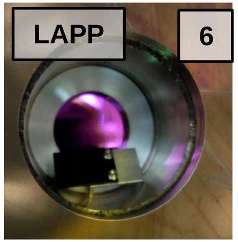

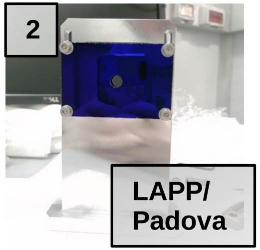

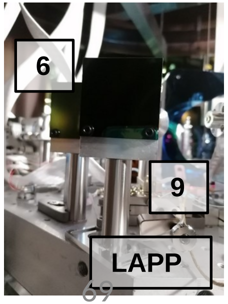

Stray light projection ingredients for O4

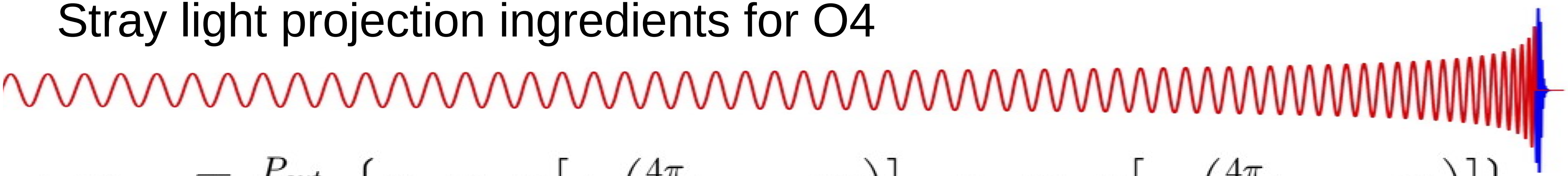

$$h_r(f) = \sqrt{f_r} \cdot \frac{P_{out}}{P_{in}} \cdot \left\{ K_{n_\phi}(f) \cdot \mathcal{F}\left[\sin\left(\frac{4\pi}{\lambda}(z_0 + z_r(t))\right)\right] + K_{\frac{\delta P}{P}}(f) \cdot \mathcal{F}\left[\cos\left(\frac{4\pi}{\lambda}(z_0 + z_r(t))\right)\right]\right\}$$

Fraction of stray light re-coupled with the main mode of the interferometer: $f_r = f_{sc} + f_{Rayleigh} + f_{sp} + \cancel{f_{extra}}$

- f_{sc} is the light scattered by an optical surface
- $f_{Rayleigh}$ is the light scattered from atoms/molecules

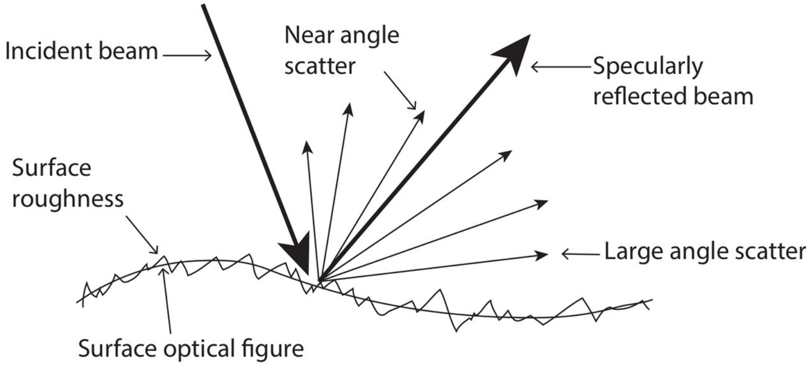

- f_{sp} is the specular reflection

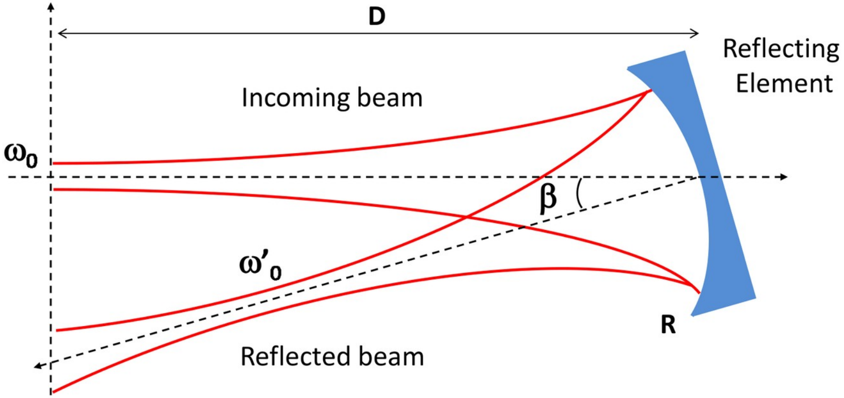

Estimation of f_r for O4

Identification of <u>critical optical elements</u> on the benches, example of SDB1 and SDB2:

- lenses perpendicular to the beam;
- highly scattering objects.

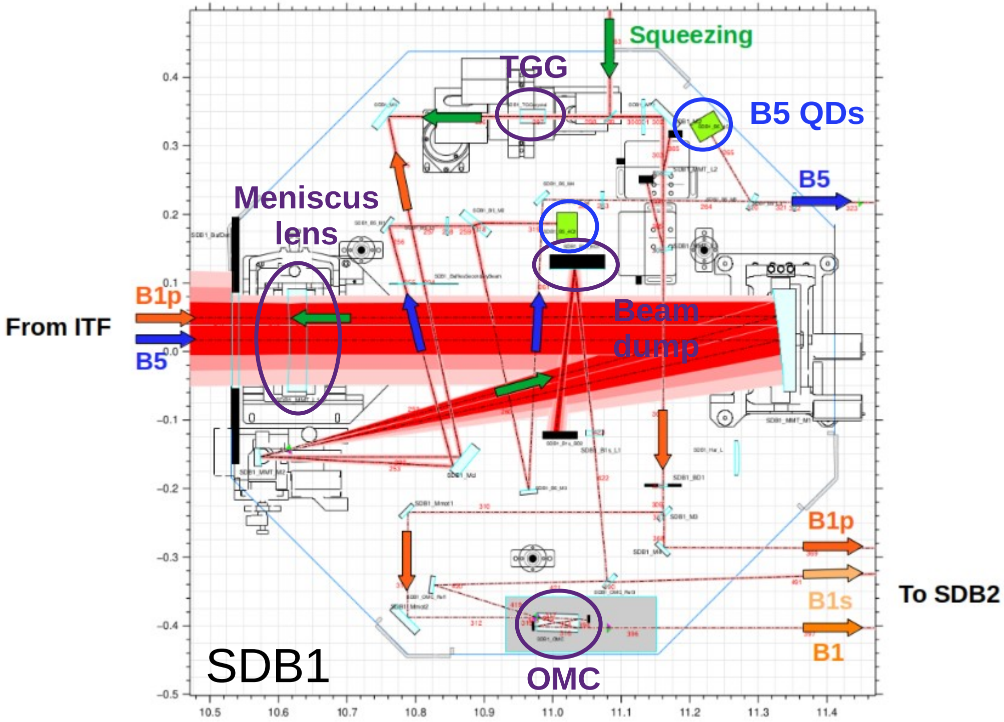

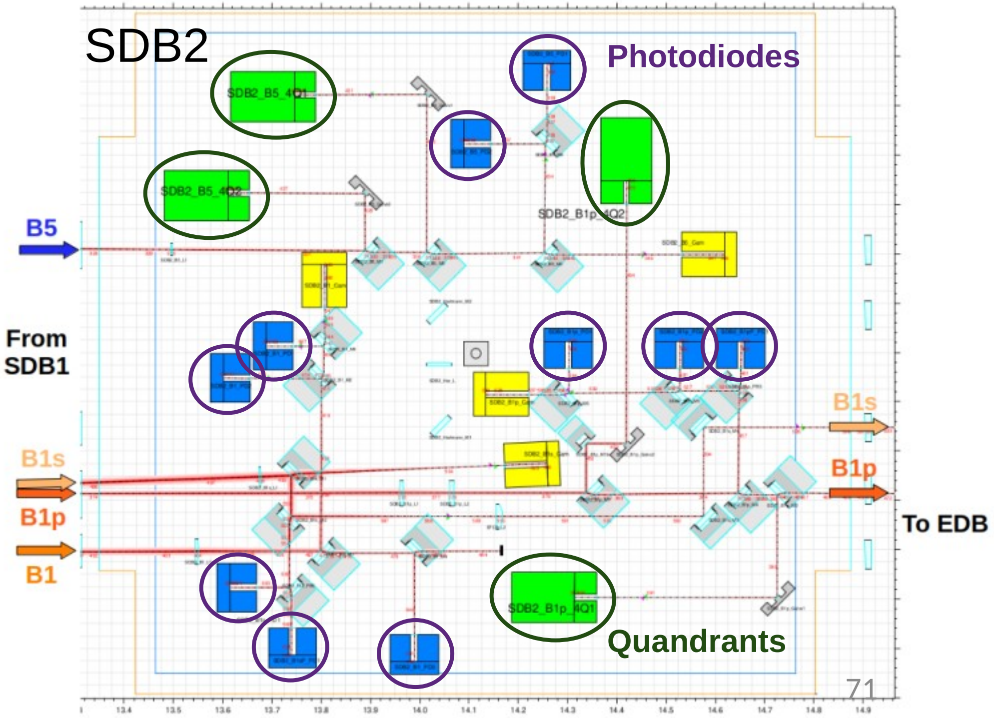

Estimation of f_{sc} for O4

- Measurement of f_{sc} with an optical set-up at LAPP using homodyne detection

$$P_1(t) - P_2(t) = \frac{P_0}{\sqrt{2}}\sqrt{f_{\text{sc}}}\cos\left(2\pi\frac{\Delta L(t)}{\lambda}\right)$$

$$A(t) = \frac{P_1(t) - P_2(t)}{P_1(t) + P_2(t)} = \sqrt{2f_{\text{sc}}}\cos\left(2\pi\frac{\Delta L(t)}{\lambda}\right)$$

$$\text{Var}(A(t)) = f_{\text{sc}}$$

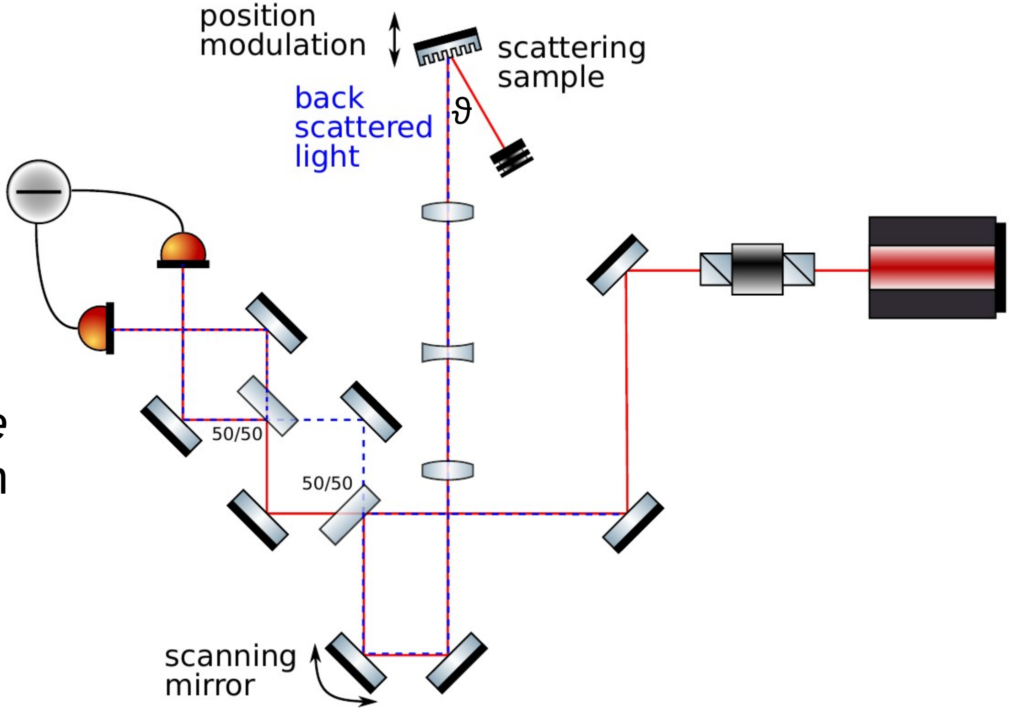

- Estimation of the *Bidirectional Reflectance Distribution Function (BRDF)* as a function of the incidence angle ϑ

$$f_{sc} \sim \alpha_p^2 \cdot \frac{BRDF(\theta)\cdot\lambda^2}{\pi\cdot w(z)^2}$$

Estimation of f_{sc} for O4

We measured the BRDF(ϑ), for angles larger than 500 μrad.

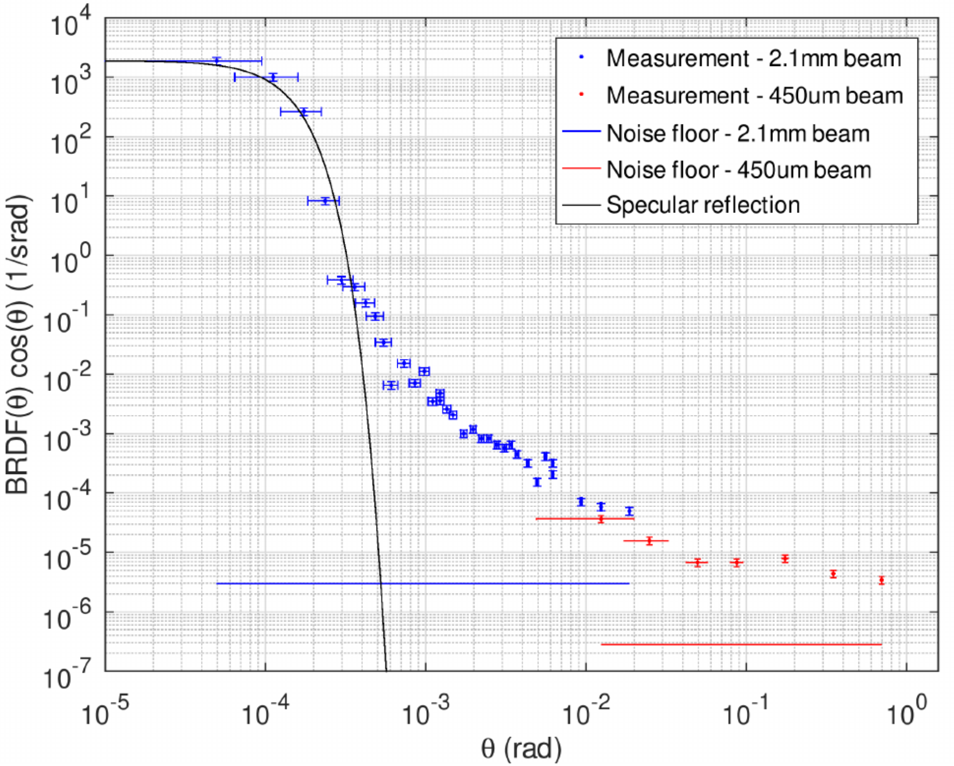

Element	θ	$BRDF(\theta)$
SDB1 quadrants (B5)	5 deg	$3.5 \cdot 10^{-3}$
SDB2/SNEB/SWEB/SPRB quadrants	5 deg	3
SDB2/SNEB/SWEB/SPRB photodiodes	20 deg	$4.9 \cdot 10^{-5}$
SNEB/SWEB Silicon beam dump	1 deg	$1.0 \cdot 10^{-4}$

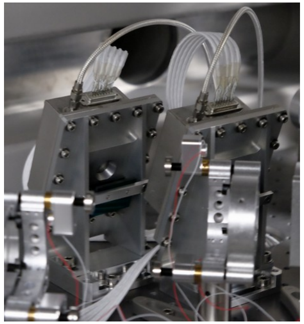

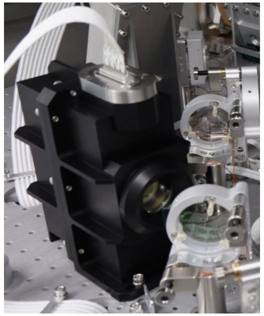

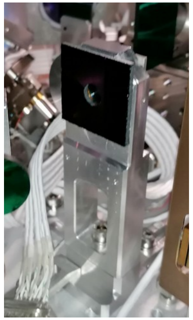

Estimation of f_{sp} for O4

The specular reflection has been considered for the lenses perpendicular to the beam and to decide how much to tilt the lenses (for example L2):

$$f_{sp} = \frac{\alpha R^2 z_o^2 \exp\left[-\frac{2\pi D^2 z_0 \beta^2}{2\lambda}\left(\frac{1}{D^2+z_0^2} + \frac{1}{(D-R)^2+z_0^2}\right)\right]}{(D^2+z_0^2)[(D-R)^2+z_0^2]}$$

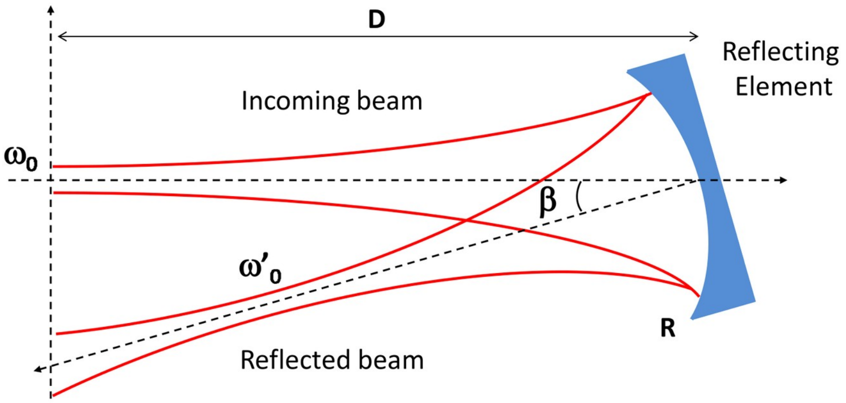

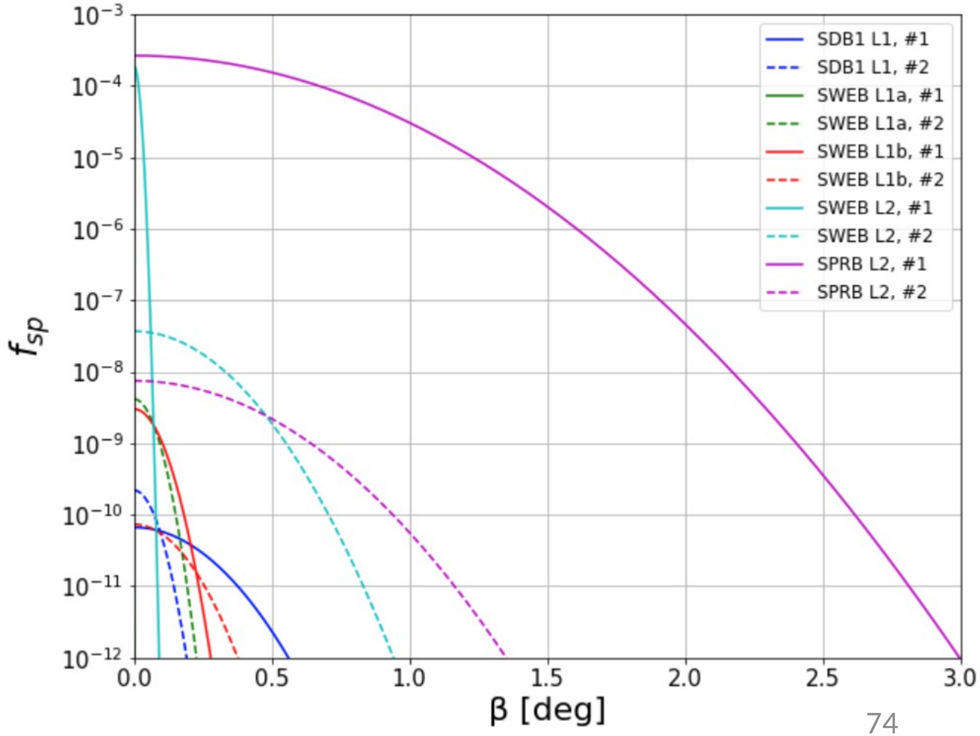

Stray light projections for O4

The projections have been performed on all the Virgo suspended benches.
The critical ones are SDB1 and SDB2.

SDB1

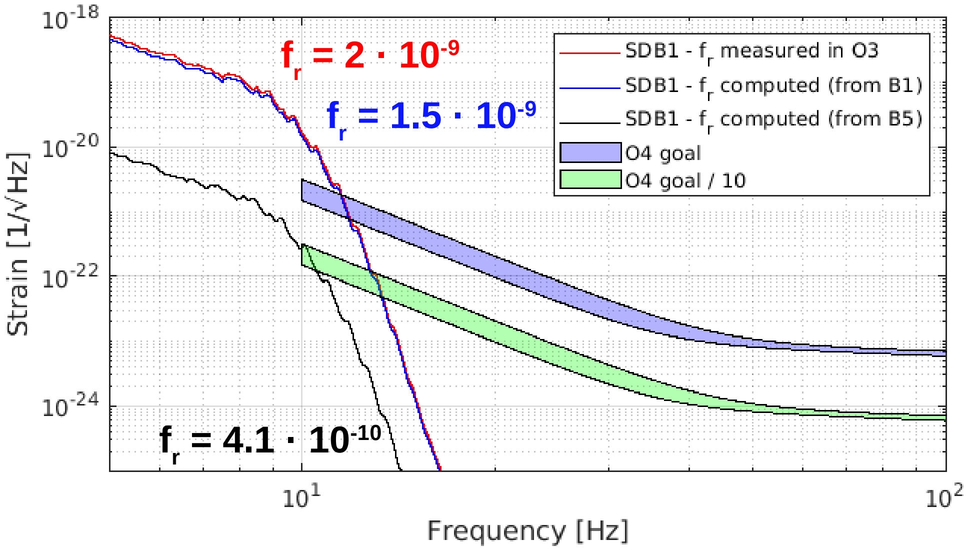

SDB2

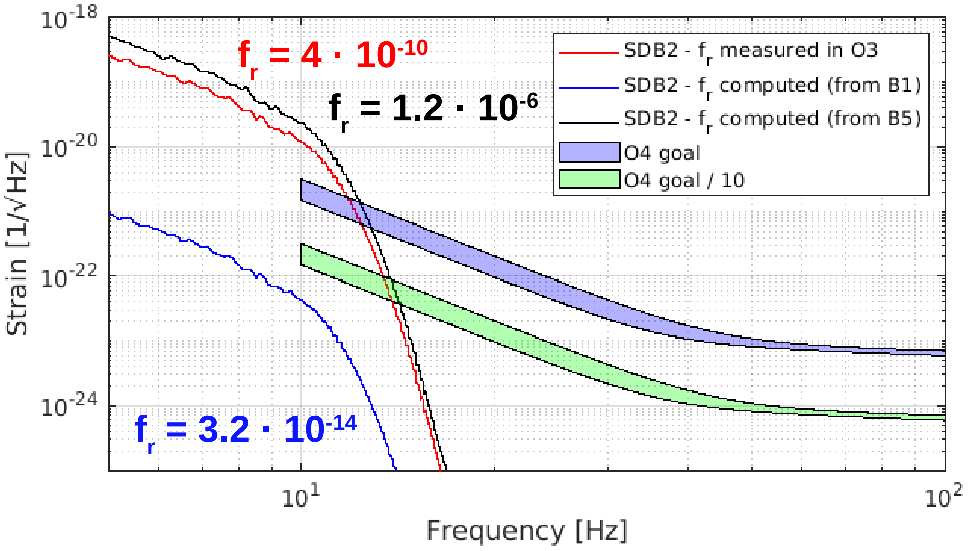

Future stray light mitigation actions

SDB1 possible actions and mitigation:

- Measure the scattering of OMC and TGG at LAPP
- Install the meniscus lens on a rotating mount
- Replace the OMC with a ring cavity
- Replace the TGG crystal by a less scattering one

SDB2 foreseen actions and mitigation:

- Install beam dumps in front of the B5 quadrants since they are not used during the run

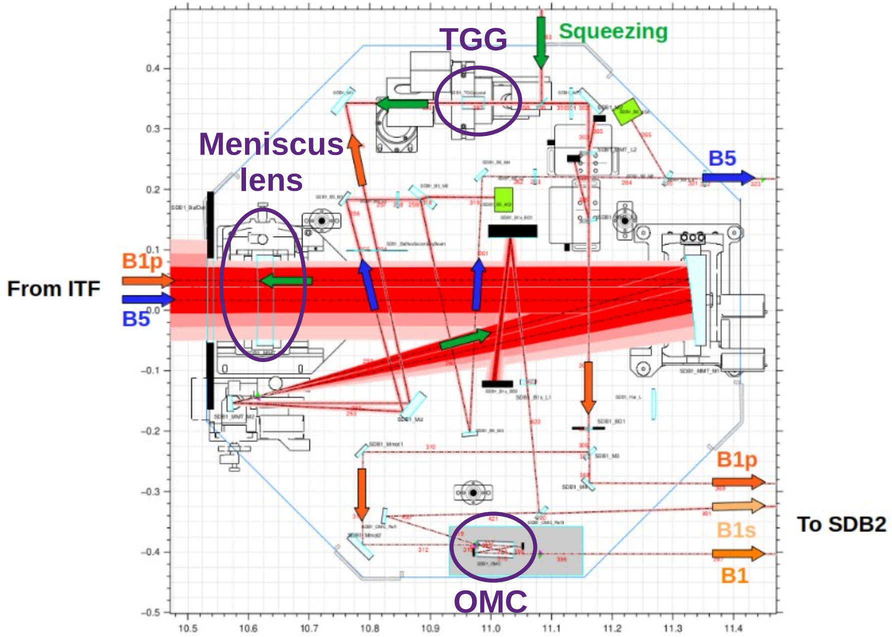

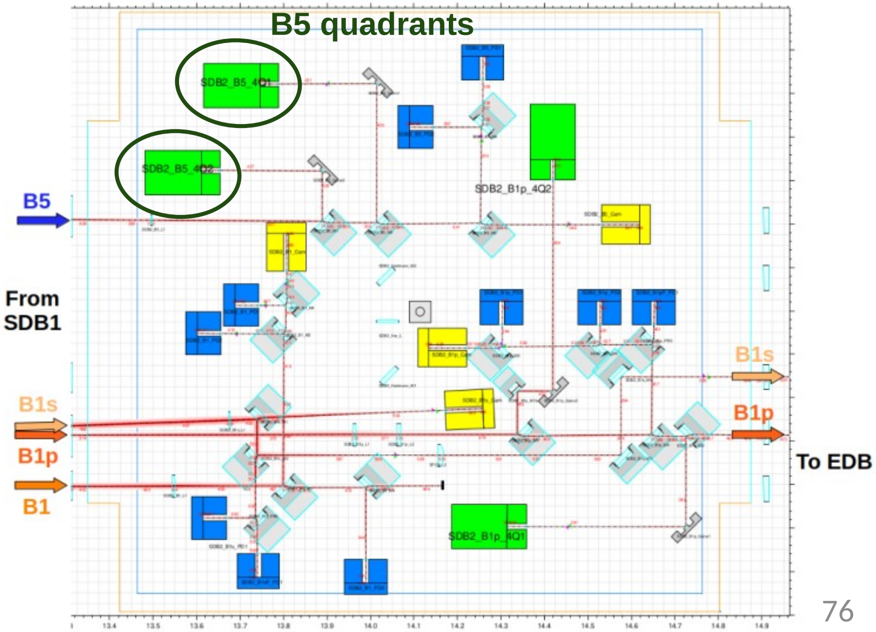

Outline

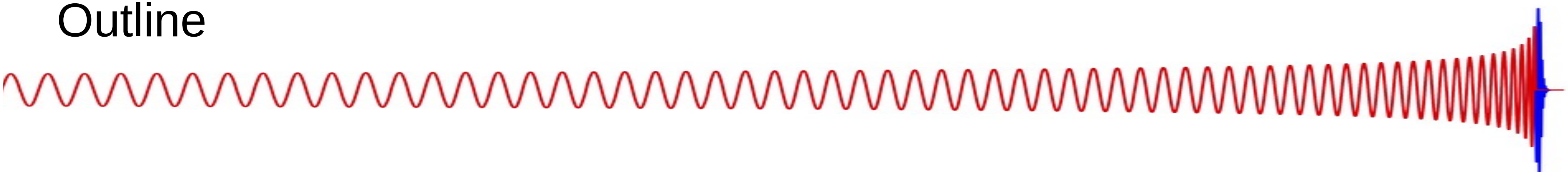

1. Gravitational waves: origin & detection
2. Quantum noise: origin & reduction strategy
3. The Virgo detector from the observing run O3 to O4
4. Frequency dependent squeezing system: installation and commissioning
5. Low loss Output Mode Cleaner: characterization, installation and commissioning
6. Scattered light noise: study and mitigation
7. Conclusions and next steps

Conclusions & next steps

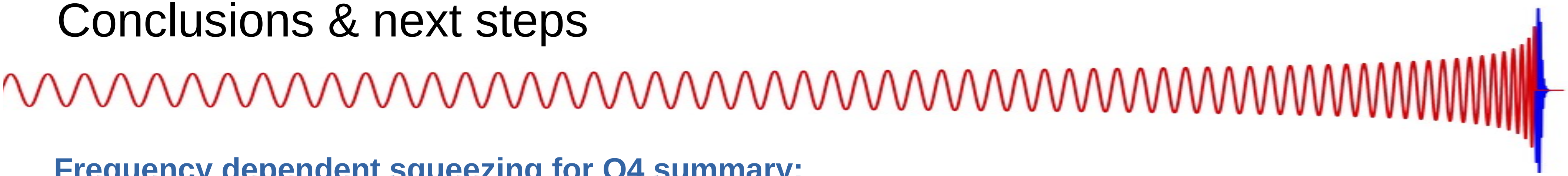

Frequency dependent squeezing for O4 summary:

- Suspended benches installed and controlled
- Full system properly aligned and controlled
- First FDS measurement performed at 25Hz
- Squeezed beam pre-aligned and pre-mode matched with the ITF beam

Next steps in O4:

- Injection of FIS/FDS in the ITF
- Fine alignment and matching (transmission of the OMC)
- Phase control of the squeezing in ITF
- Angular control of the squeezing in ITF

Next steps in O5 / post O5:

- Further squeezing degradation reduction
- Squeezer in vacuum on SQB1 (less optical losses and scattered light noise)

Conclusions & next steps

New Output Mode Cleaner for O4 summary:

- OMC cavity characterized and controlled at LAPP
- OMC cavity installed and commissioned on site
- Detection losses reduced by a factor 2 with respect to O3

Next steps in O4:

- OMC automatic alignment to keep it aligned during the run

Next steps in O5 / post O5:

- Replacement with a four mirrors bow-tie ring cavity to reduce internal losses

Conclusions & next steps

Stray light study and mitigation for O4:

- Scattered light noise from suspended benches projected for O4
- Secondary beams on suspended benches mitigated for O4
- Scatterometer at LAPP used to measure light back-scattered by optics

Next steps in O4:

- Measure at LAPP the BRDF of TGG crystal and OMC cavity
- Measure the scattered light noise coming from the benches
- Mitigation by installing beam dumps in front of quadrants on SDB2

Next steps in O5 / post O5:

- New motorized mount for the SDB1 meniscus lens
- Replacement of critical elements with low scattering ones

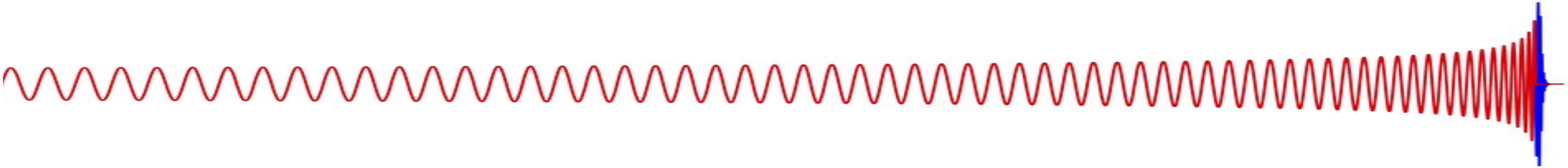

Thanks for the attention!

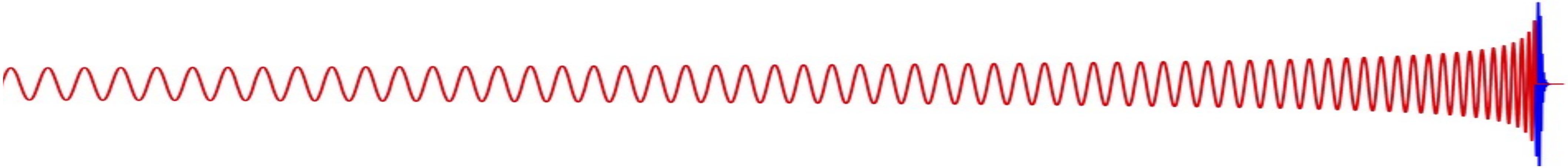

Back-up slides

Quantum noise – semi-classical approach

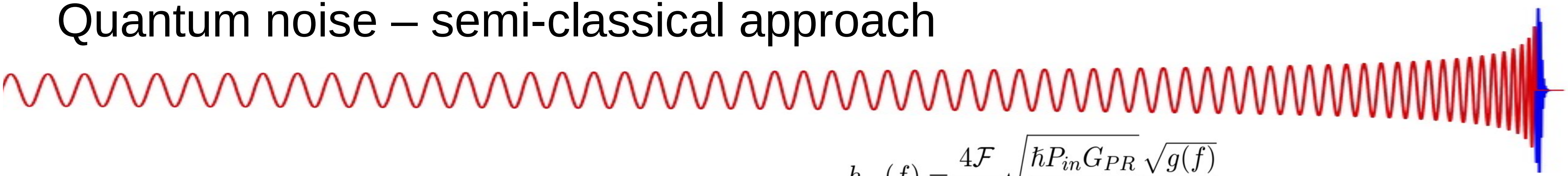

$$h_{rp}(f) = \frac{4\mathcal{F}}{ML}\sqrt{\frac{\hbar P_{in} G_{PR}}{\pi^5 c \lambda}}\frac{\sqrt{g(f)}}{f^2}$$

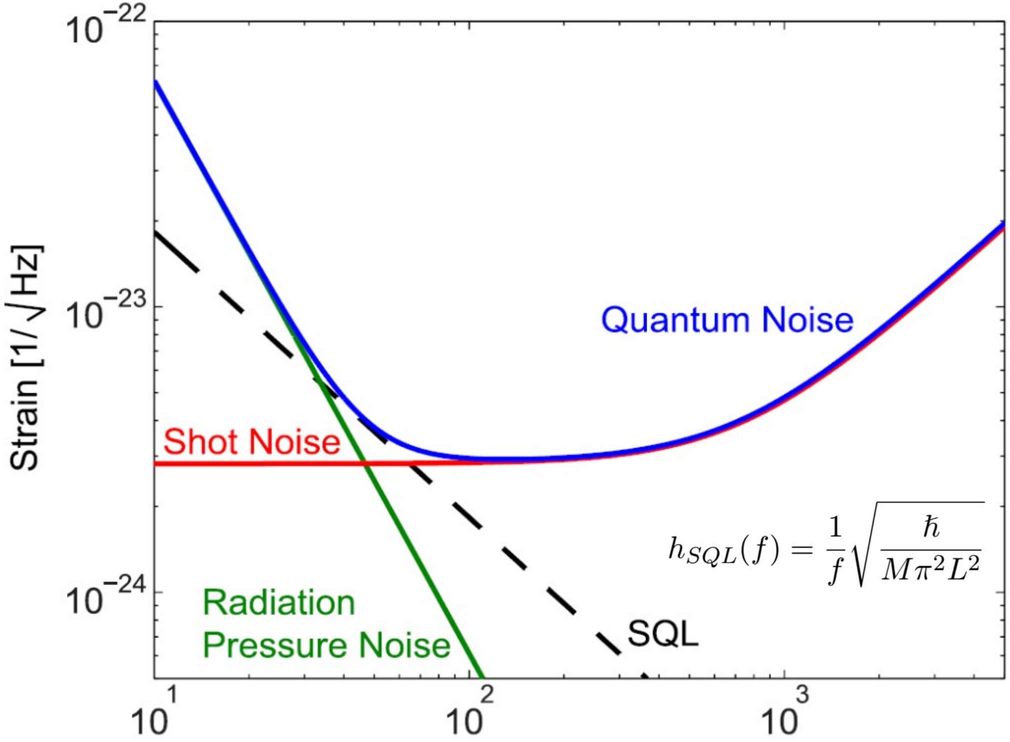

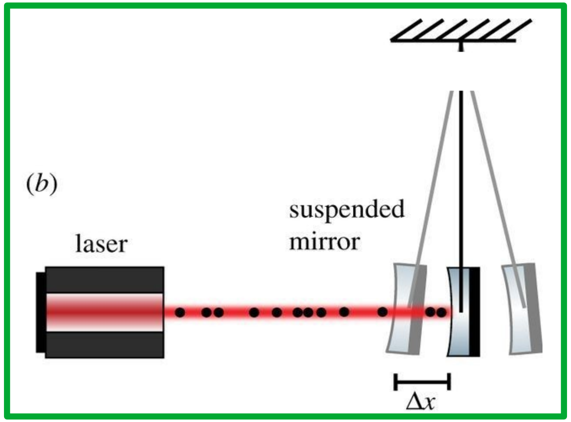

$$h_{shot}(f) = \frac{\lambda}{4\mathcal{F}L}\sqrt{\frac{\hbar\omega}{P_{in} G_{PR}}}\frac{1}{\sqrt{g(f)}}$$

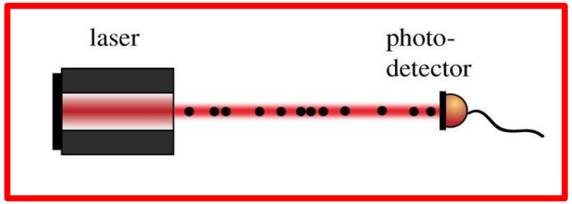

Vacuum squeezed states generation

Vacuum squeezed states are generated by the interaction of the vacuum fluctuation with a bright pump field inside a non linear crystal, called Optical Parametric Oscillator (OPO).

$$\hat{\mathcal{H}} = \hbar\omega\hat{a}^{\dagger}\hat{a} + \hbar\omega_p\hat{b}^{\dagger}\hat{b} + i\hbar\chi^{(2)}\left(\hat{a}^2\hat{b}^{\dagger} - \hat{a}^{\dagger 2}\hat{b}\right)$$

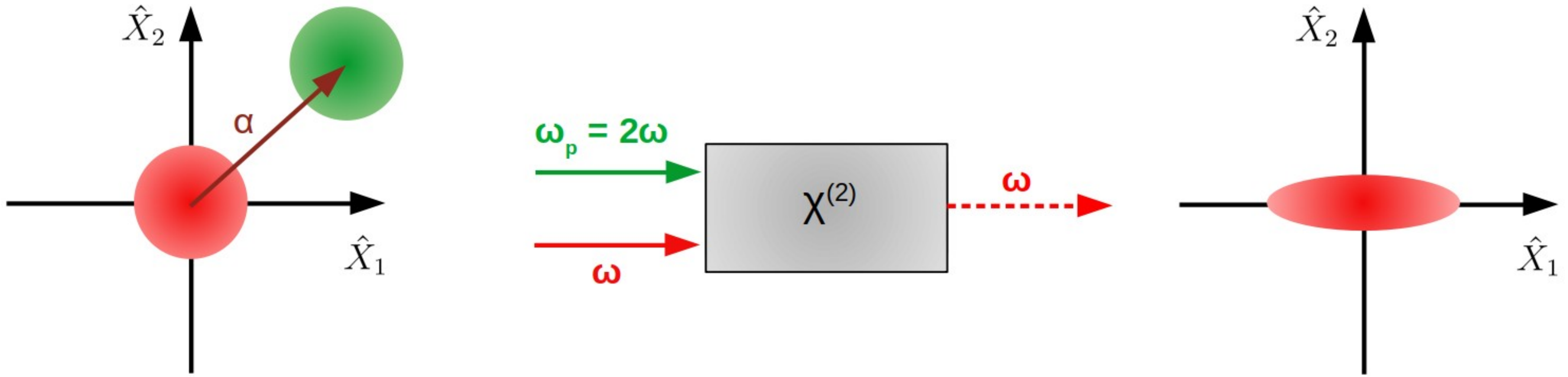

Vacuum squeezed states degradation: optical losses

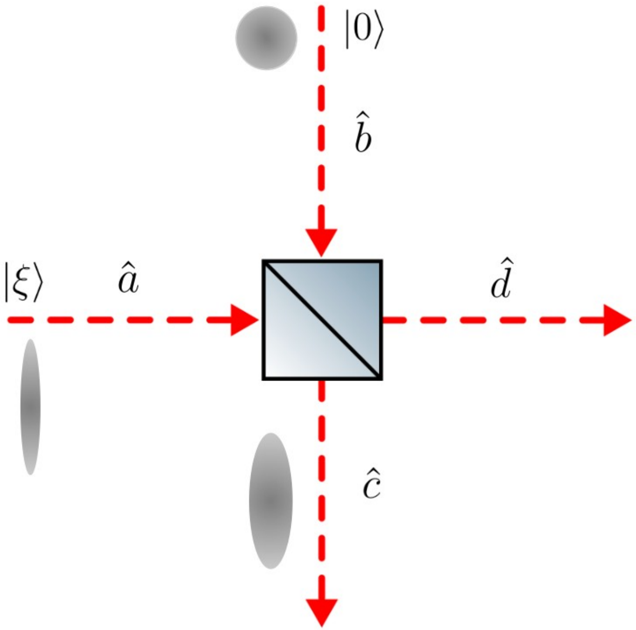

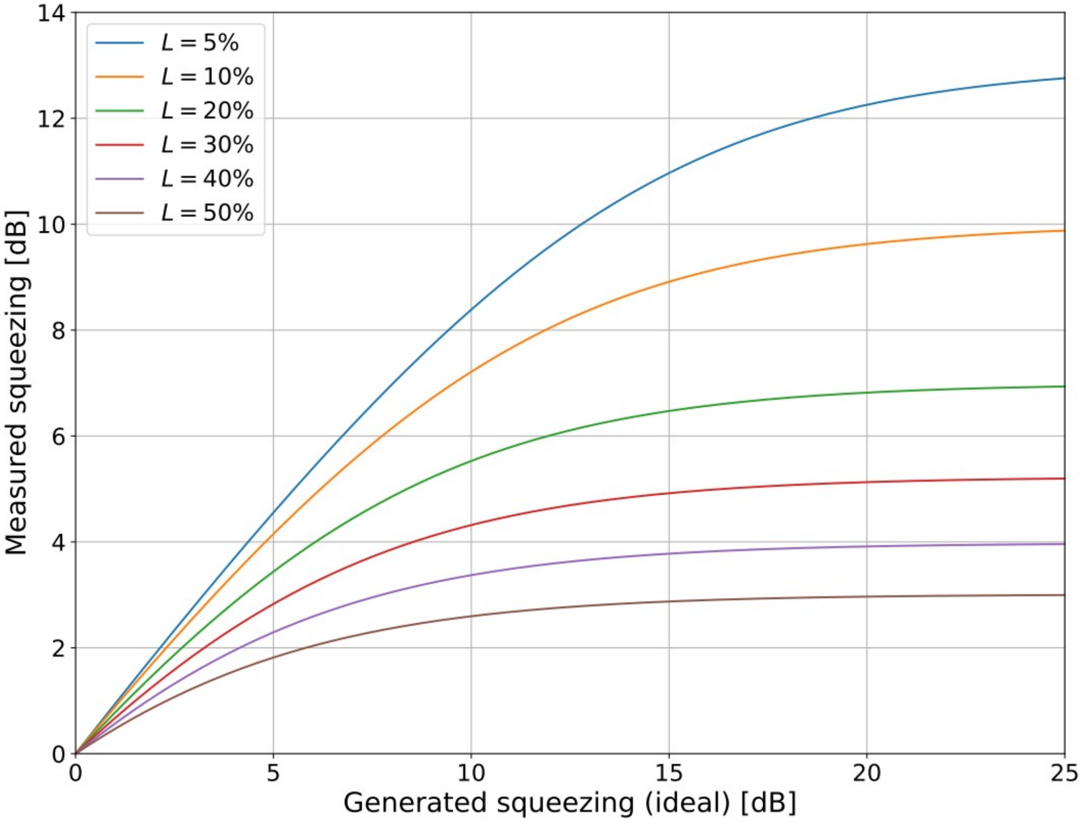

Vacuum squeezed states degradation: phase noise

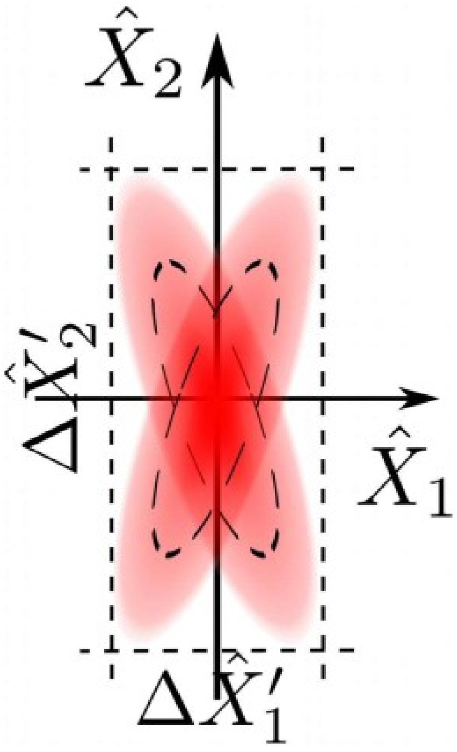

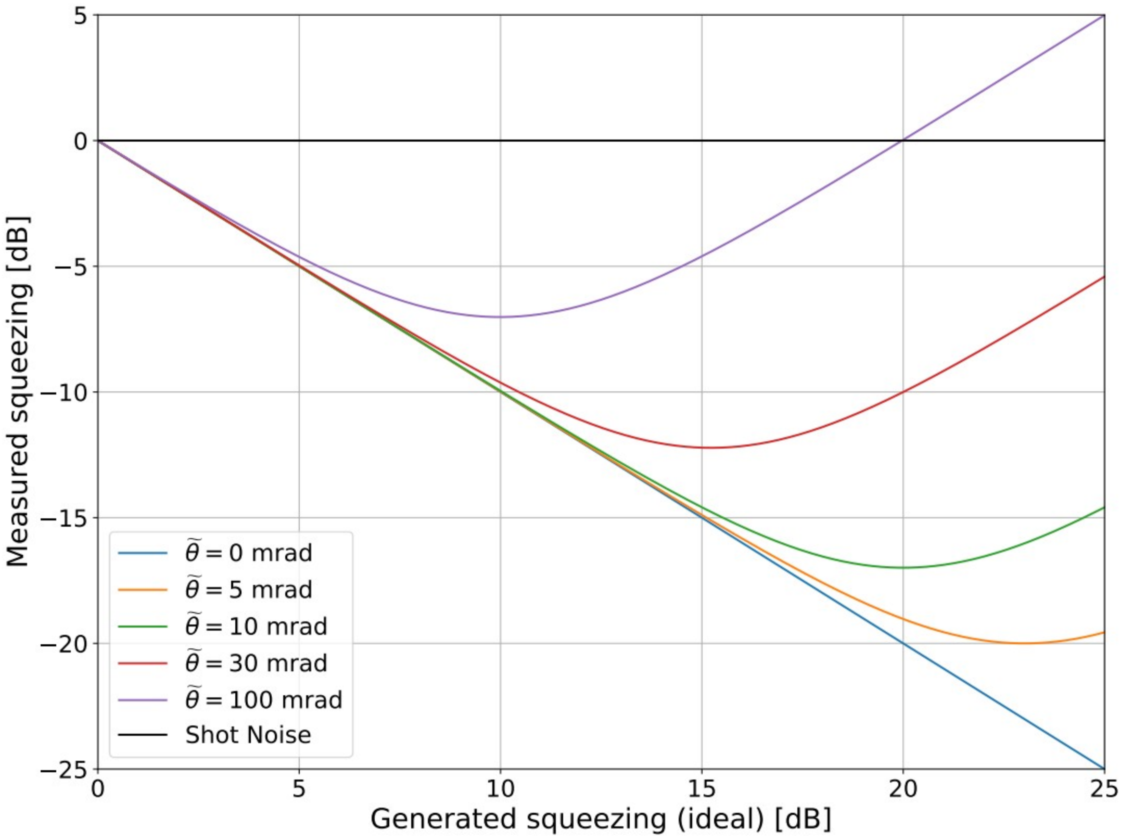

Construction of coefficient matrices: example of SQB1 TX

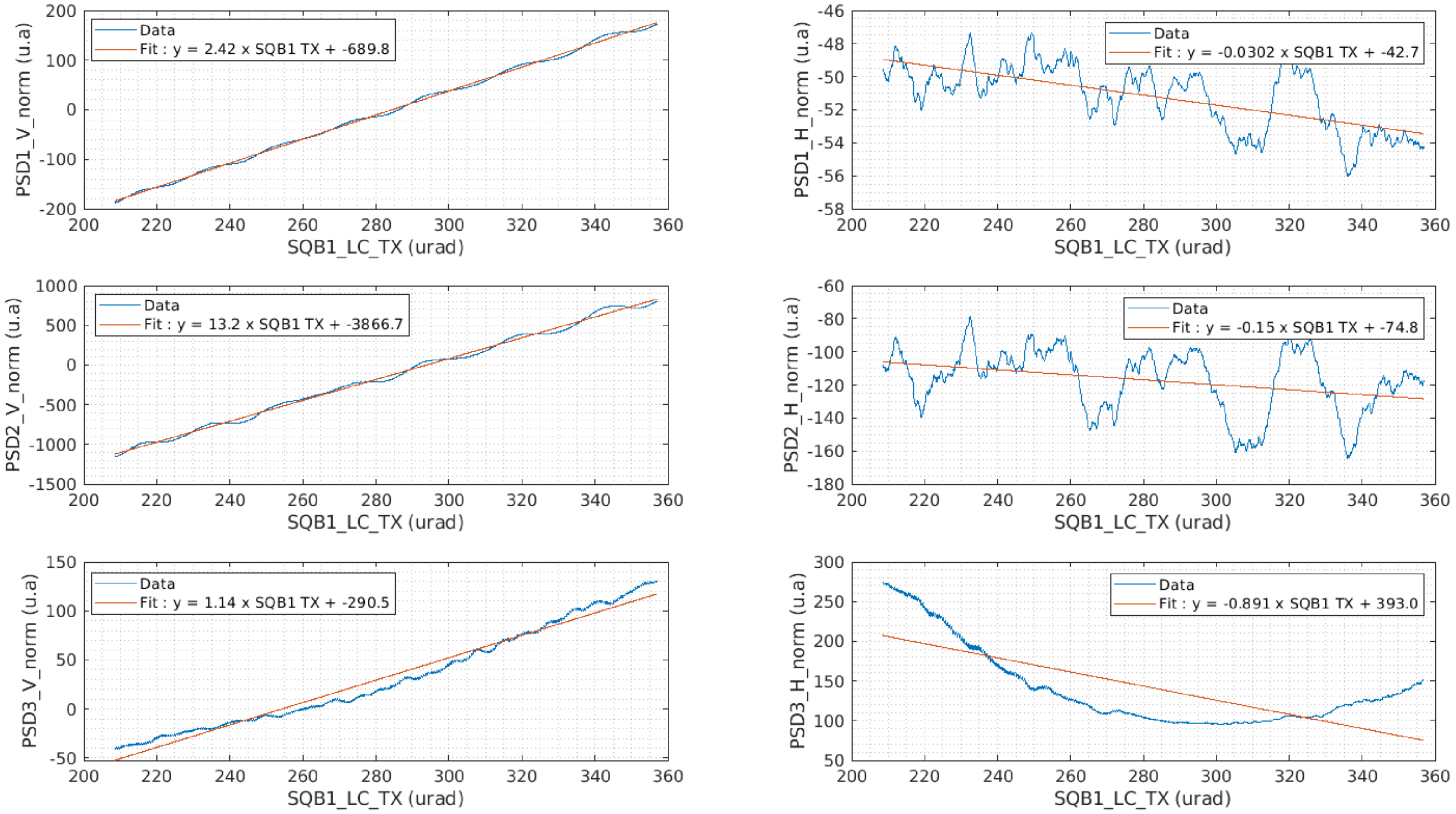

SQB1 reconstructions with sensing matrix M_A

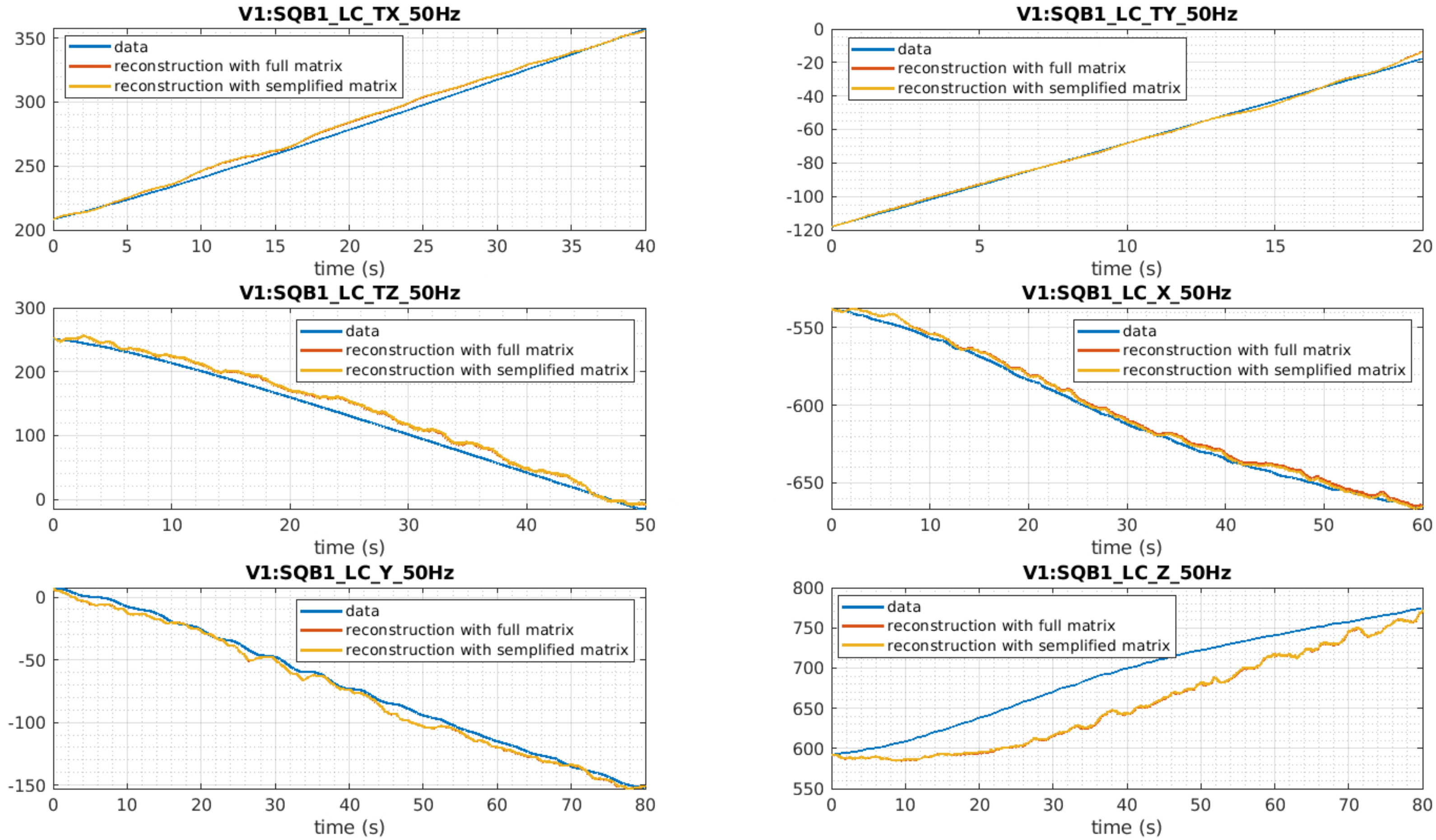

SQB1 reconstructions with sensing matrix M_B

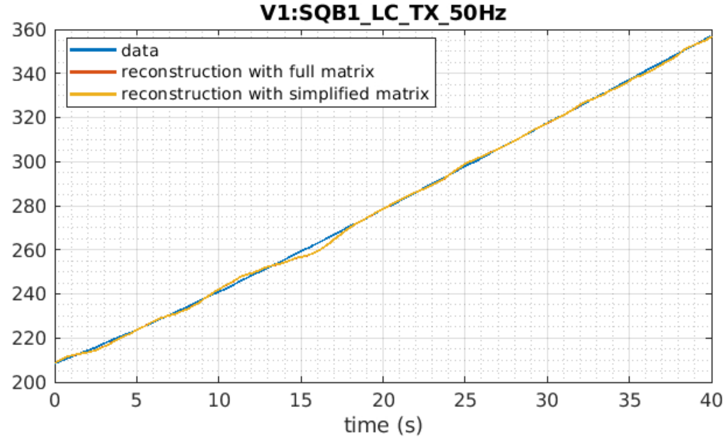

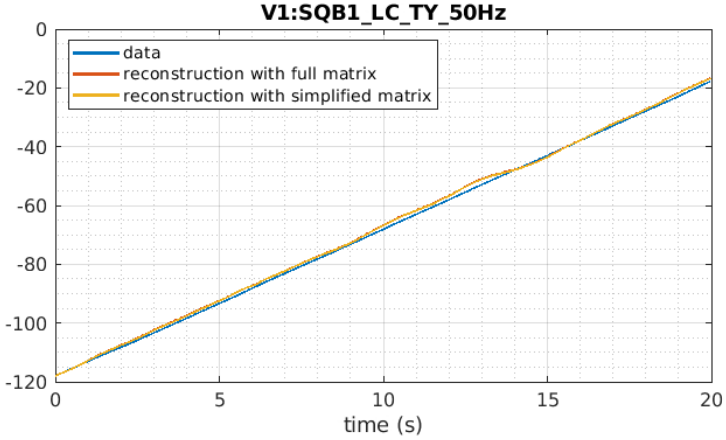

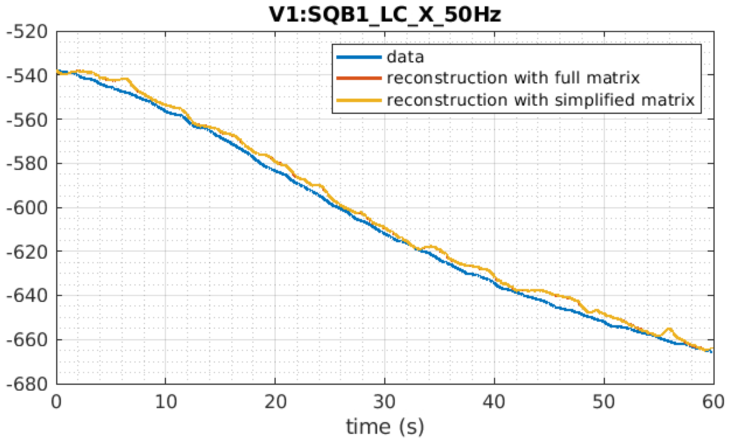

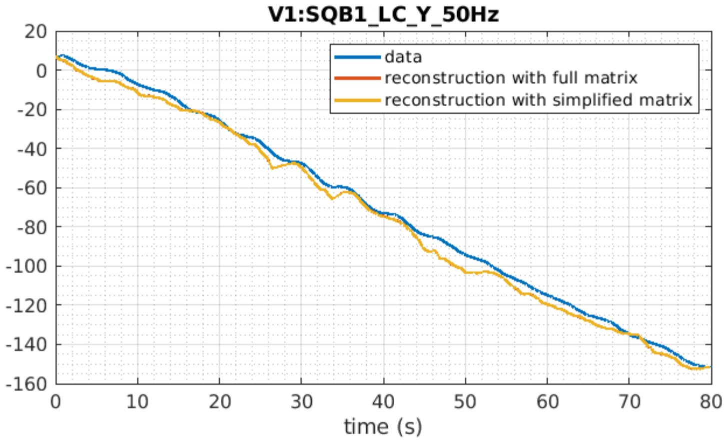

SQB1 reconstructions with sensing matrix M_C

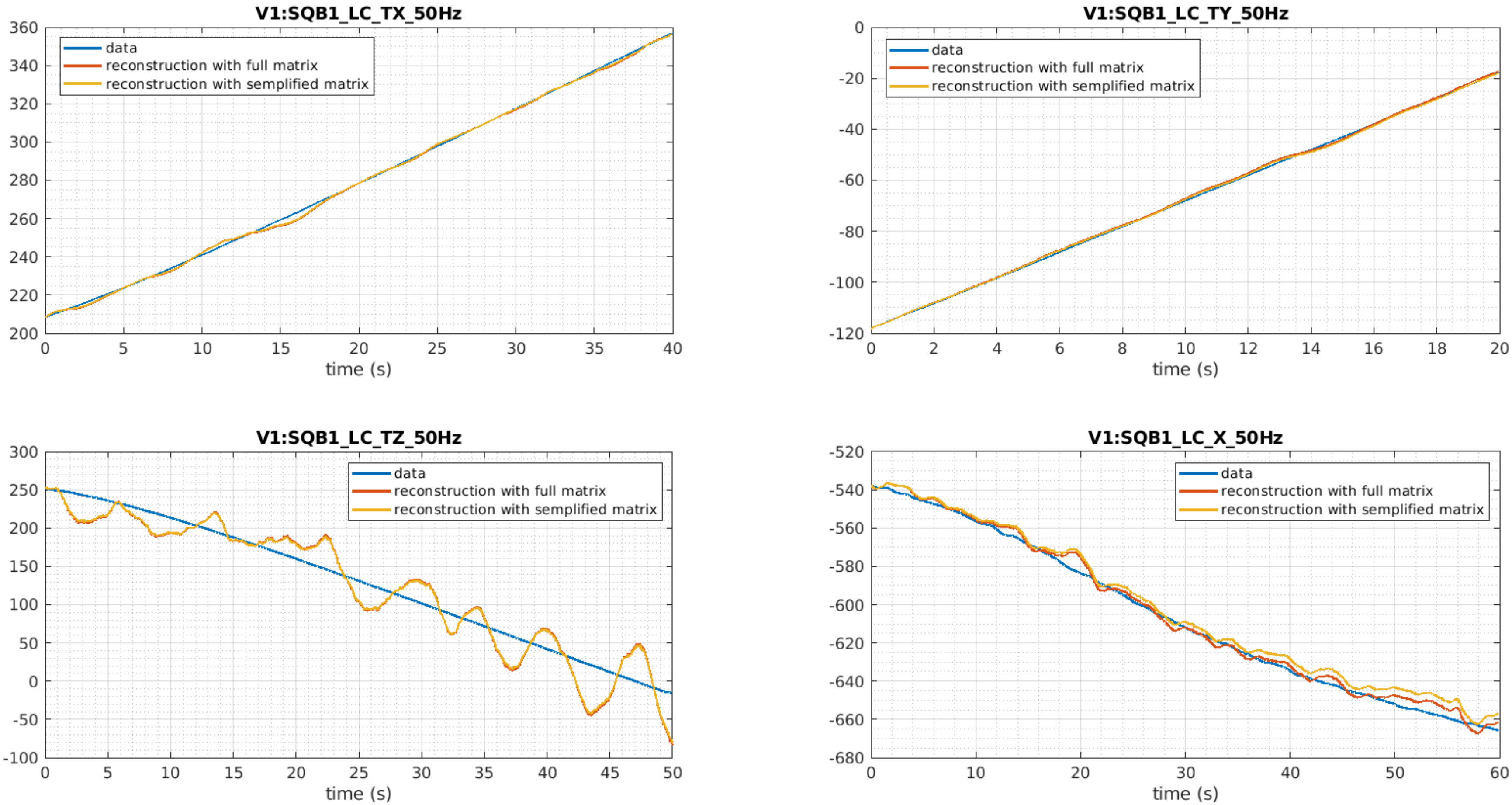

From FIS to FDS

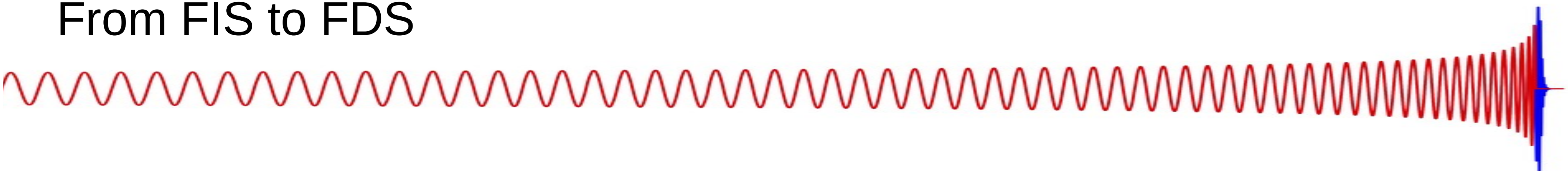

FIS in O3

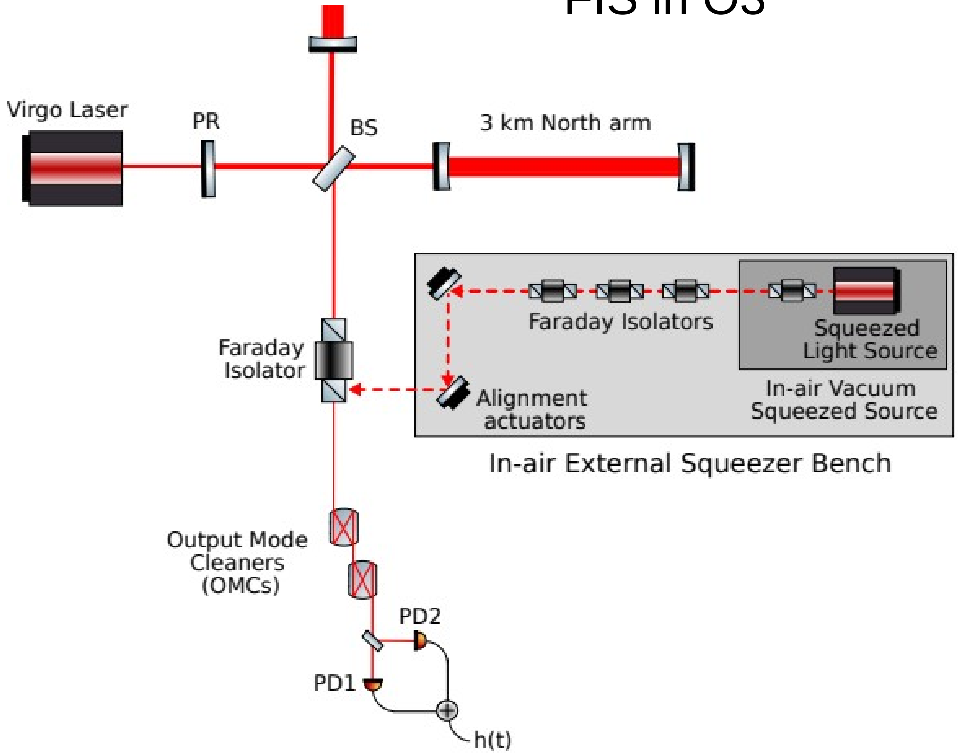

FDS for O4

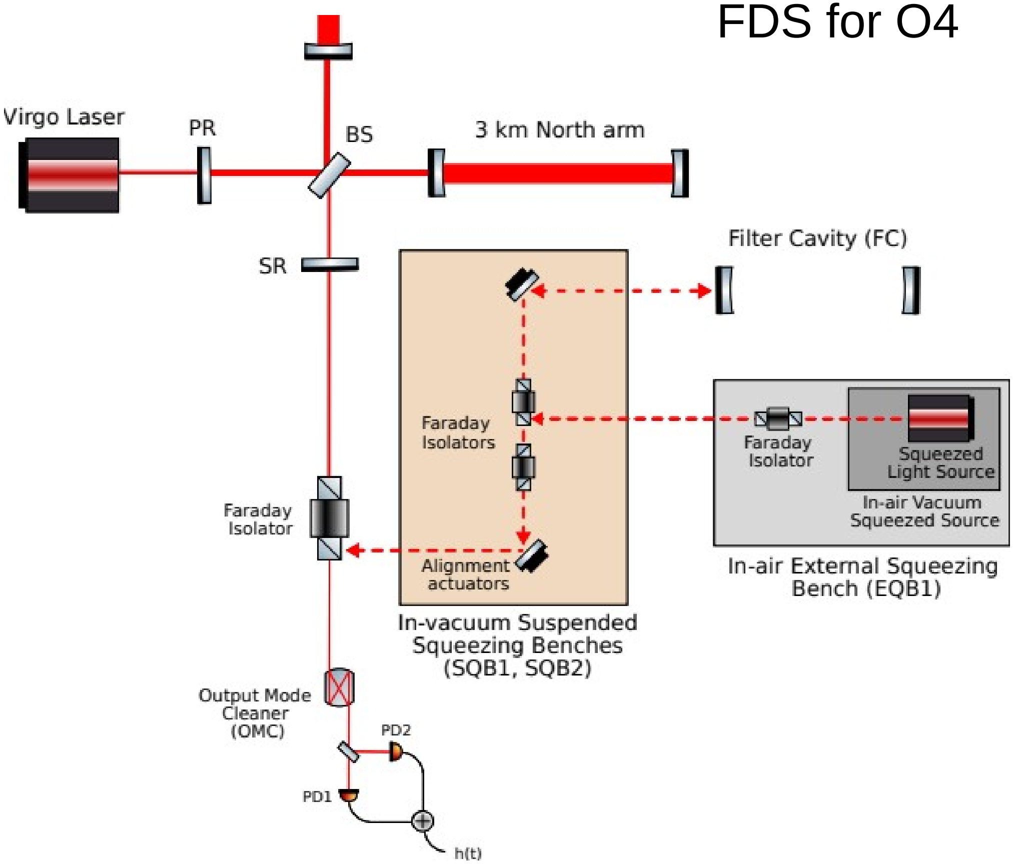

Quantum noise reduction

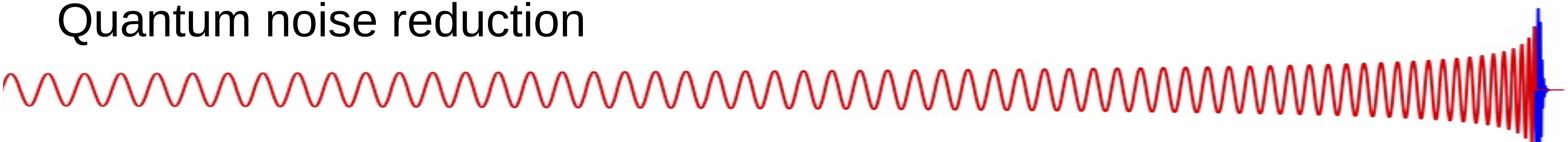

Quantum noise can be reduced by introducing vacuum squeezed states from the output port of the detector.

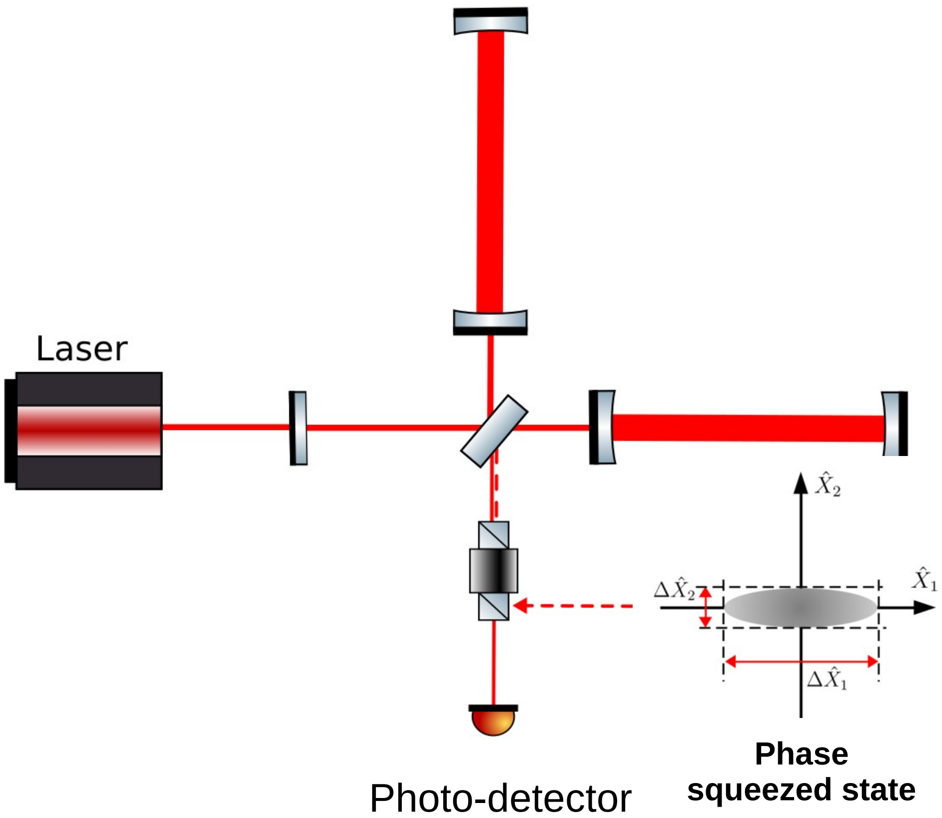

Squeezed states have smaller fluctuations in one quadrature and larger in the other for the *Heisenberg Uncertainty Principle*:

$$\Delta\hat{X}_1 > \frac{1}{4} \qquad \Delta\hat{X}_2 < \frac{1}{4}$$

They are generated by a non-linear optical process inside an **Optical Parametric Oscillator (OPO)**.

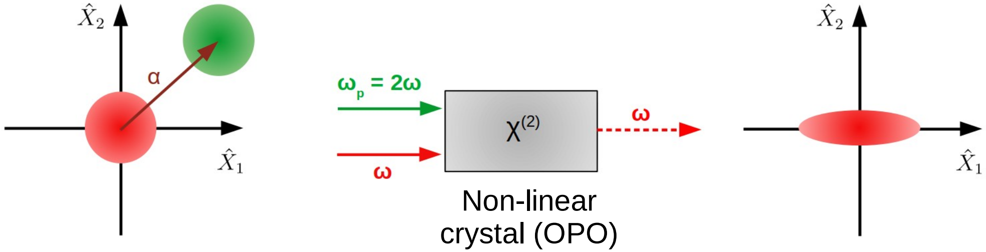

FDS loss budget

	Expected for O4	Measured in November 2021	Measured in June 2022
Filter cavity RTL	40 ppm	31 ppm	31 ppm
Phase noise	20-60 mrad	30 mrad*	30 mrad*
Filter cavity rms length fluctuation	< 1 Hz	8.3 Hz**	~ 1 Hz**
Filter cavity mode mismatch	2%	1%	1%
SC to OPA matching	2%	1%	1%
Propagation losses	2-3%	13-15%	~7%

* 30 mrad up to EQB1 does not include the extra phase noise due to the propagation in the ITF
** with 8Hz of frequency noise we can measure 4dB of high frequency SQZ in the ITF without spoiling the low frequency

OMC characterization at LAPP : Finesse and RoC

Finesse and **radius of curvature** measured from the OMC temperature scans:

F_{meas} = 1055 ± 15

RoC_{meas} = (1689 ± 2) mm

$$P_{DC} = \sum^{N} \frac{P_{max}(N)}{1 + \left(\frac{2F}{\pi}\right)^2 \sin^2\left(\frac{2\pi L_{opt}\nu}{c} - N \arccos\left(\sqrt{1 - \frac{2L_{geo}}{\rho}}\right)\right)}$$

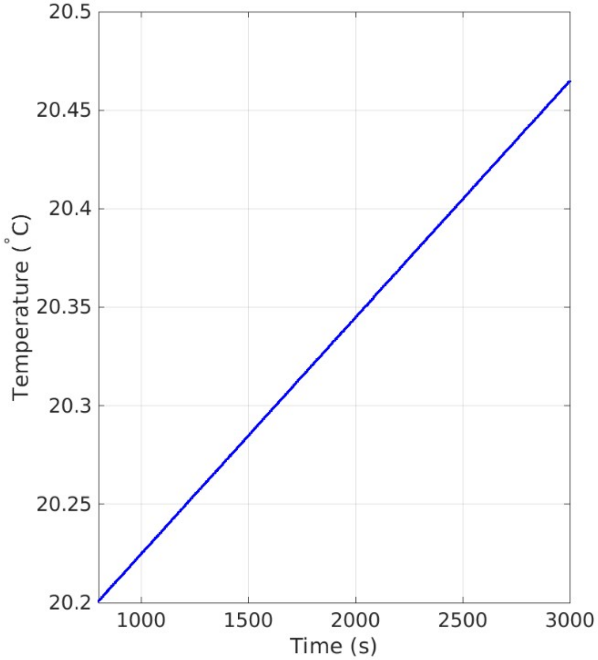

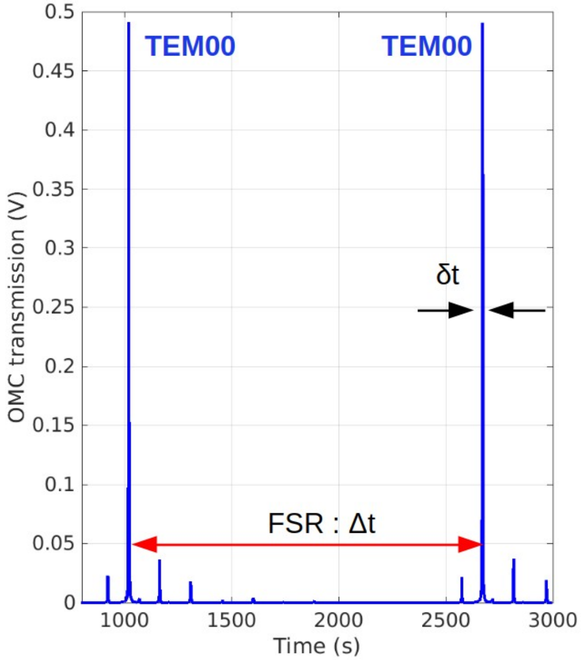

VIR-0635A-22

Stray light measurement during O3

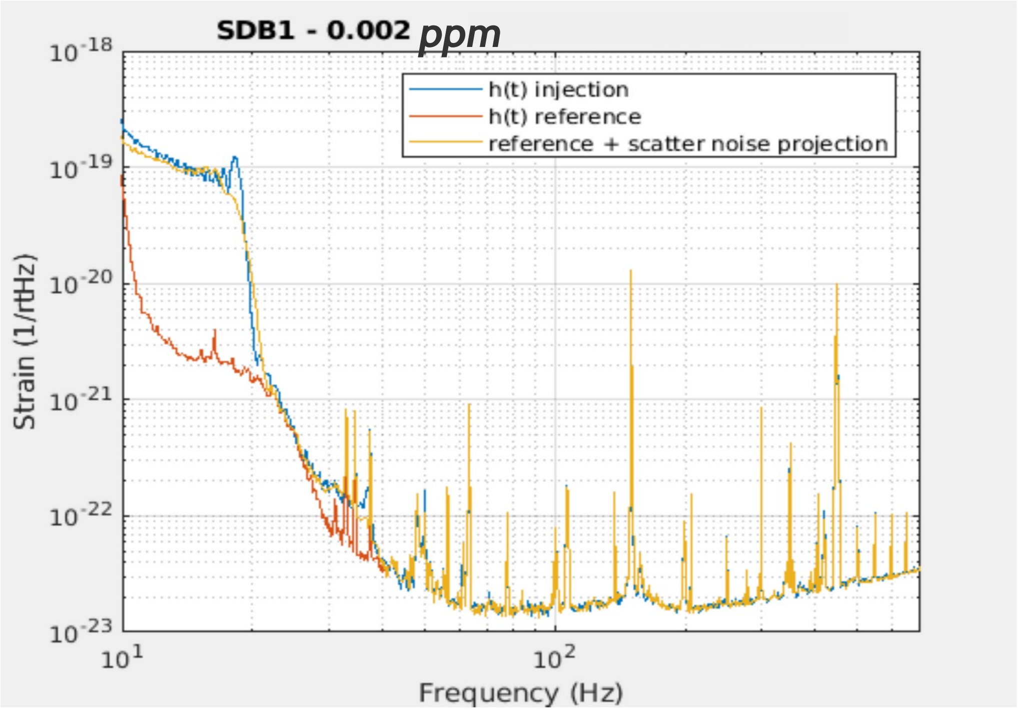

- Noise injection on the bench to be in fringe wrapping approximation – excitation up to 25 Hz:

$$h_r(f) \propto \sqrt{\frac{f_r}{f_{max}}} \cdot TF(f) \quad \text{for} \quad f < f_{max} = \frac{2v_{sc}}{\lambda}$$

- Measurement of f_r for different benches:

Bench	f_r measured in O3
SDB1	$2 \cdot 10^{-9}$
SDB2	$4 \cdot 10^{-10}$
SNEB	$3 \cdot 10^{-8}$
SWEB	$5 \cdot 10^{-9}$

VIR-1155B-19

Transfer functions for O4

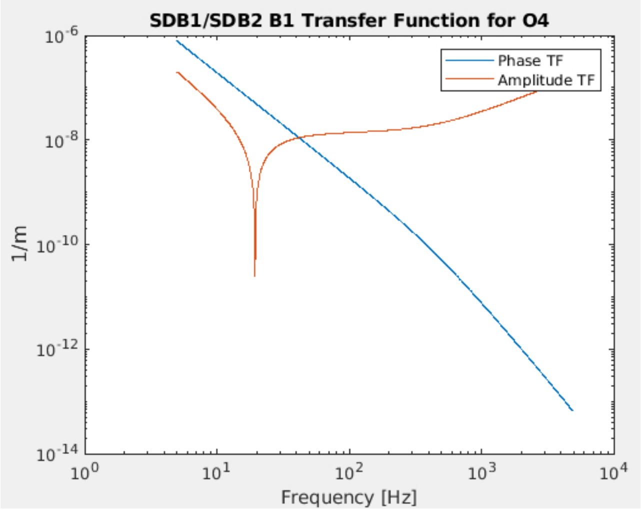

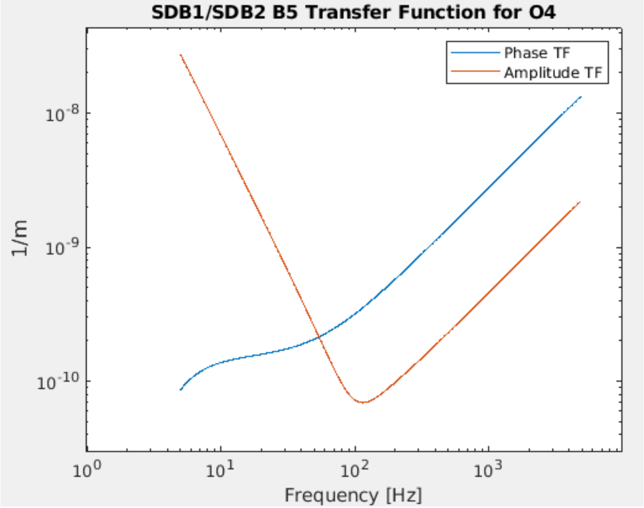

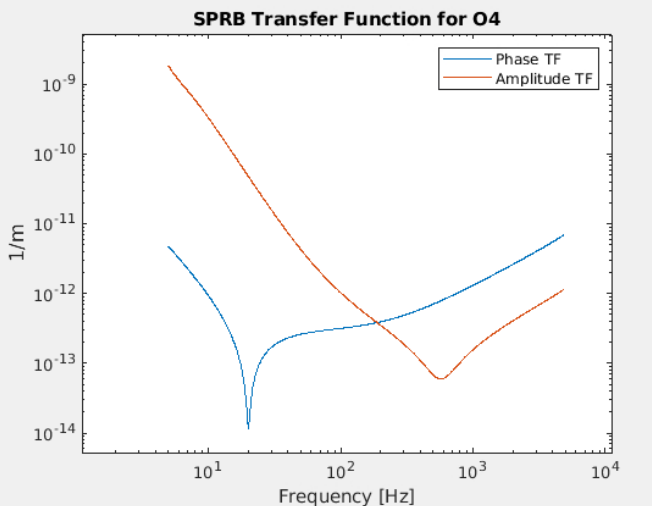

Transfer functions for O4

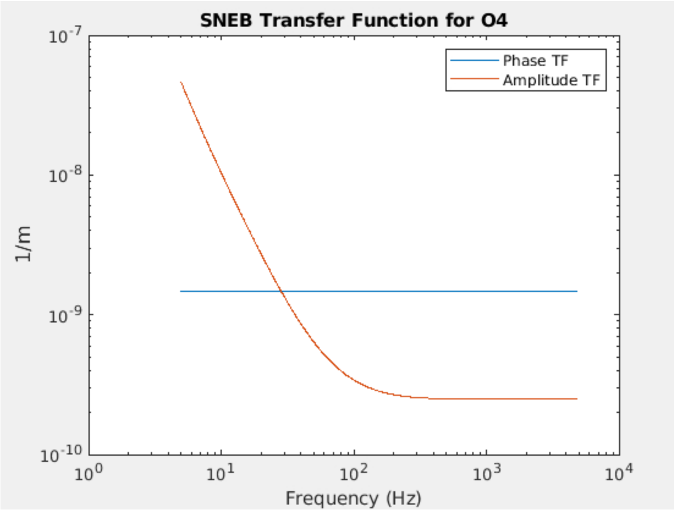

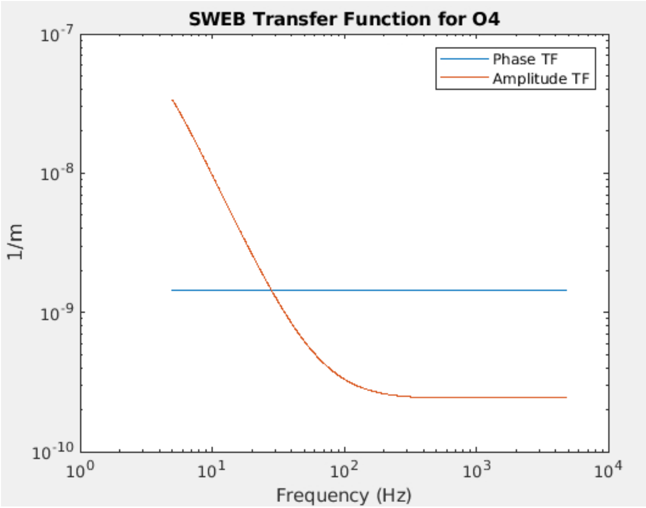

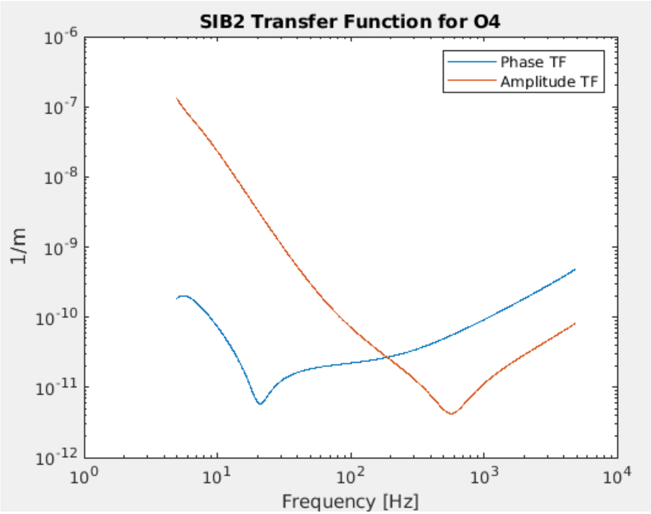

BRDF measurements at LAPP

Results

lambda	1.1E-06		
Optical efficiency	4.3E-01 (using ~50/50 beam splitter and other losses, so this is expected)		
Interferometer visibility	8.5E-01	3.9E-01	4.4E-01
Measurement efficiency	3.9E-01		
beam waist	1.6E-04	1.3E-04	
waist position	1.3E-01	1.3E-01	
Rayleigh range	7.6E-02	5.0E-02	

Object	Position (m)	Beam radius X	Beam radius Y	f_sc	BRDF (1 pol)	comments
Teflon target	0.1	1.7E-04	1.5E-04	8.0E-07	1.5E-01	
Teflon target	0.2	2.2E-04	2.2E-04	4.3E-07	1.5E-01	S-pol, scatter in both polarization equally, expect BRDF~0.16 per polarization
Teflon target	0.2	2.2E-04	2.2E-04	4.7E-07	1.6E-01	P-pol
Teflon target	0.4	5.9E-04	7.2E-04	4.7E-08	1.4E-01	S-pol
ND filter (NENIR40B-C)	0.2	2.2E-04	2.2E-04	4.0E-10	1.4E-04	S-pol, 3.3deg AOI
ND filter (NENIR40B-C)	0.2	2.2E-04	2.2E-04	1.5E-11	5.2E-06	P-pol, 3.3deg AOI
ND filter (NENIR40B-C)	0.2	2.2E-04	2.2E-04	9.0E-11	3.1E-05	S-pol, 19deg AOI
ND filter (NENIR40B-C)	0.2	2.2E-04	2.2E-04	1.6E-11	5.6E-06	P-pol, 19deg AOI
Newfocus 9809 anodized	0.2	2.2E-04	2.2E-04	1.8E-07	6.3E-02	45deg AOI
Newfocus 9809 vacuum	0.2	2.2E-04	2.2E-04	3.0E-08	1.0E-02	45deg AOI
SIN mount anoblack	0.2	2.2E-04	2.2E-04	2.2E-08	7.6E-03	45deg AOI
Silcon beam dump	0.2	2.2E-04	2.2E-04	3.0E-10	1.0E-04	1deg AOI, S-pol, measurement affected by scratch?
Silcon beam dump	0.2	2.2E-04	2.2E-04	1.1E-11	3.8E-06	1deg AOI, P-pol, measurement affected by scratch?
LAPP QPD	0.2	2.2E-04	2.2E-04	1.0E-08	3.5E-03	~5deg AOI, YAG-444-4A (Excelitas)
NIKHEF QPD	0.2	2.2E-04	2.2E-04	8.6E-06	3.0E+00	AOI as feet designed, ~5deg
Excelitas PD	0.2	2.2E-04	2.2E-04	1.4E-10	4.9E-05	AOI 20 deg (vertical inclination), S-pol for beam in bench referential
PD box window	0.2	2.2E-04	2.2E-04	2.0E-11	7.0E-06	AOI 20 deg (vertical inclination), S-pol for beam in bench referential
Glass diffuser, 1500 grit	0.2	2.2E-04	2.2E-04	2.4E-08	8.3E-03	S-pol, AOI ~ 15deg? – with power meter measured BRDF~0.02
Glass diffuser, 1500 grit	0.2	2.2E-04	2.2E-04	1.0E-09	3.5E-04	P-pol

Improved alignment of scatter measurement

Interferometer visibility		9.0E-01	3.2E-01		5.2E-01	
Measurement efficiency		5.4E-01				
Object	**Position (m)**	**Beam radius X**	**Beam radius Y**	**f_sc**	**BRDF (1 pol)**	**comments**
Teflon target	0.025	2.7E-04	3.0E-04	4.4E-07	1.9E-01	S-pol
Teflon target	0.1	1.7E-04	1.5E-04	1.1E-06	1.4E-01	S-pol
Teflon target	0.125	1.6E-04	1.3E-04	1.3E-06	1.4E-01	S-pol
Teflon target	0.15	1.7E-04	1.4E-04	1.3E-06	1.6E-01	S-pol

Measurements of BRDF performed at LAPP by Michal Was

Estimation of f_r for O4

Bench	f_r measured in O3	f_r estimate for O3	f_r estimate for O4
SDB1	$2 \cdot 10^{-9}$ (*)	$6.4 \cdot 10^{-10}$ (B1) $4.1 \cdot 10^{-10}$ (B5)	$1.5 \cdot 10^{-9}$ (B1) $4.1 \cdot 10^{-10}$ (B5)
SDB2	$4 \cdot 10^{-10}$ (*)	$2.3 \cdot 10^{-14}$ (B1) $3.2 \cdot 10^{-7}$ (B5)	$3.2 \cdot 10^{-14}$ (B1) $1.2 \cdot 10^{-6}$ (B5)
SNEB	$3 \cdot 10^{-8}$	$5.2 \cdot 10^{-8}$ (**)	$1.67 \cdot 10^{-8}$
SWEB	$5 \cdot 10^{-9}$	$7.7 \cdot 10^{-9}$ (***)	$2.16 \cdot 10^{-8}$
SPRB	-	$1.6 \cdot 10^{-7}$	$1.6 \cdot 10^{-7}$

(*) For SDB1 and SDB2 have been used the B1 transfer function.
(**) On SNEB it has been considered that one quadrant shutter was open in O3.
(***) On SWEB it has been considered that the quadrant shutters were both closed.
NB. the lenses L1a and L1b are considered perpendicular to the beam, L2 tilted.

[a]Yoshida, Hidetsugu, et al. "Optical properties and Faraday effect of ceramic terbium gallium garnet for a room temperature Faraday rotator." Optics Express 19.16 (2011): 15181-15187

[b]Chen, Xu, et al. "Rayleigh scattering in fused silica samples for gravitational wave detectors." Optics Communications 284.19 (2011): 4732-4737

SDB1:

- TGG Rayleigh[a] = $3.1 \cdot 10^{-10}$
- OMC Rayleigh[b] = $8.6 \cdot 10^{-10}$
- Meniscus lens = $2.2 \cdot 10^{-10}$ (assuming β = 0)

SDB2:

- B5 quadrants = $6 \cdot 10^{-7}$ (each)

SNEB/SWEB:

- Lenses L1a / L1b ~ $3 \cdot 10^{-9}$ (assuming β = 0)
- B7/B8 quadrants ~ $6 \cdot 10^{-9}$ (each)

SPRB:

- Lenses L1a / L1b ~ $3 \cdot 10^{-8}$
- B4 quadrants ~ $6 \cdot 10^{-9}$ (each)

Stray light projections for O4

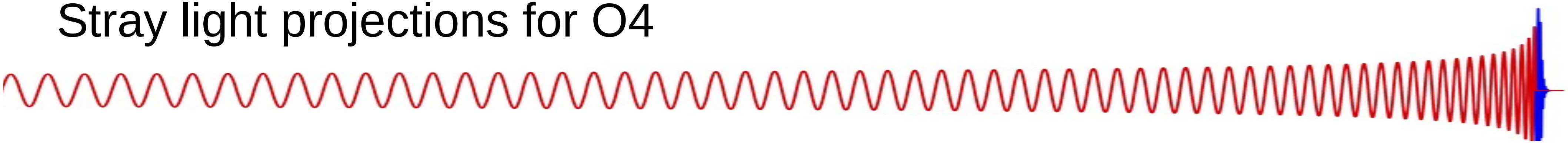

Parameter	O5	Initial post-O5	VnEXT
Injected squeezing	12 dB	12 dB	15 dB
injection losses	6.5%	5.5%	1.8%
FC losses	30 ppm	30 ppm	20 ppm
Readout losses	6%	4.5%	2.5 %
Arm-cavity roundtrip losses	75 ppm	75 ppm	75 ppm
Signal extraction cavity (SEC) roundtrip losses	1000 ppm	1000 ppm	500 ppm
Phase noise	25 mrad	15 mrad	10 mrad
Mismatching squeezing - filter cavity	0.5%	0.5%	0.25%
Mismatching squeezing - interferometer	2%	1%	0.5%
Measured squeezing at high-frequency	**5.5 dB**	**7.5 dB**	**10.5 dB**

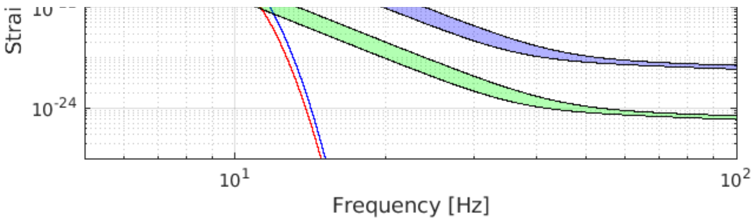

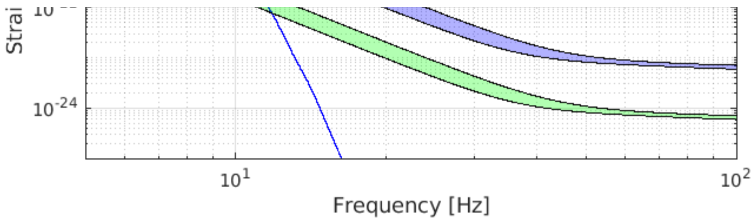

Squeezing loss budget in O5 / post O5

Parameter	O5	Initial post-O5	VnEXT
Injected squeezing	12 dB	12 dB	15 dB
injection losses	6.5%	5.5%	1.8%
FC losses	30 ppm	30 ppm	20 ppm
Readout losses	6%	4.5%	2.5 %
Arm-cavity roundtrip losses	75 ppm	75 ppm	75 ppm
Signal extraction cavity (SEC) roundtrip losses	1000 ppm	1000 ppm	500 ppm
Phase noise	25 mrad	15 mrad	10 mrad
Mismatching squeezing - filter cavity	0.5%	0.5%	0.25%
Mismatching squeezing - interferometer	2%	1%	0.5%
Measured squeezing at high-frequency	**5.5 dB**	**7.5 dB**	**10.5 dB**

FDS characterization

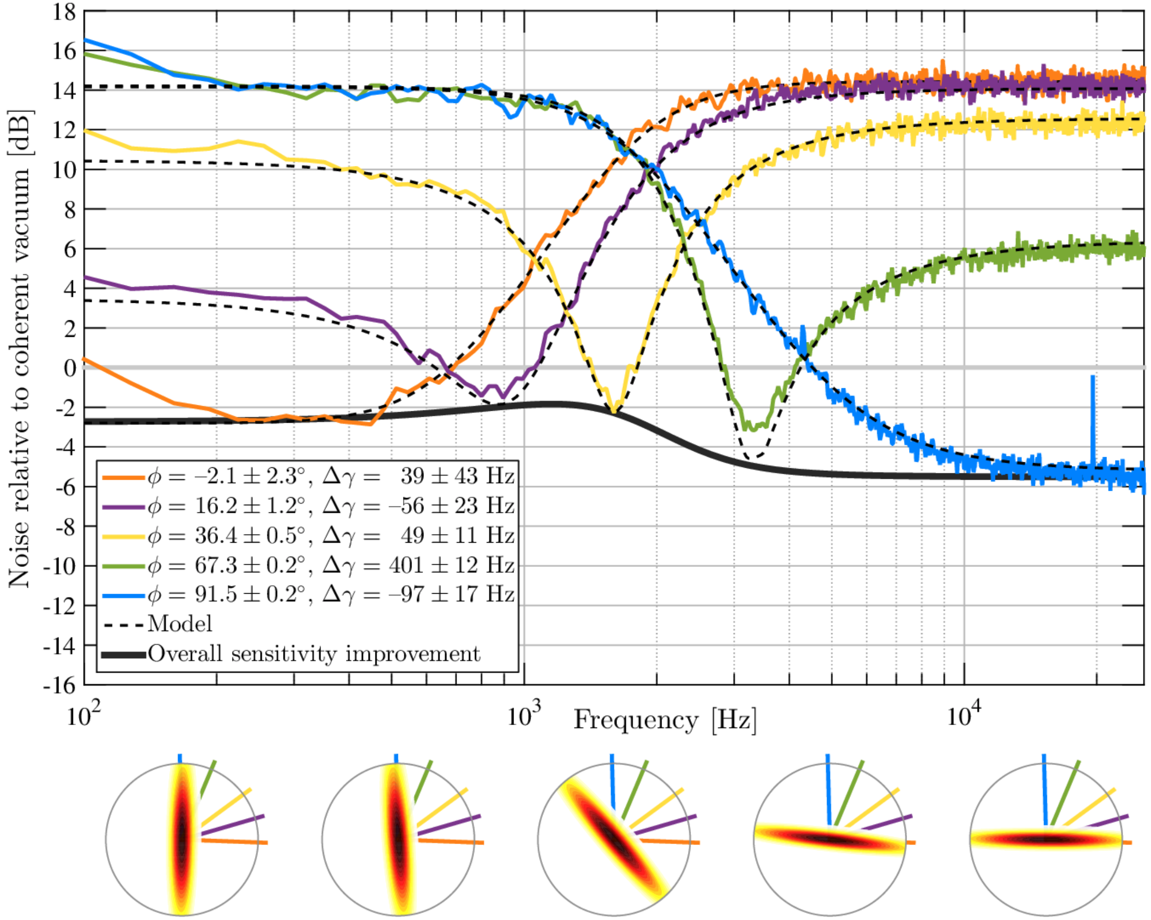

FDS characterization

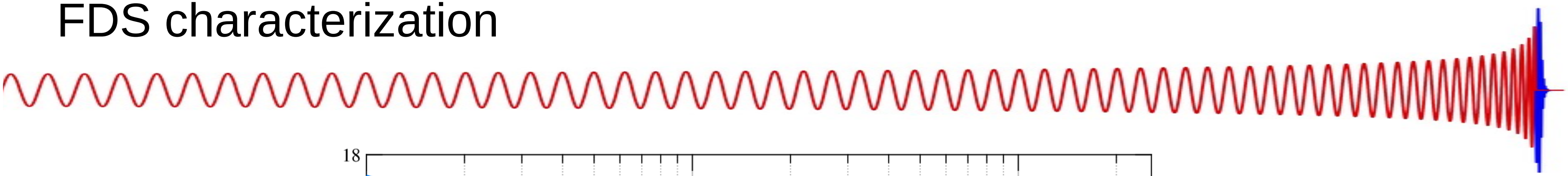

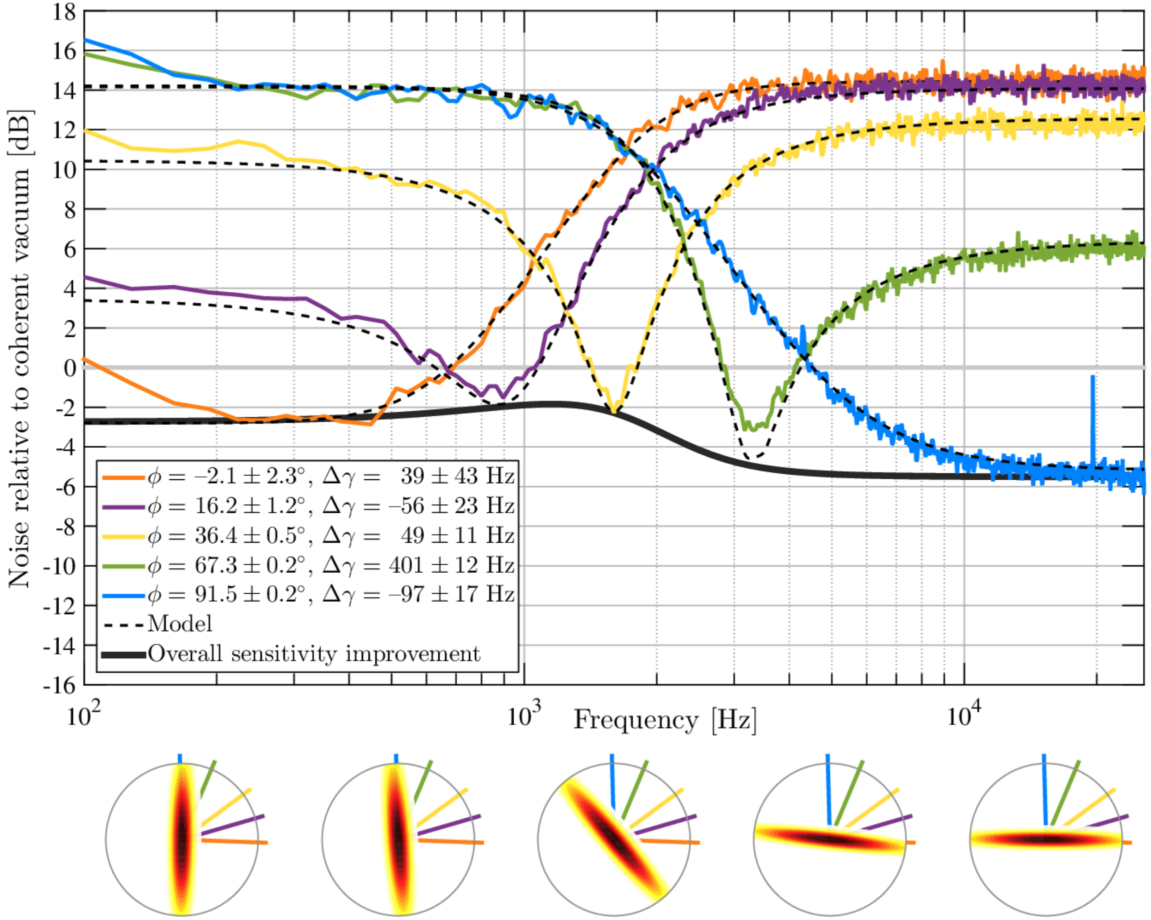

FDS loss budget

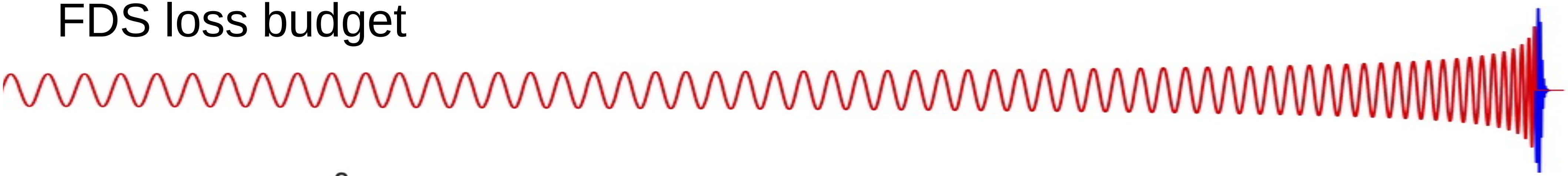

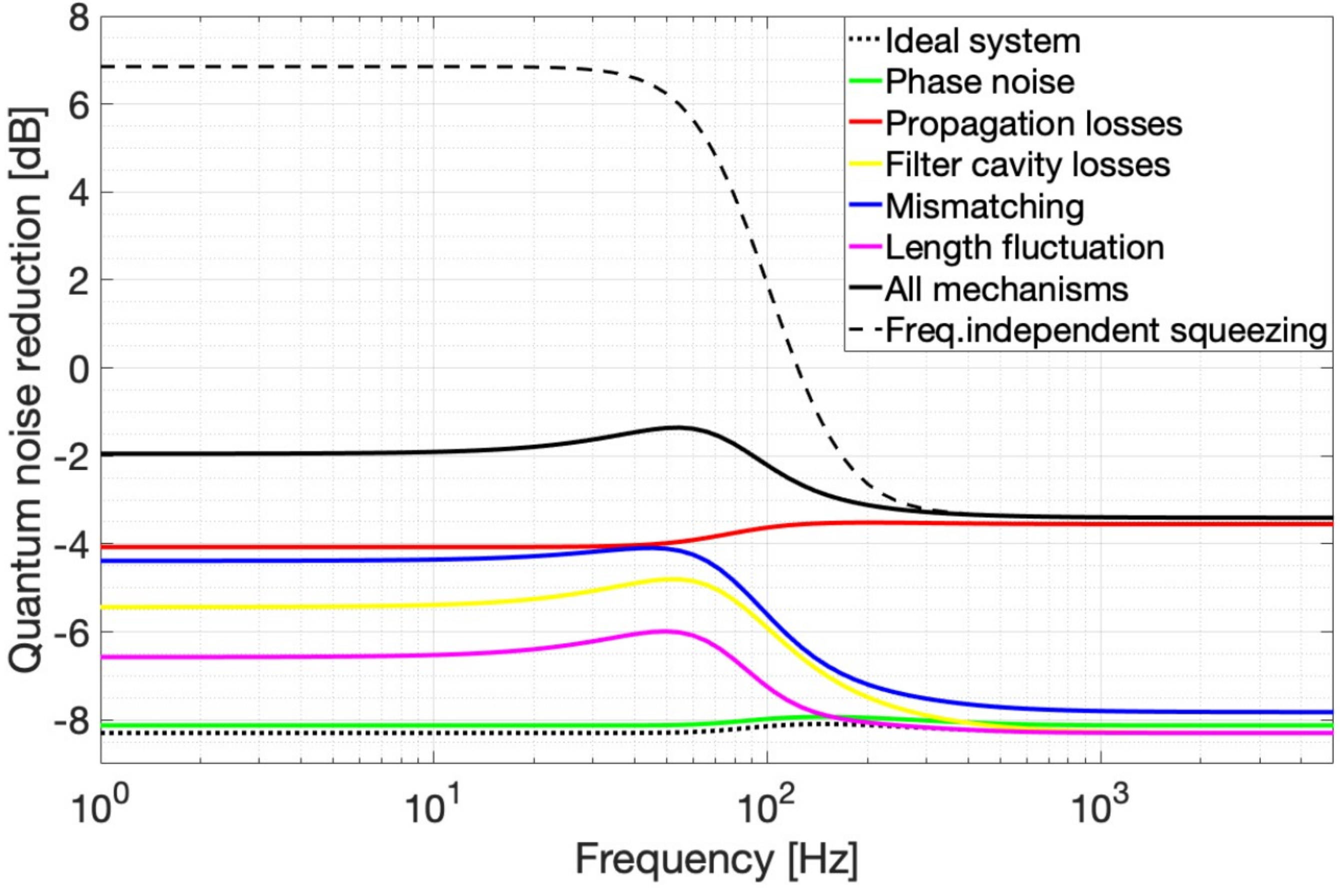

FDS measurement in TAMA

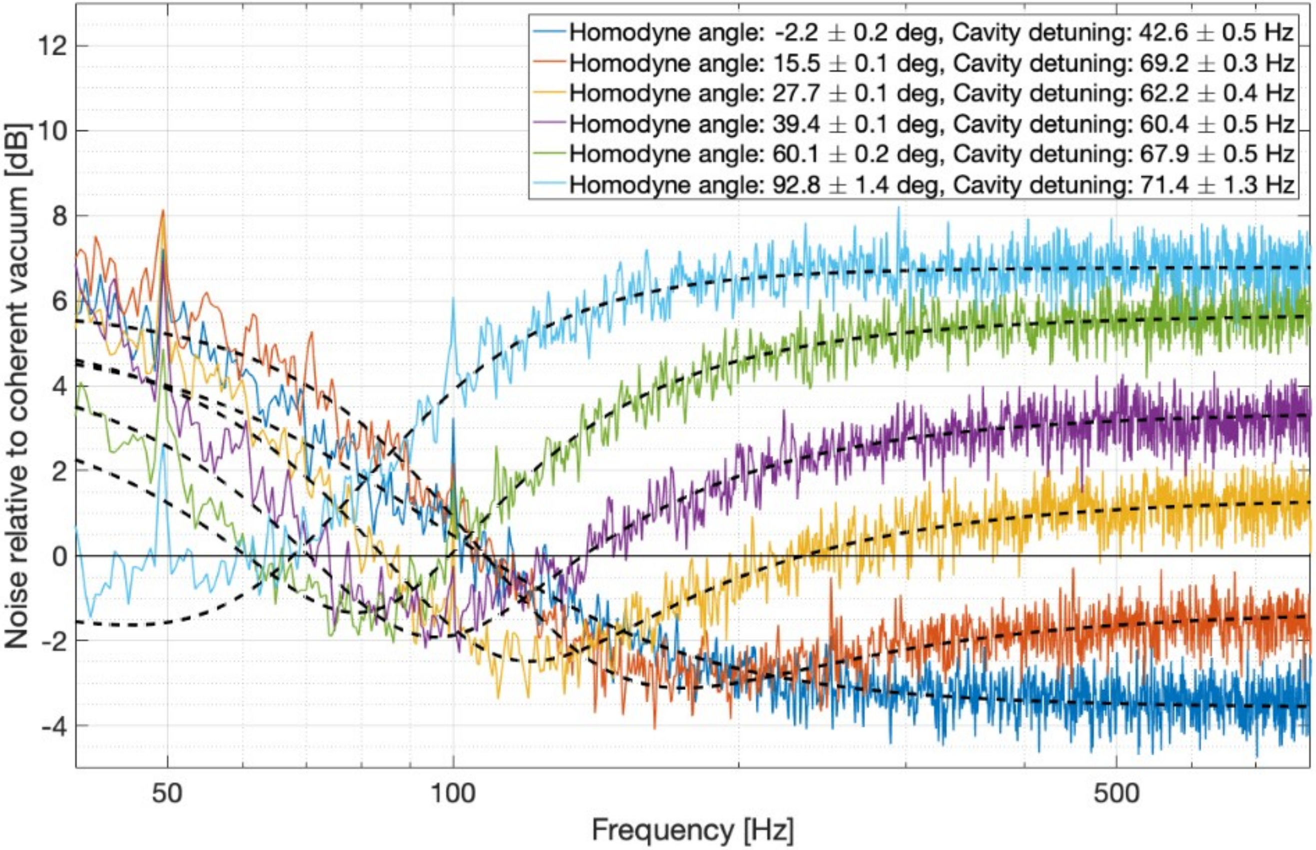

Scattered light improvement

Implementation of a **feedback control loop (SLL)** to compensate the difference in path length **δα(t)** + **δφ(t)** between the LO beam and the scattered light field.